2017

Isopeptide and Ester Bond Ubiquitination Regulate Degradation of the Human Dopamine Receptor 4

Jennifer C. Peeler

ISOPEPTIDE AND ESTER BOND UBIQUITINATION REGULATE DEGRADATION OF THE HUMAN DOPAMINE RECEPTOR 4

A Thesis Presented to the Faculty of

The Rockefeller University

in Partial Fulfillment of the Requirements for

The degree of Doctor of Philosophy

by

Jennifer Carol Peeler

June 2017

ISOPEPTIDE AND ESTER BOND UBIQUITINATION REGULATE DEGRADATION OF THE HUMAN DOPAMINE RECEPTOR 4

Jennifer Carol Peeler, Ph.D.

The Rockefeller University 2017

The human dopamine receptor 4 (hD4R) is a seven-transmembrane helical G protein-coupled receptor (GPCR) found in neural synaptic membranes. The neurotransmitter dopamine binds to and activates the hD4R, which is involved in central nervous system pathways that modulate cognition and circadian rhythms. The hD4R is the primary dopaminergic receptor for the atypical anti-psychotic drug clozapine, which is used to treat schizophrenia and other cognitive disorders. The hD4R gene is unique among the superfamily of GPCR-encoding genes because within the human population, it contains a variable number of tandem repeat (VNTR) exon polymorphism. Because of the VNTRs, the length of the primary structure of one of the intracellular loops of the hD4R can vary dramatically among individuals. Attempts have been made to correlate different VNTR structures with different behavioral traits – for example, a specific variant of hD4R is robustly correlated with attention deficit hyperactivity disorder. Like other GPCRs, hD4R functions at the plasma membrane by binding an extracellular ligand, in this case dopamine, to regulate an intracellular signaling cascade. The density of hD4R at the plasma membrane and its distribution within

the neuron/synapse dictate the cellular response to dopamine. Despite the importance of hD4R in neuronal signaling, the molecular mechanisms regulating its cellular expression and degradation are unclear. Isopeptide ubiquitination of lysine residues on the cytoplasmic surface of various GPCRs regulates receptor abundance at the membrane by promoting protein degradation. I have studied the role of the ubiquitin-proteasome system in the cellular degradation of hD4R, and show here that hD4R protein levels are regulated through both a canonical and a non-canonical ubiquitination pathway. Site-directed mutagenesis of lysine residues, as well as mutagenesis of the atypical ubiquitin acceptors serine and threonine, led to an additive increase in mutant hD4R protein abundance in a cellular expression model. Chemical inhibition of the proteasome increased levels of the wild-type hD4R, but not the lysine, serine, and threonine null mutant. Both isopeptide ubiquitination of lysine and ester bond ubiquitination of serine and threonine were detected on hD4R in a model protein expression system using immunoprecipitation techniques. A proximity ligation assay was used to quantify isopeptide and ester bond ubiquitination in this protein expression system and to detect ubiquitination of hD4R in mouse primary cortical neurons. Together, these data support the hypothesis that hD4R is proteasomally degraded after isopeptide ubiquitination of lysine residues and ester ubiquitination of serine and threonine residues. The ubiquitination and subsequent degradation of hD4R represents a mechanism for cellular control over hD4R protein levels. While the low abundance of hD4R protein produced in heterologous expression systems

has previously been limiting for biochemical and structural biology techniques, the degradation-resistant hD4R mutants presented here overcomes this limitation and may facilitate future research, including the identification of dopamine receptor interacting proteins (DRIPs). hD4R joins a small number of proteins that are known to be modified by ubiquitination via ester bonds. This work also describes novel techniques to confirm and quantify ester-bond ubiquitination for a given membrane protein within a cell.

ACKNOWLEDGEMENTS

Dr. Thomas P. Sakmar has been a kind and generous mentor. I am grateful for his scientific guidance and his support of my professional goals. Tom allowed me the independence to build an entire thesis out of an unusual western blot and was always there when I needed him.

The Sakmar Lab has been a great place to work; I have been happy to come to lab every morning for the last 6 years. My colleagues have been incredibly helpful and supportive. My fellow graduate students Dr. Amy Grunbeck Perea, Dr. Adam Knepp, Dr. He Tian, Carlos Rico, and Emily Lorenzen have been great comrades. Dr. Minyoung Park, Dr. Saranga Naganathan, Dr. Sarmistha Ray-Saha, and Dr. Thomas Huber have served as trusted advisors. The help, guidance, and friendship of Manija Kazmi have been vital to my success as a graduate student. Dr. W Vallen Graham has thoughtfully examined every piece of data I have generated and has become a dear friend.

I was able to work in the Division of Neurogeriatrics at the Karolinska Institutet thanks to the generosity of Dr. Lars Tjernberg. I am grateful to Birgitta Wiehager for her work in culturing mouse primary neurons and to Dr. Sophia Schedin-Weiss for her expertise and assistance in transfecting neurons and performing PLA.

I was able to work with two exceptional undergraduates during my time in the Sakmar lab - Carolyn Rachofsky and Mariluz Soula. I am grateful that they were willing to dedicate their precious time to my project, and I am thankful for the wonderful contributions they made to my research.

Dr. Thomas C. Peeler and Dr. Margaret T. Peeler have been constantly supportive, understanding, generous, and loving. I am lucky to be their daughter. James Peeler and Charles Peeler make me laugh. I am lucky to be their sister.

Dr. Michael S. Wheelock has been my constant teammate. I am so grateful.

TABLE OF CONTENTS

LIST OF FIGURES

LIST OF TABLES

CHAPTER 1: Introduction

1.1 G protein-coupled receptors

G protein-coupled receptors (GPCRs) are the central component in a complex signaling system that has evolved to communicate information from the extracellular environment to the cellular interior. GPCRs are polytopic membrane proteins with seven transmembrane (TM) α-helices embedded in the plasma membrane to create distinct extracellular and intracellular domains. The human genome contains genes encoding approximately 730 different GPCRs, and each GPCR has a characteristic cellular expression pattern and pharmacology. Agonistic ligands, which generally engage receptors at the extracellular surface, bind with high specificity and affinity and result in receptor activation. A ligand-induced change in protein conformation accompanies the formation of the receptor-ligand complex and extends through the TM helices to the cytoplasmic surface of the receptor. Relatively dramatic conformational changes in the receptor's cytoplasmic surface, including an opening of the helical bundle, then facilitate the binding of a specific intracellular heterotrimeric guanine nucleotide-binding regulatory protein (G protein). The formation of a "ternary complex" (ligand-receptor-G protein) induces the release of guanosine diphosphate (GDP), which is rapidly replaced with guanosine triphosphate (GTP), within the α subunit

of an intracellular G protein. The agonist-induced GDP/GTP exchange causes the dissociation of the G protein α subunit from its G protein β and γ subunits and from the active receptor. The activated G protein, which essentially functions as a molecular switching mechanism, then initiates intracellular signaling cascades either through the direct effects of the GTP-bound α subunit, or the liberated G protein βγ subunit, depending on the specific cellular context.

The basic mechanism of GPCR signaling is relatively narrowly utilized in nature. All eukaryotes – from yeast to humans – utilize GPCRs to facilitate cell-to-cell communication or to monitor the extracellular environment (de Mendoza et al., 2014), but GPCR orthologs are not found, for example, in bacterial organisms. In addition to a conserved function, GPCRs posses a highly conserved protein structure. The prototypical GPCR has an extracellular amino-terminus (N-term), seven TM domains, and an intracellular carboxy-terminus (C-term). There are three extracellular loops (EC1, EC2, and EC3), and three intracellular loops (IC1, IC2, and IC3) (Figure 1-1). Within the confines of the 7-TM structure, there is great diversity in the length and composition of the termini, loops, and TM helices. Post-translational modifications (PTMs), including N- and O-linked glycosylation, tyrosine sulfation and disulfide bond formation, especially involving the N-term tail, can vary widely among different GPCRs.

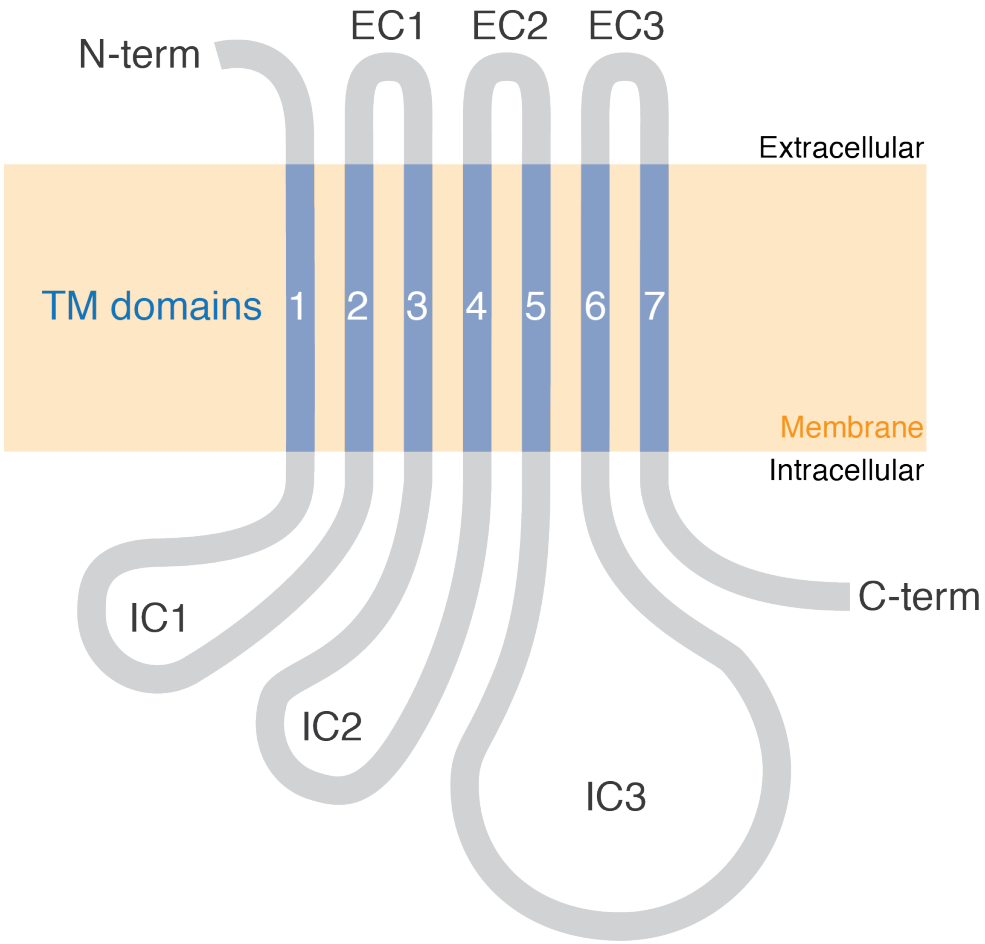

Figure 1-1 Prototypical GPCR structure.

A GPCR has an extracellular amino-terminus (N-term), seven transmembrane (TM) domains (blue), and an intracellular carboxy-terminus (C-term). There are three extracellular loops (EC1, EC2, and EC3), and three intracellular loops (IC1, IC2, and IC3). The approximate extent of the plasma membrane region is shown in orange.

Within the human genome, there are approximately 730 GPCRs (Fredriksson et al., 2003). Despite having a similar structure and general mechanism of activation, these GPCRs bind a diverse array of ligands and contribute to diverse cellular processes. GPCR ligands can range in size from a photon of light, which is detected by a chromophore cofactor in visual pigments, (Sakmar et al., 2002)to a 30-kDa protein hormone(Szkudlinski et al., 2002). The majority of GPCR ligands are small molecules and peptides, including types of odorants(Buck and Axel, 1991), neuromodulators(Civelli, 2012), and approximately 25% of all FDA-approved small-molecule drugs(Overington et al., 2006). In humans, there are four different classes of G protein α subunits that can be activated by GPCRs and, through various secondary messengers including cyclic adenosine monophosphate (cAMP), diacylglycerol (DAG), and inositol trisphosphate (IP_3), can initiate various protein signaling cascades(Wettschureck and Offermanns, 2005). Furthermore, there appear to be signaling cascades that can be activated by the interaction of GPCRs with cellular proteins other than G proteins, including β-arrestin(DeWire et al., 2007). At the cellular level, the consequences of GPCR-initiated signaling cascades can include protein phosphorylation, regulation of gene transcription, and apoptosis. At the organismal level, the consequences of GPCR-initiated signaling cascades can include sensory perception, regulation of behavior, and immune function(Wettschureck and Offermanns, 2005).

GPCRs are expressed throughout the mammalian body (Regard et al., 2008; Vassilatis et al., 2003), and at the organismal level, regulating the spatial distribution and level of cell-surface expression of GPCRs appears to be vital to human health. Aberrant expression of GPCRs has been associated with numerous disease states, including tumorigenesis. For example, the induced aberrant expression of a GPCR has been shown to be sufficient to induce tumorigenesis(Mazzuco et al., 2007) and the expression of a constitutively active GPCR has been shown to cause uveal melanoma – the first case of a GPCR oncogene(Moore et al., 2016). At the cellular level, the regulation of GPCR protein levels at the cell surface is also important to human health, and at least 20 GPCRs have been found to be upregulated in at least 14 different types of cancer, where their activation contributes to inappropriate cell survival as well as metastasis(Dorsam and Gutkind, 2007). For example, the upregulation of the C-X-C chemokine receptor 4 (CXCR4), which mediates targeted cell migration, is necessary for Her2-mediated breast cancer metastasis(Li et al., 2004). Human disease can also result from insufficient levels of protein at the cell surface. For example, a lack of the visual GPCR rhodopsin at the surface of the disc membrane in rod cells results in autosomal-dominant retinitis pigmentosa(Hollingsworth and Gross, 2012). The presence of GPCRs at the cellular surface can be dictated by rates of transcription and translation as well as multiple PTMs. One PTM often used to regulate GPCR protein levels and localization is ubiquitination, which is the primary focus of this dissertation.

1.2 Isopeptide Ubiquitination

Protein modification via covalent attachment of the small protein ubiquitin was first reported in the 1970s in a series of inter-related studies. Ira Goldknopf and Harris Busch discovered that a polypeptide could be attached to the histone protein H2A via an isopeptide (Goldknopf et al., 1977). Separately, David Schlesinger and Gideon Goldstein identified a polypeptide, which as cited in the title of their 1975 publication, “is probably represented universally in living cells.” They later renamed the polypeptide ubiquitin (Goldstein et al., 1975). Both aforementioned groups published preliminary sequential Edman degradation results for these polypeptides (Olson et al., 1976; Schlesinger and Goldstein, 1975). Margaret O. Dayhoff, the creator of the first protein sequence repository and author of the *Atlas of Protein Sequence and Structure*, determined that these polypeptides were in fact the same, and that ubiquitin was attached to H2A via an isopeptide linkage (Hunt and Dayhoff, 1977).

After 25 years of accelerating biochemical and proteomics work, we now know that covalent attachment of an ubiquitin molecule is a common PTM and is catalyzed by a series of enzymatic reactions (Figure 1-2). First, a ubiquitin-activating enzyme (E1) binds adenosine triphosphate (ATP), Mg^{2+}, and free ubiquitin. The E1 enzyme then catalyzes the acyl-adenylation of the ubiquitin C-term. The ubiquitin adenylate intermediate is then attacked by an active site

cysteine residue in the E1 enzyme, resulting in a thioester attachment between the E1 cysteine and ubiquitin C-term (Ciechanover et al., 1982)(Schulman, 2009)(Schulman and Harper, 2009). A protein-protein interaction between the E1 and the ubiquitin-conjugating enzyme (E2) then promotes the transfer of thioester ubiquitin from E1 to an active site cysteine in E2 (Hershko et al., 1983)(Olsen, 2013)(Olsen and Lima, 2013). Finally, the ubiquitin ligase enzyme (E3) is responsible for substrate recognition and the transfer of ubiquitin from E2 to the substrate (Hershko et al., 1983).

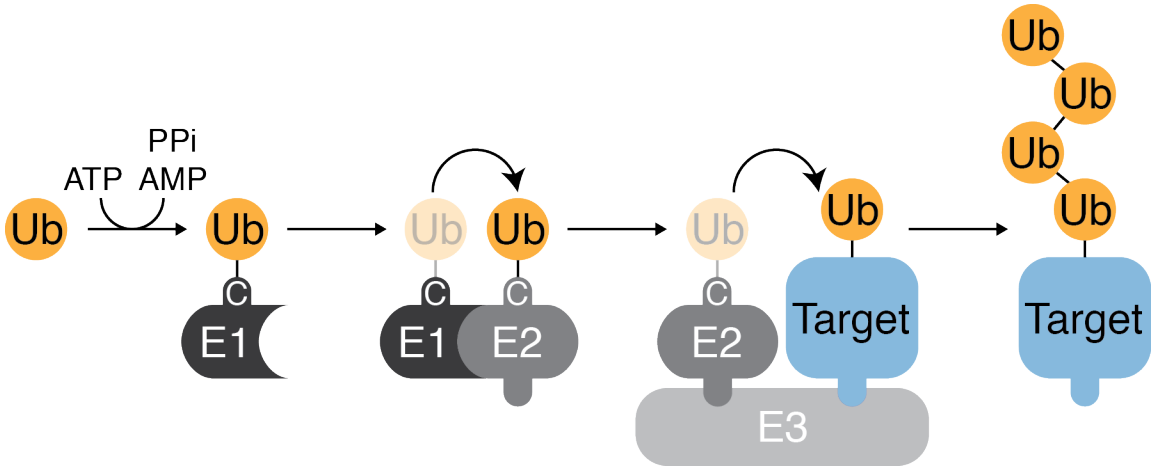

Figure 1-2 Ubiquitination reaction pathway.

Ubiquitin (Ub, orange) is attached via a thioester bond to a cysteine (C) on the ubiquitin-activating enzyme (E1, dark gray) through an ATP-dependent process. Ub is then transferred to the ubiquitin-conjugating enzyme (E2, gray), where it is also attached via a thioester bond. An ubiquitin ligase enzyme (E3, light gray) then facilitates the covalent deposition of Ub on the target protein (blue). A RING family E3 ligase is shown here as an example. Adapted from (Rotin and Kumar, 2009).

There are two major families of E3 ligases, with separate mechanisms of action. The RING domain-containing enzyme may be one component in a multi-protein complex responsible for substrate recognition and ubiquitination. In the case of the RING family of E3s, the E3 works as a scaffold that brings the substrate and E2-ubiquitin complex in close proximity (Deshaies and Joazeiro, 2009). Alternatively, in the HECT family of E3s, there is a conserved active site cysteine in the E3 that forms a thioester bond with ubiquitin before it is attached to the substrate (Rotin and Kumar, 2009).

Despite the fact that ubiquitin is attached via a thioester bond to the active-site cysteine residues of E1, E2, and in some cases E3 enzymes, until 2005 it was believed that ubiquitin was only attached to protein substrate lysine residues or N-terms via isopeptide bonds. The human genome encodes two potential E1 enzymes, 28 E2s, and over 600 E3s. The majority (95%) of E3s are members of the RING family (Li et al., 2008). There are also 79 human deubiquitinases (DUBs) that contribute to protein regulation by enzymatically removing ubiquitin residues from substrate proteins (Komander et al., 2009).

Ubiquitin can be attached to a substrate in a variety of configurations. First, a single substrate residue can be attached to a single ubiquitin molecule (monoubiquitination) or to a string of multiple ubiquitin molecules attached to one another (polyubiquitination). In the case of polyubiquitination, subsequent ubiquitin molecules can be attached at many different residues within ubiquitin, including up to seven different ubiquitin lysine residues. The most commonly

observed sites of polyubiquitination attachment within ubiquitin itself are lysine 48 and lysine 63. Furthermore, polyubiquitin chains can be linear or branched. Finally, recent evidence exists for further PTMs of the ubiquitin molecules themselves, including phosphorylation, acetylation, SUMOlyation (small ubiquitin-like modifier), and neddylation (Swatek and Komander, 2016). Neddylation is the process whereby the protein NEDD8 (neural-precursor-cell-expressed developmentally down-regulated), a ubiquitin-like polypeptide, is linked to its protein target. Any given protein substrate then may have multiple residues which can be subsequently modified, adding to the complexity and potential heterogeneity of a protein's ubiquitination state.

The potential biological consequences of protein ubiquitination was first understood in the 1980s. Aaron Ciechanover, Irwin Rose, and Avram Hershko discovered the mechanism of ATP-dependent proteolysis, which was in fact regulated by protein ubiquitination and subsequent proteasomal degradation (Ciechanover et al., 1980; Hershko et al., 1980). Degradation via the proteasome is now viewed as the canonical consequence of isopeptide ubiquitination of protein substrates. Recent work has sought to define the specific ubiquitin modification (in terms of length and linkage) that induces interaction with the proteasome. It is thought that configurations containing four ubiquitin molecules (though not necessarily all in a single chain) and lysine 48-based linkages specifically promote proteasomal degradation (Lu et al., 2015; Thrower et al., 2000).

It is also now clear that ubiquitination of protein substrates can have signaling consequences beyond proteasomal degradation (Chen and Sun, 2009). The most well understood non-proteolysis consequence of ubiquitination is the ubiquitin-dependent activation of the IκB kinase complex. The downstream consequence of IκB kinase activation is translocation of the transcription factor NF-κB from the cytoplasm to the nucleus (Chen et al., 1996). As with proteasomal degradation, an effort has been made to determine precisely which ubiquitin conformations are required for IκB kinase activation. Currently, it appears that N-term linked and lysine 63-linked polyubiquitination are both required for IκB kinase activation (Emmerich et al., 2013). Ubiquitination, but not proteasomal degradation, has also been shown to be important for DNA repair and chromatin dynamics. A family of proteins containing ubiquitin-binding domains seems to be vital to non-proteolytic ubiquitin signaling (Chen and Sun, 2009). Ubiquitination also has a role, outside of proteasomal degradation, in the regulation of membrane proteins, including GPCRs.

1.3 Trafficking and Ubiquitination of GPCRs

The ubiquitination of a GPCR was first reported in 2001. In the last 15 years it has been discovered that at least 40 GPCRs are modified by ubiquitin (Jean-Charles et al., 2016). Due to the inherent difficulties of proteomics studies of membrane proteins, most GPCR ubiquitination research has focused not on

the specific type of ubiquitin attachment, but rather on the cellular consequences of ubiquitination. In the majority of cases of known GPCR ubiquitination, the modification regulates receptor trafficking, which in turn can influence receptor signaling. The process of GPCR transport to and removal from the cell surface can be influenced by receptor ubiquitination.

GPCR mRNA is translated into the protein at the rough endoplasmic reticulum (ER), and co-translational insertion of the protein occurs, such that the N-term and EC loops are in the ER lumen and the C-term and IC loops are in the cytoplasm (a process called membrane translocation). GPCRs have been shown to interact with chaperone proteins in the ER that are capable of both assisting in protein folding and identifying misfolded proteins (Young et al., 2015). Quality control is performed in the ER to ensure that only properly folded proteins reach the cell surface. Quality control is conducted via the ER-associated degradation (ERAD) pathway, which is ubiquitin-dependent. During the ERAD process, misfolded proteins are ubiquitinated by E3 enzymes that are also embedded in the ER membrane. Substrate ubiquitination triggers the removal of the misfolded protein from the ER (a process called retrotranslocation) and degradation of the substrate via the proteasome (Figure 1-3) (Christianson and Ye, 2014). A number of GPCRs are subjected to ERAD processing, including a series of opioid receptors (Petaja-Repo et al., 2001). Additionally, ERAD is the mechanism by which disease-associated mutations in GPCRs, including the well-studied case of rhodopsin mutations associated with rod cell degeneration in autosomal-

dominant retinitis pigmentosa, lead to receptor degradation (Hollingsworth and Gross, 2012).

At least four other PTMs are known to occur on GPCRs in the ER. N-linked glycosylation is the addition of sugar molecules to asparagine residues within the GPCR N-term. O-linked glycosylation occurs at serine or threonine residues. Tyrosine sulfation also can occur in the the ER at the N-term of GPCRs, and the extent of tyrosine sulfation can affect the ligand affinity of receptor agonists as demonstrated in the case of chemokine receptors, in particular CXCR4 (Veldkamp et al., 2008). GPCR glycosylation is thought to occur in the ER and is correlated with successful surface expression (Young et al., 2015). Palmitoylation is the attachment of lipid molecules to the GPCR – canonically on cysteine residues in the C-term. Palmitoylation of GPCRs is also believed to occur during ER processing and is correlated with receptor cell surface expression (Chini and Parenti, 2009).

GPCRs that are properly folded leave the ER via vesicular transport. The GPCRs then travel through the ER-Golgi intermediate complex, the Golgi apparatus and the trans-Golgi network (Figure 1-3). It is believed that GPCRs undergo further processing in the Golgi, including additional O-glycosylation (Young et al., 2015). GPCRs then exit the Golgi, dependent upon specific protein sequence motifs in the N-term and C-term of the protein (Dong et al., 2007). Traveling via vesicle, GPCRs arrive at the plasma membrane and join the cell surface via exocytosis.

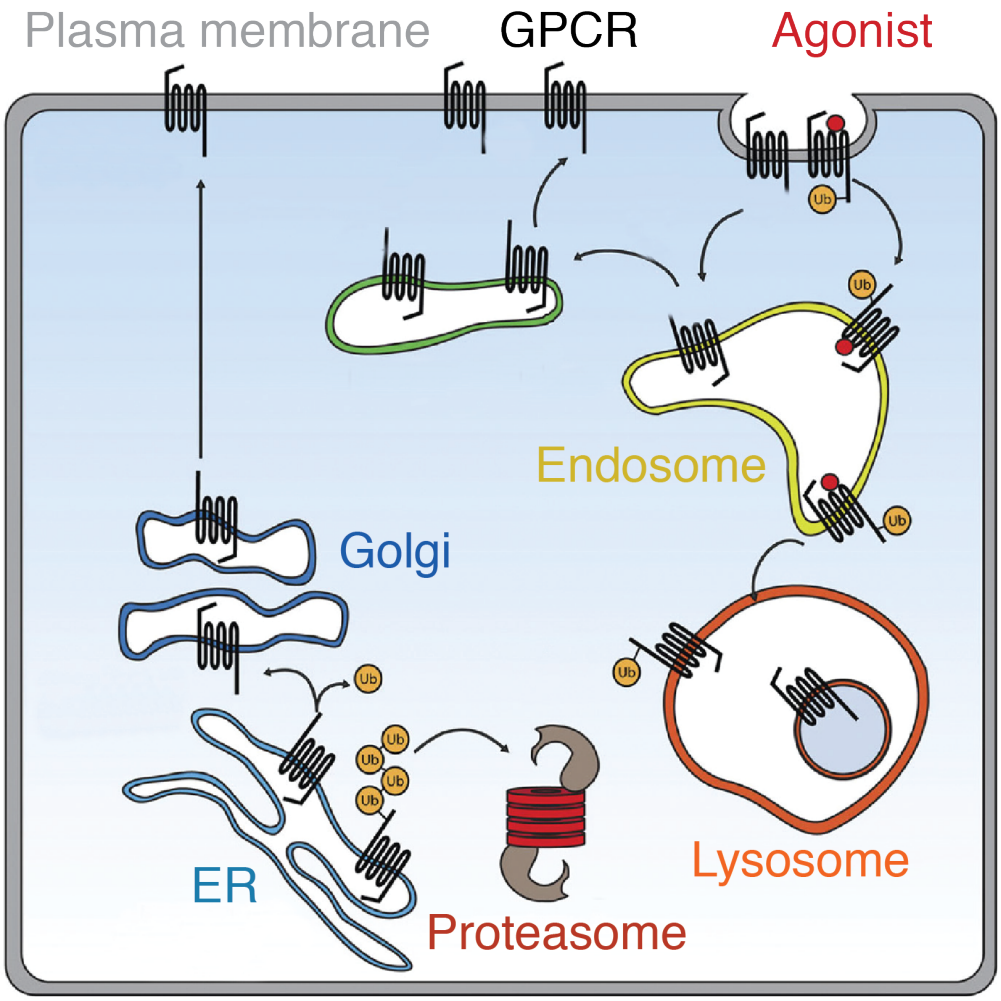

Figure 1-3 Role of ubiquitin in GPCR trafficking.

GPCRs travel from the ER (light blue), through the Golgi (dark blue), to the plasma membrane (gray). Attachment of ubiquitin (Ub, orange circle) to a GPCR in the ER targets that receptor for proteasomal degradation via ERAD. At the plasma membrane, agonist binding (red circle) promotes phosphorylation-dependent internalization of receptors into endosomes (yellow). Canonically, an ubiquitinated receptor in an endosome is destined for lysosomal degradation (orange) while non-ubiquitinated receptors can be recycled back to the plasma membrane (green). Adapted from (Dores and Trejo, 2012).

GPCR levels at the cell surface are dictated by both the rate of trafficking from the ER to the plasma membrane and the rate of removal from the plasma membrane via endocytic vesicles. The internalization of GPCRs from the cell surface after receptor activation contributes to receptor desensitization (Figure 1-3). Desensitization is the terminology for the observation that subsequent repeated stimulation of a cell or tissue by the same stimulus results in progressively less response. The desensitization process allows for fine-tuning of the linear response range, dependent on previous levels of ligand binding (Gainetdinov et al., 2004). In yeast, internalization of GPCRs is directly dependent upon receptor ubiquitination. In mammals, however, the mechanism of endocytic internalization is dependent upon another PTM: phosphorylation. After ligand binding and G protein activation, G protein-coupled receptor kinases (GRKs) phosphorylate serine and threonine residues on the cytoplasmic surface of the receptor. Phosphorylation of serine and threonine residues then recruits β-arrestin proteins that in turn recruit the protein machinery for endocytosis (Gainetdinov et al., 2004).

While the process of internalization for mammalian GPCRs is phosphorylation-dependent, the fate of internalized receptors is ubiquitin-dependent. The most widely studied and understood role of GPCR ubiquitination is in regulating whether internalized receptor will be returned to the cell surface (a process called recycling) or destroyed. According to the canonical mechanism of desensitization, an ubiquitin molecule attached to a GPCR inside an endocytic

vesicle will be bound by proteins called, endosomal-sorting-complex-required-for-transport (ESCRT) proteins. ESCRT machinery will then facilitate the combining of the vesicle with a lysosome, leading to the degradation of the receptor (Alonso and Friedman, 2013). Alternatively, if an internalized receptor is not ubiquitinated, the vesicle is not bound by ESCRT machinery and is capable of returning to the cell surface (Figure 1-3). While GPCR ubiquitination does promote receptor degradation, it is not through the proteasomal pathway that dominated ubiquitination studies of the 1980s and 1990s. Receptor ubiquitination leading to lysosomal degradation has been observed for a number of GPCRs, including the β_2 adrenergic receptor, a number of chemokine receptors including CXCR4, and opioid receptors. The enzymes required for ubiquitination and in some cases also deubiquitination for these receptors have been determined, as have the specific steps of lysosomal degradation that are ubiquitin-dependent (Jean-Charles et al., 2016).

The number of copies of a given GPCR at the plasma membrane influences how a cell responds to extracellular ligands. Ubiquitination of GPCRs helps to regulate the abundance of receptors at the plasma membrane through, 1) ERAD processes controlling the quality and number of receptors leaving the ER for the cellular surface, and 2) lysosomal degradation processes controlling the fate of receptors leaving the cellular surface after activation. It is likely that there are consequences of GPCR ubiquitination outside of their canonical roles in regulating proteasomal and lysosomal degradation. For example, ubiquitination

of GPCRs could be utilized directly in receptor signaling in a mechanism similar to the activation of IκB kinase complex. It is also likely that many more GPCRs are ubiquitinated than we currently appreciate. It has been shown in HEK293T cells that the D1, D2, and D5 dopamine receptors are ubiquitinated, though the details of ubiquitin attachment and the consequence of ubiquitination is unknown (Jean-Charles et al., 2016; Rondou et al., 2008). In the dissertation that follows, I present evidence for the ubiquitination of a dopamine-binding GPCR, the human dopamine receptor 4 (hD4R), at both lysine residues and serine/threonine residues, and determine the consequences of hD4R ubiquitination on its degradation.

1.4 Human dopamine receptor 4

The human proteome contains five GPCRs that recognize the modulatory neurotransmitter dopamine as their primary agonist ligand. Despite all binding the same endogenous ligand, these receptors vary in their distribution within the body, their protein sequence and structure, and their G protein coupling specificity. The human dopamine receptor 1 (hD1R) and the human dopamine receptor 5 (hD5R) are expressed exclusively in post-synaptic cells, contain a long C-term, and couple predominantly to $G\alpha_s$ (the “stimulatory” G protein) ultimately leading to cAMP production. Alternatively, hD2R, hD3R, and hD4R can be expressed in pre- and/or post-synaptic cells, contain a long IC3 loop, and couple

predominantly to $G\alpha_{i/o}$ (the “inhibitory” G protein, or so-called “other” G protein) leading to the inhibition of cAMP production (Beaulieu and Gainetdinov, 2011).

In 1991, only three human dopamine receptors had been discovered - hD1R, hD2R, and hD3R. At that time the antipsychotic drug clozapine used mainly for treatment of schizophrenia was characterized as “atypical” because it was hypothesized to work through both serotonin and dopamine pathways, but none of the known dopamine receptors had sufficient binding affinity for the drug to be potential targets (Meltzer, 1991). Therefore, Hubert Van Tol and colleagues hypothesized that a fourth dopamine receptor must exist. Through homology-based cloning, Van Tol cloned the gene *DRD4* that encodes hD4R and showed that hD4R affinity for clozapine was an order of magnitude greater than its affinities for hD1R, hD2R, and hD3R (Van Tol et al., 1991).

Shortly after cloning *DRD4*, Van Tol and coworkers noticed that a number of variants of *DRD4* were present in the human population. They described a 48-base pair variable number of tandem repeat (VNTR) polymorphism in the third exon of *DRD4,* which encodes the IC3 loop in hD4R (Van Tol et al., 1992). There can be anywhere from 2 to 11 repeats in *DRD4*, though the most common are 2, 4, or 7 repeats (Figure 1-4). These are not perfect repeats; while all repeats are proline-rich, the exact amino acid sequence is not identical for each repeat segment within a variant. Further variability exists in that multiple alleles of the 2, 4, or 7 repeat exist with minor codon changes within the repeat region (Lichter et al., 1993).

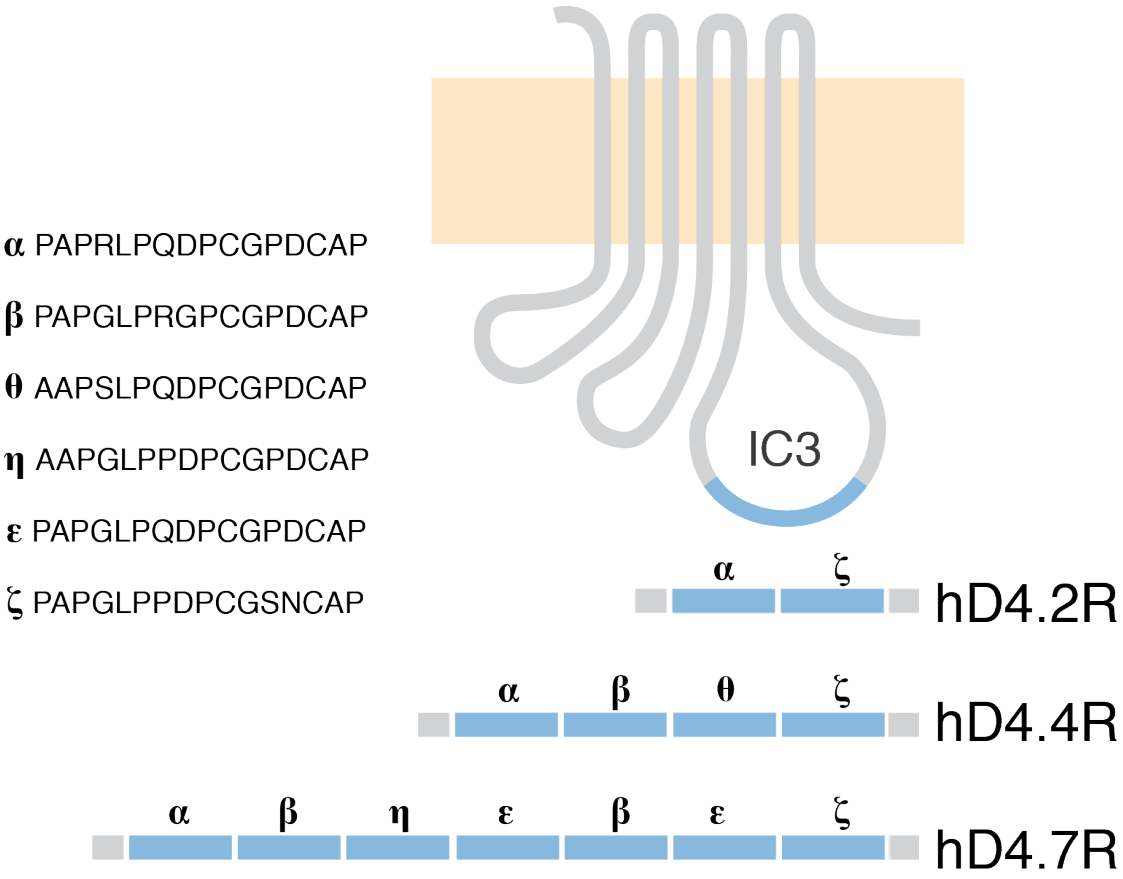

Figure 1-4 VNTR in hD4R IC3.

hD4R contains 2-11 repeats (blue squares) in IC3. Repeats are 16-amino acid residues long; repeat sequences are not identical, but are proline-rich. The most common hD4R variants are 2-repeat (hD4.2R), 4-repeat (hD4.4R), and 7-repeat (hD4.7R). The amino acid sequence for the most common allele of each variant is shown.

The hD4R receptor gained public recognition after two articles reported a correlation between the 7-repeat variant of DRD4 and novelty seeking behavior in humans (Benjamin et al., 1996) (Ebstein et al., 1996). The correlation between the 7-repeat variant and novelty seeking has not withstood meta-analysis (Kluger et al., 2002), but the initial articles spurred the publication of numerous further studies checking for associations between DRD4 variants and various aspects of human behavior, personality traits, and mental health. The U.S. National Library of Medicine online database PubMed.gov shows that an average of nearly 1 paper per week has been published analyzing *DRD4* polymorphisms from 2004 to 2016. The majority of results that do find a positive correlation are not reproducible, in part because of great variability in the methods used to classify alleles (Pappa et al., 2015).

However, one association does seem to be routinely reproduced and holds true during meta-analysis: the correlation between the *DRD4* 7-repeat alleles and diagnosis of attention deficit hyperactivity disorder (ADHD) (Li et al., 2006). An outstanding question in the field is how the correlation between the 7-repeat variant and ADHD may be explained by the molecular pharmacology of hD4R, its cell biology, and its neural signaling.

Understanding the expression pattern of hD4R protein in the brain has been challenging due to difficulties in finding antibodies or ligands that are sufficiently selective for hD4R over hD2R and hD3R. One immunohistology study did provide evidence that hD4R is likely expressed in g-aminobutyric acid

(GABA) ergic (or GABA-producing) neurons within a variety of brain structures, including the cerebral cortex and hippocampus. Additionally, evidence exists for hD4R expression in pyramidal neurons, especially in the prefrontal cortex (Mrzljak et al., 1996). These results have been corroborated by evidence from mRNA- and ligand-based studies (Vullhorst, 2013). hD4R expression has also been observed at high levels in the human retina (Matsumoto et al., 1995) and pineal gland (Bai et al., 2008).

In the brain hD4R seems to be present specifically in fast-spiking, parvalbumin-expressing (PV+), GABAergic interneurons. These neurons are relatively easy to identify in the brain and have therefore become a highly studied cell type – both at the molecular and circuit levels. It is clear that PV+ interneurons have a role in a number of brain functions, including gamma-oscillations (Hu et al., 2014). Gamma-oscillations are measurable neural oscillations between 20-80 Hz. The presence of gamma-oscillations is correlated with attention (Benchenane et al., 2011), and decreased gamma-oscillations are correlated with cognitive impairment and psychiatric disease (Uhlhaas and Singer, 2012). The activation of PV+ interneurons is associated with the generation of gamma-oscillations while the inhibition of PV+ interneurons is associated with reduction in gamma-oscillations (Cardin et al., 2009; Sohal et al., 2009). A role has emerged for hD4R in the regulation of these gamma-oscillations. A specific hD4R agonist is capable of increasing gamma-oscillation power (Andersson et al., 2012b). It seems that hD4R works with ErbB4 (a

receptor tyrosine kinase with neuregulin-1 as a ligand) and N-methyl-D-aspartate (NMDA) receptor (a glutamate activated ion channel) to exert a modulatory effect on gamma oscillations (Andersson et al., 2012a). These studies have renewed interest in hD4R as a drug target – now focusing on ameliorating cognitive deficits as opposed to being an anti-psychotic agent.

The cell biological and signaling properties of hD4R are of great interest and have the potential to serve as a bridge between genetic- and circuit-level understanding of the receptor. However, detailed studies of hD4R variants have been hampered because expression levels of the receptor in heterologous expression systems are extremely low, the receptor appears to be heterogeneous due to PTMs, and its signaling pathways appear to be pleiotropic. hD4R is glycosylated on the N-term and palmitoylated on the C-term (Zhang and Kim, 2016). Proper folding of hD4R may be a limiting factor in trafficking of the receptor to the cell surface (Van Craenenbroeck et al., 2005), and it appears that hD4R may not be internalized through the canonical phosphorylation- and β-arrestin-dependent mechanism (Spooren et al., 2010). hD4R binds endogenous dopamine and activates predominantly $G\alpha_{i/o}$ which leads to a decrease in cAMP production . Depending on the cellular context, hD4R activation can have various downstream signaling outcomes. A few examples include activation of NF-κB (Zhen et al., 2001), transactivation of the receptor tyrosine kinase PDGFRβ (Gill et al., 2010), and suppression of NMDA function (Qin et al., 2016) .

Identification of dopamine receptor interacting proteins (DRIPs) of hD4R is also an activate field of study. It is hypothesized that identifying additional DRIPs will increase our knowledge about hD4R signaling and its regulation. The IC3 loop of hD4R is extremely proline-rich and filled with potential SH3 (Src-homology 3) binding domains, a common motif in protein-protein interactions. Oldenhoff and colleagues demonstrated that the SH3 domain-containing adaptor proteins Grb and Nck2 interact with the hD4R IC3 (John Oldenhof et al., 1998). hD4R has also been shown to interact with other GPCRs. hD4R and hD2R dimerize to regulate release of glutamate in the striatum (González et al., 2012a). Dimerization of hD4R with adrenergic receptors in the pineal gland regulates melatonin production (González et al., 2012b). hD4R has also been shown to directly interact with potassium channels and regulate their trans-membrane voltage currents (Lavine et al., 2002). The lab of Kathleen Van Craenenbroeck identified the E3 adaptor protein KLHL12 as a hD4R DRIP. They determined that overexpression of KLHL12 promoted hD4R ubiquitination, including on non-lysine residues, but did not find evidence of KLHL12-associated degradation of hD4R (Rondou et al., 2008) (Rondou et al., 2010) (Skieterska et al., 2015).

The many genetic studies that correlate *DRD4* VNTR alleles with variations in human behavior and health have motivated a series of experiments comparing the function of hD4R protein variants. The 2-repeat protein variant (hD4.2R) has a repeat region in IC3 that is 32-amino acid residues in length while the 7-repeat protein variants (hD4.7R) has a repeat region that is 112-amino acid

residues in length (Figure 1-4). The difference in IC3 loop size is substantial, especially considering that the non-repeat region of the receptor is 355-amino acids in length. The repeat region causes hD4R variants to have hugely different cytoplasmic surfaces in the region attributable to G protein binding. However, standard GPCR functional assays show little to no change in hD4R ligand binding, G protein coupling, or downstream signaling (Kazmi et al., 2000) (Asghari et al., 1994) (Asghari et al., 1995). Functional differences in VNTR variants have appeared in a few studies characterizing hD4R-DRIP interactions, including hD2R dimerization (González et al., 2012a). Recent data have suggested that hD4R in pyramidal neurons of the prefrontal cortex has two potentially related roles, 1) regulating NMDA receptor levels, and 2) regulating neural oscillations. It seems that expression of hD4.7R, but not hD4.4R, leads to both aberrant NMDA degradation and imbalance in excitatory/inhibitory network bursts in the prefrontal cortex (Qin et al., 2016; Zhong et al., 2016). The authors suggest that the difference in hD4.7R function in pyramidal neurons may explain the correlation between the 7-repeat *DRD4* allele and diagnosis of ADHD.

Further understanding the cellular regulation of hD4R is critical if we aim to utilize hD4R as a drug target in the context of cognitive disorders or ADHD. Through my thesis research project on hD4R, I have discovered a mechanism that regulates hD4R protein levels. Regulation of hD4R protein levels is dependent upon both canonical ubiquitination of hD4R lysine residues and non-canonical ubiquitination of serine and threonine residues.

1.5 Ester and Thioester Ubiquitination

As described earlier, it has been known that ubiquitin attachment to the substrate protein could occur via isopeptide bonds with the primary amine of lysine residues. However, in 1998 it was also discovered that the primary amine on the N-term of a protein is also sufficient for isopeptide ubiquitination (Breitschopf et al., 1998). Now, N-term ubiquitination is widely recognized, even within polyubiquitin chains (Swatek and Komander, 2016). It has also long been recognized that the attachment of ubiquitin to cysteine residues via thioester bonds occurs in the active sites of enzymes of the ubiquitination pathway (Figure 1-2).

An additional example of non-canonical cysteine ubiquitination was more recently recognized. Upon infection with Kaposi's sarcoma-associated herpesvirus (KSHV), host immune defense proteins are downregulated. Major histocompatibility complex I (MHC I) molecules are ubiquitinated by the modulator of immune recognition 1 (MIR1) E3 ubiquitin ligase encoded in the genome of KSHV and subsequently degraded. In 2005, Cadwell and Coscoy determined that, unexpectedly, mutation of the MHC I molecule's cytoplasmic lysine residues to arginine did not fully prevent degradation. A cytoplasmic cysteine residue was sufficient for down-regulation of MHC I in a MIR1-dependent pathway (Cadwell and Coscoy, 2005). Therefore, it was hypothesized that MIR1 was able to ubiquitinate MHC I on lysine via isopeptide bonds as well

as cysteine residues via thioester bonds in order to promote degradation (Figure 1-5).

The degradation of host defense proteins after viral E3 ubiquitination on non-lysine residues is not unique to MIR1. It was quickly determined that lysine-less MHC-I molecules could also be marked for degradation via the mK3 E3 ubiquitin ligase encoded in the genome of the mouse γ-herpesvirus. In the case of mK3, lysine, serine, and threonine residues, but not cysteine residues were sufficient for degradation (Wang et al., 2007). Ubiquitination of hydroxyl-containing residues serine and threonine would require the attachment of ubiquitin via ester bonds (Figure 1-5). The E3 ligase Vpu, encoded by the human immunodeficiency virus (HIV) is capable of inducing degradation of two host defense proteins – CD4 and BST-2/tetherin. Vpu ubiquitinated targets lysine, serine, and threonine residues in order to promote degradation (Magadán et al., 2010) (Tokarev et al., 2011).

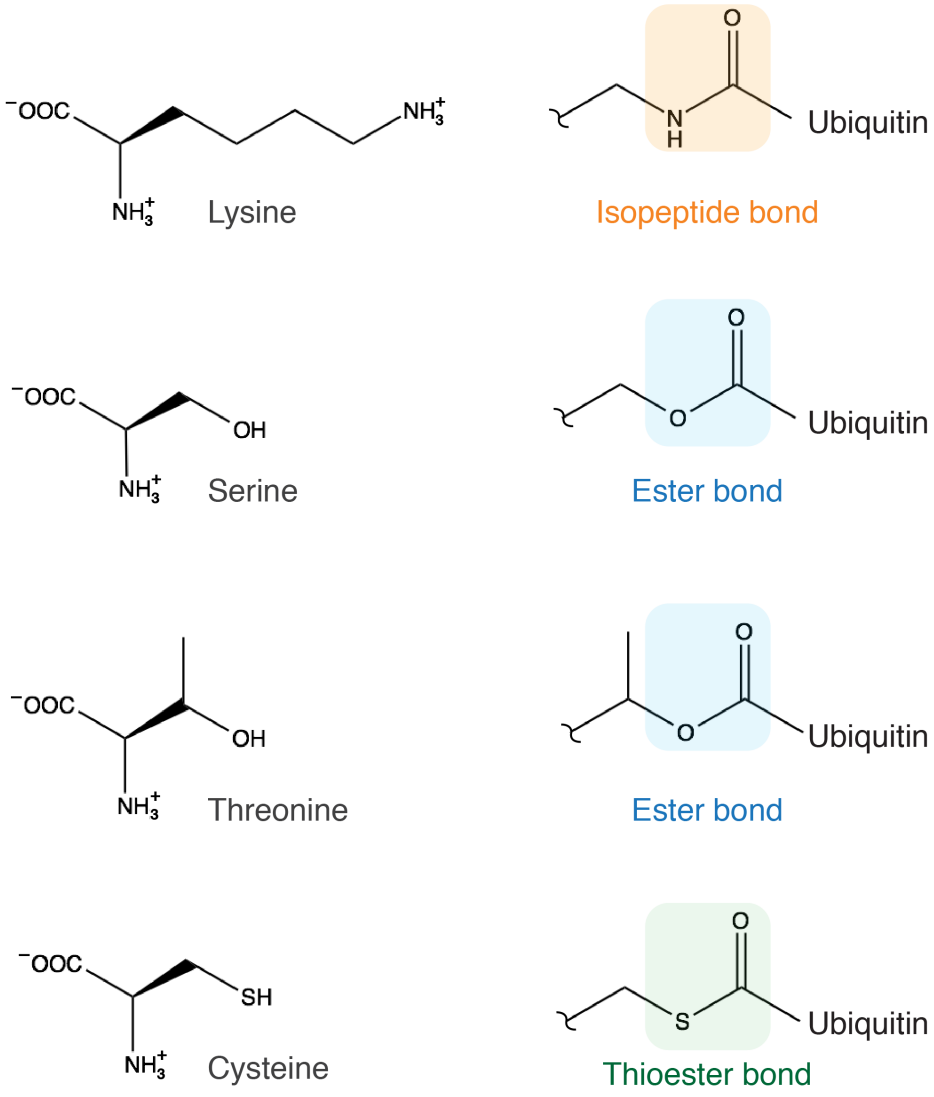

Figure 1- 5 Ubiquitin acceptor residues and linkage bonds.

Ubiquitin can be attached to target proteins on lysine residues through isopeptide bonds (orange), serine and threonine residues through ester bonds (blue), and cysteine residues through thioester bonds (green).

The catalysis of ester and thioester ubiquitination of protein substrates is not limited to viral E3 ligases. Ester and/or thioester ubiquitination of proteins in the absence of viral infection has been observed in yeast, plants, flies, frogs, and mammals (Weber et al., 2016) (Gilkerson et al., 2015) (Domingues and Ryoo, 2012) (Vosper et al., 2009) (Tait et al., 2007).

A predominant consequence of known cases of ester and thioester ubiquitination has been in targeting proteins for proteasomal degradation, especially via ERAD. Shimizu and colleagues determined that a mammalian ERAD E3 ligase Hrd1 ubiquitinates the known ERAD substrate NS-1 nonsecreted immunoglobulin light chain via ester ubiquitination. Furthermore, Shimizu determined that chemical disruption of ER protein folding increased overall cellular levels of ester ubiquitination, suggesting ester ubiquitination may be a common mechanism of ERAD E3s (Shimizu et al., 2010). Recently, it was also shown that a yeast ERAD E3 ligase, Doa10, is capable of inducing ubiquitination of ester as well as isopeptide ubiquitination of ERAD substrates. Separate E2 ubiquitin conjugating enzymes, however, were used for isopeptide and ester ubiquitination (Weber et al., 2016).

Proteasomal degradation of ester and thioester ubiquitinated proteins can also occur outside of the ER. For example, the proneural transcription factor Ngn2, which is active for only a small temporal window in development, is ubiquitinated via isopeptide, ester, and thioester ubiquitination before being proteasomally degraded (McDowell et al., 2010). The pro-apoptotic protein Bid is

auto-inhibited by its N-term. In order for apoptosis to proceed, the N-term is cleaved from Bid by a protease, and the N-term fragment must be degraded in order to prevent further binding. It has been shown that the N-term fragment is ubiquitinated by isopeptide, ester, and thioester bonds in order to induce rapid proteasomal degradation (Tait et al., 2007).

Though the majority of examples of ester and thioester ubiquitination lead to protein degradation, just as with isopeptide ubiquitination, there is at least one example of ubiquitin serving to regulate protein function. The proteins Pex5p and Pex20p serve to shuttle proteins from the cytosol to the peroxisome. In order to return to the cytosol to bind more peroxisome-bond proteins, thioester ubiquitination of these proteins is required (Carvalho et al., 2007) (Léon and Subramani, 2007).

Ester and thioester ubiquitination are still under-recognized and under-studied PTMs. In part, the lack of recognition is likely due to the difficulty in ester and thioester ester bond identification using mass spectrometry analysis – a widely used technique in the ubiquitination field. I present herein evidence for ester ubiquitination, but not thioester ubiquitination, in the regulation of protein levels of hD4R, and I provide a quantitative method for detecting hD4R ester ubiquitination.

CHAPTER 2: Materials and Methods

2.1 DNA constructs and mutagenesis

DNA constructs for hD4.2R-1D4, hD4.4R-1D4, hD4.7R-1D4 and the non-physiological hD4.NRR-1D4 in the pMT vector were constructed by Dr. Lenore Snyder (Kazmi et al., 2000). The open reading frames of these constructs were cloned into the pcDNA3.1 vector using EcoRI and NotI restriction enzymes. The original pMT constructs include a C-term 1D4 epitope (amino acid sequence: TETSQVAPA) and a 9-amino acid linker between the C-term of hD4R and the 1D4 epitope sequence (amino acid sequence: GKNPLGVRK). In all pcDNA3.1 constructs used in this thesis, the 9 amino acid linker region is present, but the two lysine residues are mutated to arginine. Mutations were made utilizing the QuikChange Lightning Multi Site-Directed Mutagenesis Kit (Agilent Technologies). In the creation of the KØ mutant all 4 endogenous lysine residues were mutated to arginine. In the creation of the STØ mutant cytoplasmic serine and threonine residues were mutated to alanine. The KSTØ mutant combines KØ and STØ mutations. For the CØ mutant, 4 cysteine residues in the IC3 loop of the hD4.2R-1D4 were mutated to alanine. The TagMaster Site-Directed Mutagenesis Kit (GM Biosciences) was used to create an hD4R mutant with N-term myc epitope as well as a mutant with the OLLAS epitope between hD4R C-term and 1D4. For baculovirus generation, hD4R-1D4 genes were added to

pFBDM using EcoRI and NotI restriction enzyme sites. The pCMV10-3XFLAG-ubiquitin construct was a gift of Dr. Andrian Marchese, Medical College of Wisconsin (Marchese and Benovic, 2001). The Gqi5 construct was a gift of Dr. Bruce Conklin (Coward et al., 1999) (Addgene plasmid # 24501). The pGEX2T-Nck and pGEX2T-Grb2 constructs were gifts from Dr. Hubert Van Tol (John Oldenhof et al., 1998). A control expressing only glutathione s-transferase (GST) was created using the QuikChange Lightning Site-Directed Mutagenesis Kit (Agilent) to delete the Nck gene from the pGEX2T-Nck construct.

2.2 Baculovirus production

The pBFDM constructs containing hD4R-1D4 genes were transformed into DH10BAC *E. coli* cells and plated on LB Agar with kanamycin, tetracycline, gentamicin, X-gal, and IPTG for a blue/white screen. A single white colony was grown in LB liquid media (plus kanamycin, tetracycline, and gentamicin) overnight and the resulting Bac-mid was isolated using a modified mini-prep kit (Qiagen) and isopropanol precipitation. The 10-15 µg of bac-mid was then transfected into $10x10^6$ Sf9 cells in 1 mL Grace's Insect Medium (Invitorgen) using 15 µL of Cellfectin II reagent (ThermoFisher Scientific). Cells were cultured at 27 °C without CO_2, rotating at 120-150 rpm. After 4 hours cells were supplemented with 4 mL Sf-900 II SFM (Gibco). 48 hours after transfection cells were supplemented with an additional 5 mL Sf-900 II SFM. 96 hours after

transfection 1 mL of FBS (Gemini BioProducts) was added to the media, and the P1 virus was harvested and filtered. The P2 virus was generated by infecting $3x10^8$ Sf9 cells (in 100 mL of Sf-900 II SFM) with 1 mL of P1 virus. 24 hours after infection, 100 mL of media were added. 72 hours after infection, 10 mL of FBS was added to the media, and the P2 virus was harvested and filtered. The P2 virus was then used for infection of HEK293T cells. The bac-mid and P1 virus are stable for up to 6 months. The P2 virus is also stable up to 6 months and can be snap frozen in liquid nitrogen and stored at -80 °C with little effect on infection efficiency.

2.3 HEK293T cell culturing and protein expression

HEK293T cells were grown in Dulbecco's Modified Eagle's Medium (DMEM) with GlutaMAX and 4.5 g/L glucose (Gibco) containing 10% FBS (source) in a 5% CO2 atmosphere at 37 °C. All cells used in this thesis were between passage number 3 and 25.

2.3.1 Transient transfection of HEK293T

For most experiments presented in this thesis, HEK293T cells were transiently transfected with Lipofectamine and Plus reagents. Exceptions are detailed below. For transfection in a 6-well plate, HEK293T cells were plated at

$7x10^5$ cells per well onto PDL-coated plates 1 day before transfection. On the day of transfection, 0.875 µg total of plasmid DNA was combined with 5 µL Plus Reagent (Invitrogen) in 200 µL of DMEM (no FBS) and incubated for 15 minutes. A mixture of DMEM (200 µL) and Lipofectamine reagent (Invitrogen, 10 µL) was then added to the DNA solution, and the mixture was incubated for an additional 15 minutes. The mixture was then added to the cells in a total volume of 1 mL. After 3-5 hours the cells were supplemented with 1 mL of DMEM with 20% FBS. 24 hours after transfection, the media was removed and replaced with 2 mL of DMEM with 10% FBS. Assays were initiated 48 hours after transfection. For transfection in a 10 cm dish, HEK293T cells were split at a ratio of 1:5 24 hours before transfection, and a similar protocol was performed using 3.5 µg DNA with 10 µL Plus reagent in 750 µL DMEM and 17 µL Lipofectamine reagent in 750 µL DMEM. The total volume of transfection was 4 mL, and the cells were supplemented with 4 mL DMEM with 20% FBS. 24 hours post-transfection the media was replaced with 8 mL of DMEM with 10% FBS.

For most sodium dodecyl sulfate polyacrylamide gel electrophoresis (SDS-PAGE) assays, the entire quantity of transfected DNA was pcDNA3.1-hD4R-1D4. For ubiquitination experiments, half the DNA was pcDNA3.1-hD4R-1D4 and half was 3X-FLAG-ubiquitin. For immunofluorescence experiments and qualitative PLA in HEK293T cells, 1/7 of the total DNA was pcDNA3.1-hD4R-1D4 and the remainder was empty pcDNA3.1 vector.

2.3.2 Treatment with inhibitors

For lysosome inhibition experiments, cells were grown in the presence of chloroquine diphosphate (Sigma) for 4 hours and SDF1α (PeproTech) for 3.5 hours before collection. For proteasomal inhibition experiments, cells were grown in the presence of bortezomib (Cell Signaling Technology, 1 pM to 1 μM) for 12 hours before collection. For the initial screening of degradation inhibitors, the following concentration of each inhibitor was included in the cell culture media for 6 hours before collection: 10 μM MG132 (Cayman Chemical), 10 μM ALLM (Santa Cruz Biotech), 10 μM Eeyarestatin I (Sigma), 10 μM bortezomib (Cell Signaling), 50 μM Chloroquine diphosphate (Sigma), 10 μL of DMSO.

2.3.3 Transient transfection of HEK293T for calcium flux assay

For calcium flux assays, HEK293T cells were transiently transfected directly into a poly-D-lysine (PDL)-coated 384-well plate (Corning) using Lipofectamine 2000 (Invitrogen). The day of transfection, 30 ng/well of DNA was incubated in 5 μL/well DMEM for 5 minutes. A mixture of 0.075 μL/well Lipofectamine 2000 and 5 μL/well DMEM was then added to the DNA solution and incubated for an additional 20 minutes. HEK293T cells were then trypsinized and resuspended in DMEM with 20% FBS, and 10 μL/well of cell solution (at $8x10^5$ cells/mL) was added to the DNA and Lipofectamine 2000 mixture. A total

of 20 µL of solution was then added to each well of the 384-well plates and incubated for 48 hours before the assay. The ratio of $G_{qi}5$ DNA to pcDNA3.1-hD4R-1D4 was 1:10.

2.3.4 Baculovirus infection of HEK293T

HEK293T cells were infected with pFBDM baculorvirus. On the day of infection, HEK293T cells were trypsinized and resuspended in 20% FBS DMEM. 1 mL cells (at $1.5x10^5$ cells/mL) was added to each gelatin-coated 35 mm glass bottom dishes No 1.5 (MatTek), followed by the addition of 0.8 mL of P2 virus and 0.2 mL DMEM (no FBS). Cells were incubated for 48 hours before processing.

2.4 Membrane preparations of HEK293T cells

For preparation of membranes containing hD4R-1D4, transiently transfected HEK293T cells were harvested via scraping with a rubber policeman in 1 mL PBS with aprotinin and leupeptin per 10 cm plate. Cells were then washed in an additional 1 mL per 10 cm plate PBS with aprotinin and leupeptin. Washed cell pellets were resuspended in hypotonic lysis buffer (1 mM Tris-HCl pH 6.8, 10 mM EDTA, 0.1 mM PMSF, and 10 µg/mL aprotinin and leupeptin) – approximately 1 mL buffer per 3 10 cm plates. Cells were then forced through a

23-guage needle 3 times, and a 26-guage needle 3 times. 1 mL of 35.5% (w/w) sucrose solution in buffer A (20 mM Tris-HCl pH 6.8, 150 mM NaCl, 1 mM MgCl2, 1 mM $CaCl_2$, 10 mM EDTA) was added to a TLS-55 centrifuge tube (Beckman). The lysed pellets were slowly layered on top of the sucrose solution. Tubes were centrifuged at 22,000 rpm at 4 °C for 20 min. The membrane layer was removed with a 23-guage needle and moved to TLA 100.3 centrifuge tubes (Beckman) and washed with 3 mL of buffer A with PMSF. Membranes were centrifuged at 60,000 rpm, 4 °C, for 30 minutes. The membrane pellet was then resuspended in 1 mL buffer A with PMSF using a 27-guage needle and washed again with 3 mL buffer A with PMSF and spun at 60,000 rpm, 4 °C, for 30 minutes. Pellets were frozen -20 °C.

2.5 SDS-PAGE and immunoblot

In order to perform SDS-PAGE analysis, transiently transfected HEK293T cells were washed in 1 mL per 10 cm plate PBS with protease inhibitors and then scraped from the plate in an additional 1 mL of PBS with protease inhibitors using a rubber policeman. After harvesting, cell pellets were solubilized with RIPA buffer (Thermo) with protease inhibitors, PMSF, NaF, Na_3VO_4, and benzonase at 4 °C for 1 hour. Lysates were spun at 10,000 rpm, 4 °C for 10 min and then normalized for total protein using the DC Protein Assay (BioRad). Normalized

lysates were combined with LDS load buffer (NuPAGE) and DTT (100 mM) and run on a 4-12% Bis-Tris gel (NuPAGE) at approximately 150 V.

2.5.1 Chemiluminescent detection of immunoblot

For detection with chemiluminescent reagents, gels were transferred to immobilon-P membrane (Millipore). The membranes were blocked with 5% milk and immunoblotted with 1D4 antibody (1:1000 dilution for the detection of hD4R-1D4) and anti-mouse-HRP secondary (Novex 16066). A sample processing control was analyzed by SDS-PAGE and immunoblotting with actin antibody (Abcam 8227, 1:10,000 dilution) and anti-rabbit HRP secondary (Novex 16110). Membranes were treated with ECL detection reagents (Thermo Scientific) prior to being exposed to HyBlot CL autoradiography film (Denville Scientific Inc.).

2.5.2 IR detection of immunoblot

For some experiments (including the chloroquine incubation assays, CØ mutant expression analysis, and variant protein levels), IR-conjugated secondary antibodies were used to detect immunoblots. In this case, a gel was transferred to immobilon-FL membrane (Millipore). The membrane was blocked with Odyssey blocking buffer (LI-COR) and co-incubated with 1D4 and actin primary

antibodies. Secondary antibodies were conjugated to IR probes (LI-COR) and scanned using the LI-COR Odyssey Sa.

2.5.3 Quantification of immunoblots

In order to measure the increase in protein expression upon bortezomib treatment, chemiluminescent immunoblots were quantified. Films were scanned, and Adobe Photoshop was used to convert images to gray scale. Using ImageJ, the relative area of each band on a single film was measured using the "analyze gels" function. The intensity of the 1 pM band for each mutant was normalized to 1 – resulting in the fold-change value for all higher concentration samples. The fold-change for each concentration in biological replicates (2 for wt, and 3 for KØ, STØ, and KSTØ) were averaged, and standard deviation was calculated. In order to insure that high expression mutants were being analyzed in the linear range of chemiluminescent detection, KSTØ hD4.4R-1D4 samples were diluted 10-fold before SDS-PAGE and immunoblot analysis. The trend of little to no increase in KSTØ protein levels with increasing bortezomib concentrations was maintained. Furthermore, 1 biological replicate for each mutant was also analyzed by SDS-PAGE and immunoblot analysis with IR detection. Quantification of IR detection immunoblots yielded the same trend observed for quantified chemiluminescent immunoblots.

2.6 Expression and purification of GST-DRIPs

pGEX2T constructs (GST alone, GST-Nck, or GST-Grb2) were transformed into BL21 DE3 Gold *E. coli* (Agilent) and plated onto LB-Agar plates with ampicillin. Bacteria were grown in liquid LB with ampicillin to an OD of approximately 0.6. Protein expression was then induced with the addition of 1 mM IPTG. After 2 additional hours of growth, cells were pelleted and frozen. In order to purify GST-DRIPs, cell pellets were thawed and resuspended in Lysis buffer (PBS with 1% Tween-20, & TritonX-100, 10 mM DTT, aprotinin, and leupeptin). The cell solution was sonicated and centrifuged. The resulting lysate was incubated with glutathione sepharose 4B slurry (Amersham) for 1 hour at room temperature, shaking. The beads were washed twice with lysis buffer before lysate binding. After lysate binding, the beads were washed three times with lysis buffer. In cases where specific elution of GST or GST-DRIPs was required, beads were incubated in 50 mM glutathione (reduced) for 30 minutes at room temperature, shaking. For DRIP IPs proteins were also concentrated using microcon spin columns (Sigma). In some cases, Grb2 was cleaved from the GST fusion by incubating GST-Grb2 attached to glutathione sepharose beads with thrombin overnight at room temperature.

2.7 Immunoprecipitations (IPs) and pulldowns

In order to detect protein-protein interactions as well as covalent protein modifications such as ubiquitination, proteins and protein complexes were purified from cellular lysates and membranes using IPs and glutathione-based pulldowns.

2.7.1 GST pulldowns

GST-DRIPs or GST alone were expressed and bound to glutathione beads, as detailed in section 2.7. After washing the GST-bound beads with lysis buffer to remove non-specific interactions, the coated beads were resuspeded in RIPA buffer. The coated beads were then combined with membrane preparations containing hD4R-1D4 (also resuspended in RIPA), and the bead and protein complexes were incubated overnight at 4 °C, rotating. The beads were then washed 3 times with RIPA buffer before non-specific elution of protein complexes with LDS and DTT for 1 hour at 37 °C, shaking. The quantities of GST-DRIPs were assay by SDS-PAGE and coomassie staining while the presence of hDR-1D4 was assayed by SDS-PAGE and immunoblot with 1D4 antibody.

2.7.2 1D4 IPs

HEK293T cells expressing hD4R-1D4 were washed in 1 mL PBS with protease inhibitors and then scraped from the plate in an additional 1 mL of PBS with protease inhibitors using a rubber policeman. After harvesting, cell pellets were solubilized with RIPA buffer (Thermo) containing protease inhibitors, PMSF, NaF, Na_3VO_4, and benzonase at 4 °C for 1 hour. Lysates were centrifuged at 10,000 rpm, 4 °C for 10 min and then normalized for total protein using the DC Protein Assay (BioRad). For ubiquitination IP assays, normalized lysates were incubated with limiting quantities of 1D4 antibody-coated protein G dynabeads (Invitrogen 10003D) incubated overnight at 4 °C. For hD4R-DRIP co-IPs, membrane preparations containing hD4R-1D4 were solubilized with RIPA and combined with purified GST or GST-DRIPs and 1D4-conjugated sepharose beads for overnight incubation a 4 °C. Beads were washed three times in RIPA buffer, and then the protein was eluted either specifically with 1D5 peptide (approximately 350 µg/mL peptide, on ice, 1 hour) or generally using LDS buffer and DTT (37 °C, 1 hour, shaking).

2.7.3 Distinguishing ester versus isopeptide ubiquitination

In order to identify ester bond ubiquitination via IP, HEK293T cells were co-transfected with hD4R-1D4 mutants and 3X-FLAG-ubiquitin. After IP with the 1D4

antibody, 1D5 eluates were treated with PNGaseF (NEB), and then split in half. One aliquot was incubated with 50 mM NaOH (pH 12.3) for 1 hour at 37 °C. The other aliquot was incubated with an equivalent volume PBS (pH 7.6) for 1 hour at 37 °C. The samples were then analyzed by SDS-PAGE and immunoblot with 1D4 and anti-FLAG antibodies.

2.7.4 myc IPs

Co-IP of GST-DRIPs with myc epitope-tagged hD4R constructs was performed similarly to 1D4 co-IP detailed in section 2.8.2, but using anti-myc 9E10 antibody (Sigma) and ultralink A/G resin (Pierce).

2.7.5 OLLAS IPs

In order to perform co-IP of GST-DRIPs with OLLAS epitope-tagged hD4R constructs, protein G dynabeads (Invitorgen) were coated with purified anti-OLLAS antibody. The beads were then used to isolate hD4R proteins by incubating solubilized membrane preparations with antibody-coated beads for 1 hour at 4 °C. The beads were then washed 3 times in RIPA buffer and combined with bacterial lysates containing GST-Grb2, purified GST-Grb2, or cleaved Grb2. Protein complexes were incubated with the beads overnight at 4 °C, shaking, before washing and elution with LDS and DTT for 1.5 hours at 37 °C.

2.8 Calcium flux assays

48 hours after transfection, HEK293T cells expressing hD4R-1D4 and $G_{qi}5$ were incubated with FLIPR calcium 4-assay kit dye for 1 hour in the tissue culture incubator. The fluorescence (Ex 488 nM, Em 530 nM) of the wells were then recorded, using Flex Station II 384 (Molecular Devices) while a dose curve of quinpirole was added to wells, in triplicate, from 0-100 nM (wt and KØ) or 0-500 nM (STØ and KSTØ). Normalized Max-Min fluorescence for each well was plotted for each dose curve, and a 4-parameter fit was used to calculate EC_{50} for each construct.

2.9 Immunofluoresence (IF)

The following conditions were optimized using IF: fixation conditions, blocking solution, primary antibody concentration, and antibody incubation times. The optimal protocol is listed here. HEK293T cells were transiently transfected as described in section 2.4.1. 24 hours after transfection, cells were trypsinized and plated on gelatin-coated coverslips. 24 hours after trypsinization, cells were washed with PBS containing calcium and magnesium and fixed in ice-cold methanol at -20 °C for 5 minutes. Samples were blocked with 0.5% BSA in PBS containing calcium and magnesium for 1 hour at room temperature. Primary antibodies against 1D4 and endogenous ubiquitin (Abcam 7780) were diluted in

the BSA blocking solution at 1:1000 and 1:250, respectively. Fixed cells were incubated with primary antibodies overnight at 4 °C before washing and incubation with anti-mouse-Alexa594 and anti-rabbit-Alexa488 secondary antibodies. After washing and staining with nuclear dye, cells were imaged at 60X magnification using the FSX100 microscope.

2.10 Proximity ligation assays (PLA)

Qualitative PLA in HEK293T cells was performed on HEK293T cells transiently transfected with wt hD4R-1D4. PLA was performed following DuoLink detection kit (Red, Sigma) recommendations, and the custom solutions for fixation, blocking, and antibody dilution detailed above for IF. Samples were mounted in Duolink mounting medium with DAPI (Sigma-Aldrich).

For quantitative PLA, HEK293T cells were infected with baculovirus as described in section 2.4.4. PLA was performed as described for qualitative PLA, but using the Abcam 134953 ubiquitin primary antibody at 1:1000 dilution and the DuoLink Detection Reagents Green (Sigma-Aldrich) kit. Anti-mouse-Alexa594 fluorescent secondary antibody was used to detect infected cells. Samples were mounted in Duolink mounting medium with DAPI (Sigma-Aldrich).

Mouse cortical neurons were cultured and transfected as described in section 2.12. After 48 hours, cells were washed twice in DPBS, fixed in 10% formalin for 10 min at RT, washed again with DPBS, and permeabilized with

0.4% CHAPSO for 10 min at RT. Cells were then processed following manufacturer's instructions for DuoLink Detection Reagents Far Red (Sigma-Aldrich), using 1D4 and anti-ubiquitin (Abcam 7780) primary antibodies. After PLA processing, cells were stained with phalloidin-Alexa488 in order to visualize neuronal architecture. Samples were mounted in Duolink mounting medium with DAPI (Sigma-Aldrich).

2.10.1 Microscopy of PLA

Confocal images of PLA-treated neurons were acquired with a Nikon A1RSi point scanning confocal inverted microscope using a 60X oil immersion objective. Excitation lasers of 405, 488, and 640 nm were used. Images from single confocal planes are shown. Image processing (cropping and adding of scale bars) were done in NIS Elements. The brightness and intensity of the images was adjusted in Adobe Photoshop CS6 and the final figure was made in Adobe Illustrator CS6.

For quantitaive PLA in HEK293T cells, 20X magnification Z-stack images (every 1.5 to 2 µm) were captured using FSX100 Olympus microscope. Exposure times were held constant while imaging samples within each experimental replicate. A total of four fields of view were obtained for each sample. All image processing was done using ImageJ. Nuclei were counted to obtain the total number of cells per image. Z-stacks were used to calculate maximum

projections, and the channels were split. The green channel was converted to a 32-bit grayscale image and the number of PLA dots were programmaticaly detected. To obtain the number of infected cells, 1D4 IF (red) and DAPI (blue) were used. Cells were considered transfected if a full ring of red surrounded the entire circumference of the blue nucleus.

2.10.2 Analysis of quantitative PLA

Quantifications of PLA in HEK293T cells were performed by Mariluz Soula under my mentorship. The average number of PLA signals per cell of a control-infected plate was considered the background signal. For each image, the average background signal (average of all four images obtained from the control infection) was multiplied by the total number of cells to give the total number of backround foci in the image. The number of background foci were subtracted from the total number of PLA signals in the image. The difference was divided by the number of infected cells to account for variable infection efficiencies, resultting in the average number of PLA signals per transfected cell per image. For each of the five biological replicates there were four fields analyzed for each mutant.

Data from the five replicates was pooled for each mutant giving a total of 20 fields analyzed. Using Prism, a one way ANOVA followed by Tukey's multiple

comparisons test was used to compare the mean of each group to that of every other group. Significance was determined by a p-value <0.05.

2.11 Culturing and transfection of mouse cortical neurons

Mouse cortical neurons were cultured by Birgitta Wiehager. Transfections were performed by Dr. Sophia Schedin-Weiss, with my input. Cortices were dissected from 16-17-day C57Bl/6 mouse embryos (E16.5). The isolated cortical neurons were seeded on the inner well of 35 mm glass bottom dishes No 1.5 (MatTek) that had been pretreated with PDL. The neurons were grown for 6 days *in vitro* (DIV) in selective Neurobasal medium containing 2% B27 (Invitrogen) and 1% L-glutamine (Invitrogen) at 37 °C in a cell incubator (humidified, 5% CO_2) until the day of transfection. Primary neurons were transfected with 0.2 µg pcDNA3.1-hD4R-1D4 using 0.6 µL Lipofectamine 3000 and 0.4 µl P3000. Growth medium was removed to keep a total volume of 70 µl during the initial stage of the transfection. After incubating for 4 hours, excess growth medium was added to the dishes.

2.12 Antibody production

The 1D4 antibody and the antibody against the *E.coli* OmpF Linker and mouse Langerin fusion Sequence (OLLAS) epitope were prepared by protein G purification of the culture media from hybridoma cell lines grown in a hollow fiber cartridge. This work was performed in collaboration with Manija Kazmi and Dr. W Vallen Graham.

2.12.1 Culturing 1D4 hybridoma

The 1D4 mouse hybridoma cell line was cultured in a hollow fiber cartridge (FiberCell) in serum-free DMEM with GluatMAX for 11 months, following FiberCell protocol instructions. Cultured media containing secreted antibody was harvested from the cartridge every 48-72 hours, depending on the glucose consumption rate of the cells. Harvested media was frozen and -20 °C.

2.12.2 Purifying 1D4 antibody

1D4 antibody was purified from cultured media using FPLC and a HiTrap Protein G column (GE healthcare). A total of 3 g of antibody was purified. Antibody was concentrated to 1 or 10 mg/mL and stored in PBS with 10% glycerol and 0.02% sodium azide at -80 °C.

2.12.3 Culturing OLLAS antibody hybridoma

The rat hybridoma cell line expressing the antibody against the OLLAS epitope was cultured in serum-free DMEM in a hollow fiber cartridge (FiberCell) for 6 months. Cultured media containing secreted antibody was harvested from the cartridge every 48-72 hours, depending on the glucose consumption rate of the cells. Harvested media was frozen and stored at -20 °C.

2.12.3 Purifying OLLAS antibody

Antibody recognizing the OLLAS epitope was purified from cultured media using FPLC and a HiTrap Protein G column (GE healthcare). A total of 300 mg of antibody was purified. Antibody was concentrated to 10 mg/mL and stored in PBS with 10% glycerol and 0.02% sodium azide at -80 °C.

CHAPTER 3: Proteasomal degradation of hD4R through isopeptide and ester ubiquitination

3.1 Degradation of hD4R

3.1.1 Mutation of hD4R lysine residues increases hD4R protein levels

hD4R contains four lysine residues, all of which are located on the cytoplasmic surface of the receptor (Fig 3-1). Three lysine residues are present in IC3, near but not within the VNTR polymorphism; the fourth lysine residue is in the cytoplasmic tail. The four lysine residues of hD4R are conserved in number and position in the mouse D4R homolog (Fig 3-1), while the rat homolog contains one additional lysine residue. In the most common variant of hD4R, hD4.4R, lysine residues comprise less than 1% of the total amino acids. All other human dopamine receptors have 2.25-5% lysine residues (Figure 3-1). Although the lysine residues in hD4R are conserved, their role in regulating hD4R was previously unappreciated.

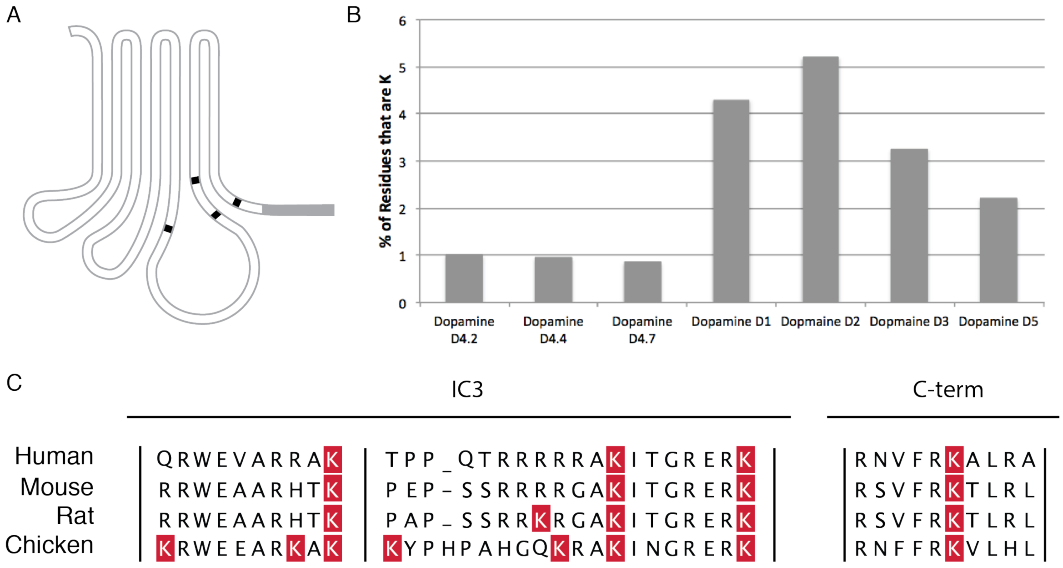

Figure 3-1 Lysine residues of D4R.

A) Graphic representation of the lysine residues (black) in hD4R. The 1D4 epitope is shown in gray. B) Comparison of percentage of residues that are lysine for hD4R compared to other human GPCRs. C) Conservation of lysine residues in D4R orthologs.

I proposed to label the four lysine residues of hD4.4R with chemical crosslinkers in order to identify hD4R DRIPs (described in further detail in Chapter 4). I created a mutant of hD4.4R-1D4 where all four lysine residues were mutated to arginine (KØ). KØ hD4.4R-1D4 was intended to serve as a negative control for crosslinking of hD4R/DRIP since lysine but not arginine residues can be labeled with N-hydroxysuccinimide (NHS). Unexpectedly, SDS-PAGE immunoblot analysis revealed that a much greater amount of KØ hD4.4R-1D4 is present in transiently transfected HEK293T cells compared with wild type (wt) hD4.4R-1D4 (Fig 3-2).

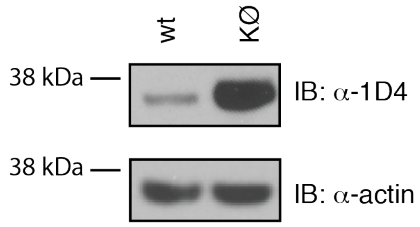

Figure 3-2 Protein levels of wt and KØ hD4R-1D4.

HEK293T cells transiently transfected with hD4R-1D4 constructs were solubilized. Normalized cellular lysates were subjected to SDS-PAGE and immunoblot analysis with 1D4. Sample processing controls were subjected to immunoblot with anti-actin antibody.

To verify that the change in protein level was due to the absence of lysine residues rather than the presence of arginine residues, lysine residues were mutated to alanine (Fig 3-3). Individual lysine to arginine mutations were also created, and these individual mutants show that there was an additive effect for

all four lysine residues (Fig 3-3). Based on the serendipitous observation of protein level changes after lysine mutation, it was hypothesized that lysine residues regulate protein levels of hD4R through ubiquitination and subsequent degradation.

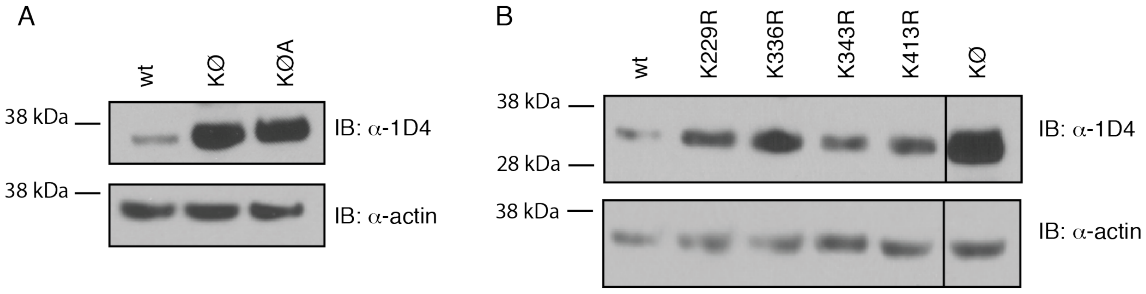

Figure 3-3 Lysine residues contribute additively to hD4R protein levels.

A) Mutation of lysine to arginine versus alanine. HEK293T cells transiently transfected with hD4R-1D4 constructs – wt, KØ, or a mutant where all four lysine residues were mutated to alanine (KØA) - were solubilized. Normalized cellular lysates were subjected to SDS-PAGE and immunoblot analysis with 1D4. Sample processing controls were subjected to immunoblot with anti-actin antibody. B) Individual mutations of hD4R lysine residues. HEK293T cells transiently transfected with hD4R-1D4 constructs containing a single lysine to arginine point mutant were solubilized. Normalized cellular lysates were subjected to SDS-PAGE and immunoblot analysis with 1D4. Sample processing controls were subjected to immunoblot with anti-actin antibody.

3.1.2 hD4R is degraded proteasomally but not lysosomally

Ubiquitination of lysine residues can mediate protein degradation through several pathways. In order to test whether and how wt hD4R protein is being degraded, cells expressing wt hD4.4R-1D4 were incubated with inhibitors to various protein degradation pathways. GPCRs that have been ubiquitinated at the plasma membrane are canonically degraded by lysosomes. Therefore, cells were incubated the lysosomal inhibitor chloroquine diphosphate. Cells were incubated with inhibitors of proteasomal degradation (bortezomib, MG132), the ERAD pathway (Eeyarestatin I), and calpain degradation (ALLM, MG132). Protein levels of wt hD4.4R-1D4 increased substantially upon incubation with bortezomib, a potent and specific inhibitor of the 26S proteasome. Chloroquine diphosphate had little effect on hD4.4R-1D4 protein levels (Fig 3-4).

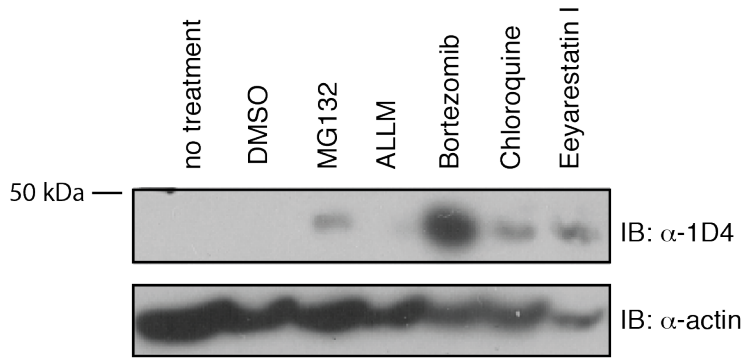

Figure 3-4 The effect of degradation inhibitors on hD4.4R-1D4 protein levels.

HEK293T cells expressing wt hD4.4R-1D4 were incubated with inhibitors to proteasome (10 μM MG132, 10 μM bortezomib), calpain (10 μM MG132, 10 μM ALLM), lysosome (50 μM chloroquine disphosphate), and ERAD (10 μM Eeyarestatin I) degradation pathways. Normalized cellular lysates were subjected to SDS-PAGE and immunoblot analysis with 1D4. Sample processing controls were subjected to immunoblot with anti-actin antibody.

Cells expressing wt hD4.4R-1D4 were incubated with increasing concentrations of lysosomal and proteasomal inhibitors (Figure 3-5). A five-fold increase in chloroquine diphosphate had no impact on hD4.4R-1D4 protein levels. The chemokine receptor CXCR4 is known to be ubiquitinated and lysosomally degraded after treatment with the agonist SDF1-α (Marchese and Benovic, 2001). Therefore CXCR4-1D4 was used as a positive control for lysosomal degradation assays. Cells expressing CXCR4 were incubated with SDF1-α in the presence or absence of chloroquine diphosphate (Figure 3-5). 250 μM chloroquine diphosphate was sufficient to inhibit SDF1-α-induced degradation of CXCR4, but had no effect on hD4R protein levels. These data suggest that constitutive hD4R degradation is not lysosome-dependent. Next, cells expressing wt hD4.4R-1D4 were treated with a dose curve of bortezomib. There was a striking positive correlation between bortezomib concentration and hD4.4R-1D4 protein levels. A quantification of two biological replicates of this bortezomib dose curve show an approximately five-fold increase in protein level for cells incubated with 1 μM bortezomib versus 1 pM. These data suggest that wt hD4R is constitutively degraded proteasomally, and not lysosomally in HEK293T cells.

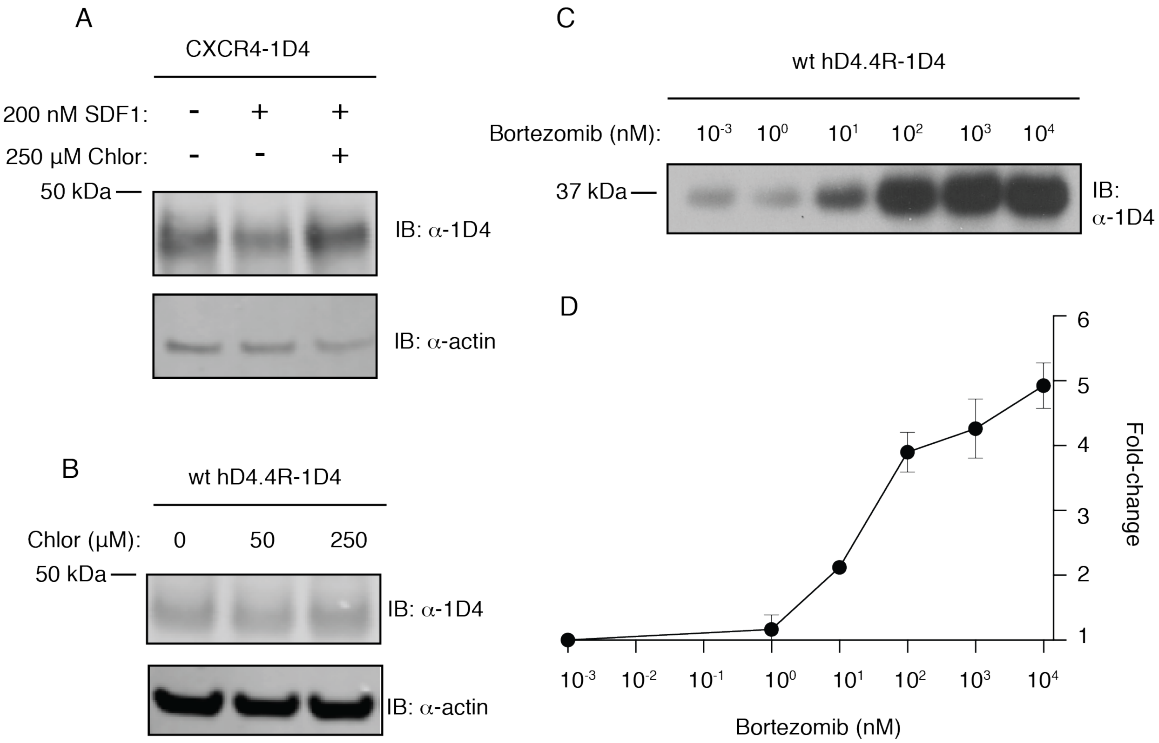

Figure 3-5 hD4R is degraded proteasomally but not lysosomally.

A) HEK293T cells expressing CXCR-1D4 were incubated with the agonist SDF1-α in the presence or absence of chloroquine diphosphate. Normalized cellular lysates were subjected to SDS-PAGE and immunoblot analysis with 1D4 and anti-actin antibody. B) HEK293T cells expressing wt hD4R-1D4 were incubated with increasing concentrations of chloroquine diphosphate. Normalized cellular lysates were subjected to SDS-PAGE and immunoblot analysis with 1D4 anti-actin antibody. C) HEK293T cells expressing wt hD4R-1D4 were incubated with increasing concentrations of bortezomib. Normalized cellular lysates were subjected to SDS-PAGE and immunoblot analysis with 1D4. D) Immunoblot bands from C, plus 1 additional replicate, were quantified via densitometry. The fold-change increase in intensity compared to the 1 pM bortezomib sample is plotted against bortezomib concentration.

To test whether low levels of wt hD4R protein were the result of post-translational degradation or low rates of protein expression, attempts were made to determine the half-life of wt hD4.4R-1D4 protein. Radioactive pulse-chase experiments as well as translation inhibition experiments were performed. However, neither protocol yielded clear or quantifiable results. Protein levels of wt hD4R before inhibition of translation or pulse-chase are already near the limit of detection by immunoblot and autoradiogram. These assays failed likely because they were dependent upon quantifying decreases in wt hD4R-1D4 protein levels. Experiments utilizing degradation inhibitors (Figure 3-4 and 3-5) and residue mutation (Figure 3-2 and 3-3) are not subject to this limitation as they increase wt hD4R protein levels and therefore have been used successfully.

3.1.3 Mutation of hD4R lysine residues does not disrupt receptor function

The KØ hD4.4R-1D4 mutant may be useful for understanding the role of lysine residues in hD4R degradation. However, residue mutation can lead to misfolding of the protein, which can disrupt protein levels. To confirm that the KØ hD4.4R-1D4 mutant was a biologically relevant control, KØ hD4.4R-1D4 function was tested through a GPCR signaling assay. I utilized the calcium flux assay, which quantifies the extent of intracellular calcium release after ligand binding and G protein activation. Calcium flux is canonically a consequence of GPCR activation through the of $G\alpha_q$ subunit. However, hD4R has been shown to bind

most strongly to $G\alpha_i$ and $G\alpha_o$ subunits. In order to more robustly measure the calcium flux of hD4R, a chimeric G protein was co-expressed with hD4R-1D4. The chimeric protein ($G_{qi}5$) is composed of the $G\alpha_q$ subunit fused to the five C-term residues of $G\alpha_i$ that mediate GPCR binding; $G_{qi}5$ was shown previously to boost calcium flux signaling for GPCRs whose primary interaction is not with $G\alpha_q$ (Coward et al., 1999). I optimized the use of this chimera in a high-throughput calcium flux assay previously adapted in the Sakmar lab. The results of calcium flux after activation of wt hD4.4R-1D4 by the agonist quinpirole in the presence or absence of the $G_{qi}5$ chimera is shown in Figure 3-6. Fluorescence levels increase after ligand addition at 20 seconds, indicative of calcium release in the absence of the $G_{qi}5$ chimera, but the maximum fluorescence level is greatly increased upon chimera expression. HEK293T cells expressing $G_{qi}5$ without co-expression of hD4.4R-1D4 show no fluorescence increase upon quinpirole stimulation.

With an optimized high-throughput calcium flux assay, hD4R activation was quantified using a dose curve of quinpirole, and an EC_{50} for the agonist with the receptor was calculated. A representative dose curve for wt hD4.4R-1D4 is shown in Figure 3-6. Repeated dose curves with wt hD4.4R-1D4 routinely yielded EC_{50} for quinpirole between 1 nM and 2 nM.

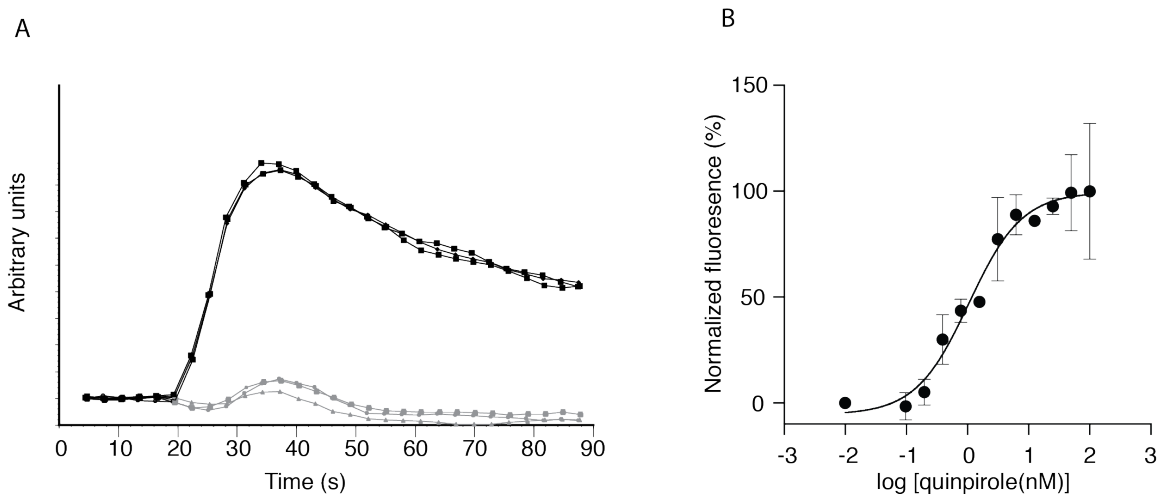

Figure 3-6 Calcium flux assay for wt hD4R with the ligand quinpirole.

A) Representative fluorescence during calcium flux assay for HEK293T cells expressing wt hD4R-1D4 in the presence (black) or absence (gray) of $G_{qi}5$ when stimulated with 2 μM quinpirole at 20 sec. B) Representative dose curve of wt hD4R-1D4 stimulated with quinpirole in the presence of $G_{qi}5$. EC_{50} of wt hD4R-1D4 is 1.1 nM.

Calcium flux assays with KØ hD4.4R-1D4 (Figure 3-7) show that the EC_{50} for quinpirole with KØ hD4.4R-1D4 was also between 1 and 2 nM. The fact that the efficacy of calcium flux is equivalent for the KØ and wt receptor suggests that the lysine mutations in KØ hD4.4R-1D4 do not substantially change the receptor folding or function, making it a biologically relevant control for studying lysine-mediated degradation of hD4R.

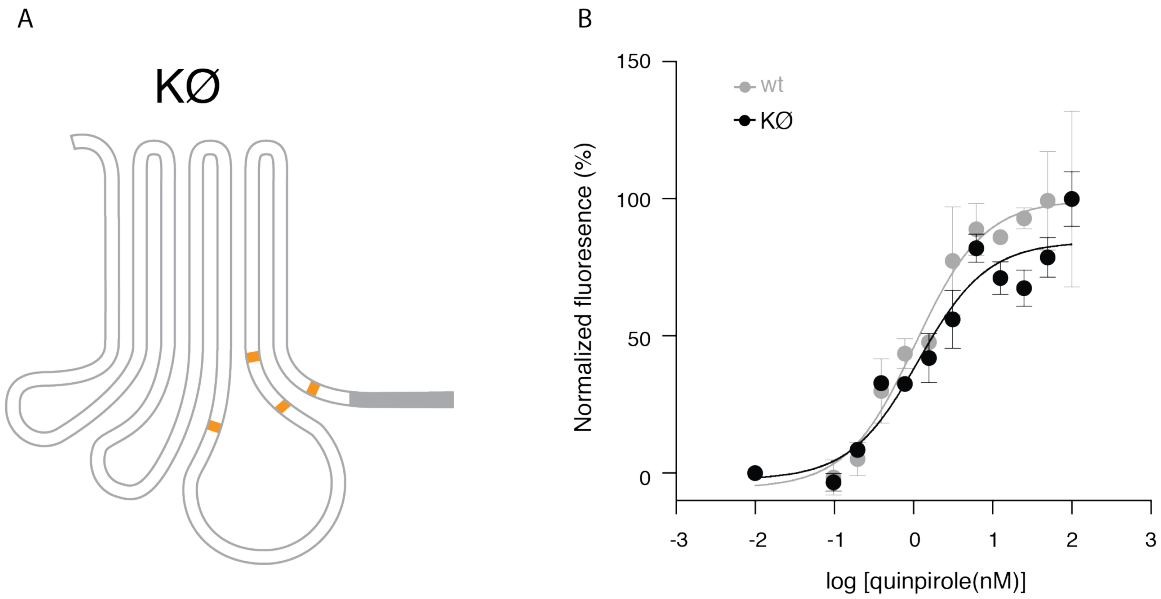

Figure 3-7 Calcium flux of KØ hD4R-1D4.

A) Graphic representation of the lysine to arginine mutations (orange) in KØ hD4R-1D4. The 1D4 epitope is shown in gray. B) Representative dose curve of wt hD4R-1D4 (gray) and KØ hD4R-1D4 (black) stimulated with quinpirole in the presence of $G_{qi}5$. EC_{50} of KØ hD4R-1D4 is 1.2 nM.

3.1.4 KØ hD4R is degraded proteasomally

The role of lysine residues in the proteasomal degradation of wt hD4.4R-1D4 was tested using the KØ hD4.4R-1D4 mutant. It was predicted that there would be little to no effect of bortezomib concentration on KØ hD4.4R-1D4 protein levels since the receptor should be unable to undergo lysine-mediated ubiquitination and degradation. Surprisingly, however, there was a dose-dependent increase in protein level for KØ hD4.4R-1D4 upon proteasome inhibition (Figure 3-8). Protein levels increased approximately 3-fold between 1 pM and 100 nM bortezomib. The total fold change of KØ hD4.4R-1D4 was less than that of wt receptor. These data support the hypothesis that lysine residues play some role in degradation of the receptor, but do not completely account for the massive degradation of wt hD4R.

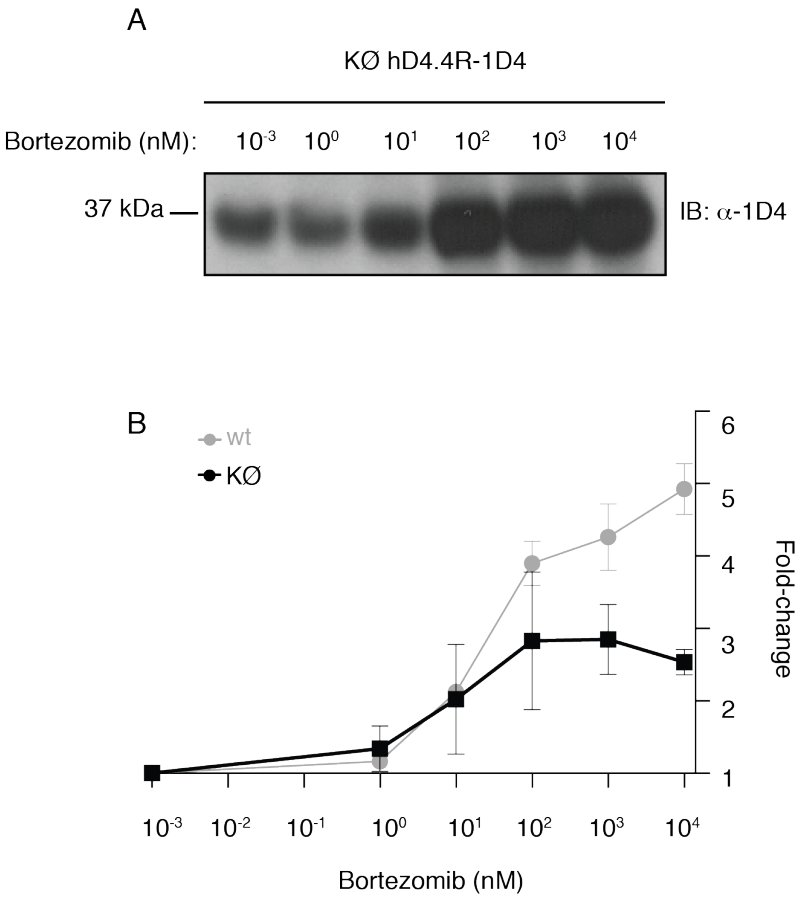

Figure 3-8 Proteasomal degradation of KØ hD4R-1D4.

A) HEK293T cells expressing KØ hD4R-1D4 were incubated with increasing concentrations of bortezomib. Normalized cellular lysates were subjected to SDS-PAGE and immunoblot analysis with 1D4. B) Immunoblot bands from A, plus 2 additional replicates, were quantified via densitometry. The fold-change increase in intensity compared to the 1 pM bortezomib sample for KØ hD4R-1D4 is plotted against bortezomib concentration. KØ hD4R-1D4 fold-change (black) is compared to wt hD4R-1D4 fold-change (gray).

3.1.5 Generation of serine and threonine null hD4R mutants

In the past decade it has become clear that residues other than lysine can be ubiquitinated (see section 1.5). One form of non-lysine ubiquitination is ester ubiquitination on serine or threonine residues. Ester bond ubiquitination is less thermodynamically stable than isopeptide bond ubiquitination on lysine residues, but has still been shown to promote protein degradation. In order to test if hD4R is ubiquitinated on serine and threonine residues through an ester bond, a cytoplasmically serine and threonine null mutant of hD4.4R was made. There are 38 total serine and threonine residues in hD4.4R. Mutations were limited to cytoplasmic residues, which would be accessible to enzyme cascade required for ubiquitination. 15 serine and threonine residues exist on the cytoplasmic surface of hD4.4R (Figure 3-9). Utilizing a multi-site mutagenesis strategy all 15 of cytoplasmic serine and threonine residues were to alanine. Additionally, a mutant that was null in cytoplasmic serine and threonine residues and null in lysine residues was made.

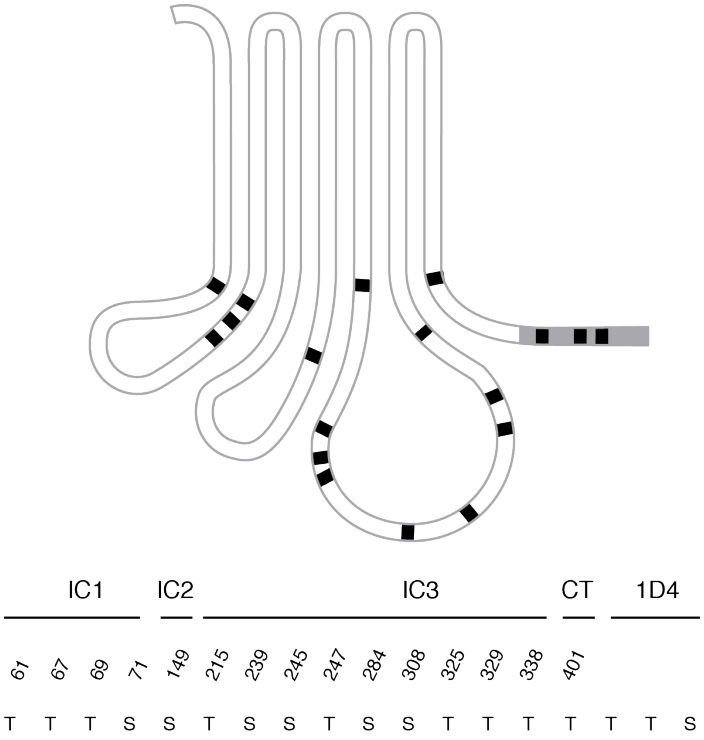

Figure 3-9 Cytoplasmic serine and threonine residues in hD4R-1D4.

Graphic representation of the cytoplasmic serine and threonine residues (black) and 1D4 epitope (gray) in hD4R-1D4. Residue number and identity are shown.

The mutants completely lacking cytoplasmic serine and threonine residues were incapable of fluxing calcium after stimulation with quinpirole, as shown in Figure 3-10. Shifts in the EC_{50} of a receptor mutant would suggest changes to ligand affinity or G protein coupling. However, such a dramatic inability to signal is likely due to massive changes in the protein including misfolding and potentially mistrafficking of the receptor. hD4.4R mutants which were unable to induce calcium flux in the presence of quinpirole were considered not physiologically relevant. Therefore, starting with the fully cytoplasmic serine and threonine null receptor, individual residues were mutated back to serine or

threonine in order to find the mutant that had the least number of potentially ubiquitinatable residues while still maintaining receptor function.

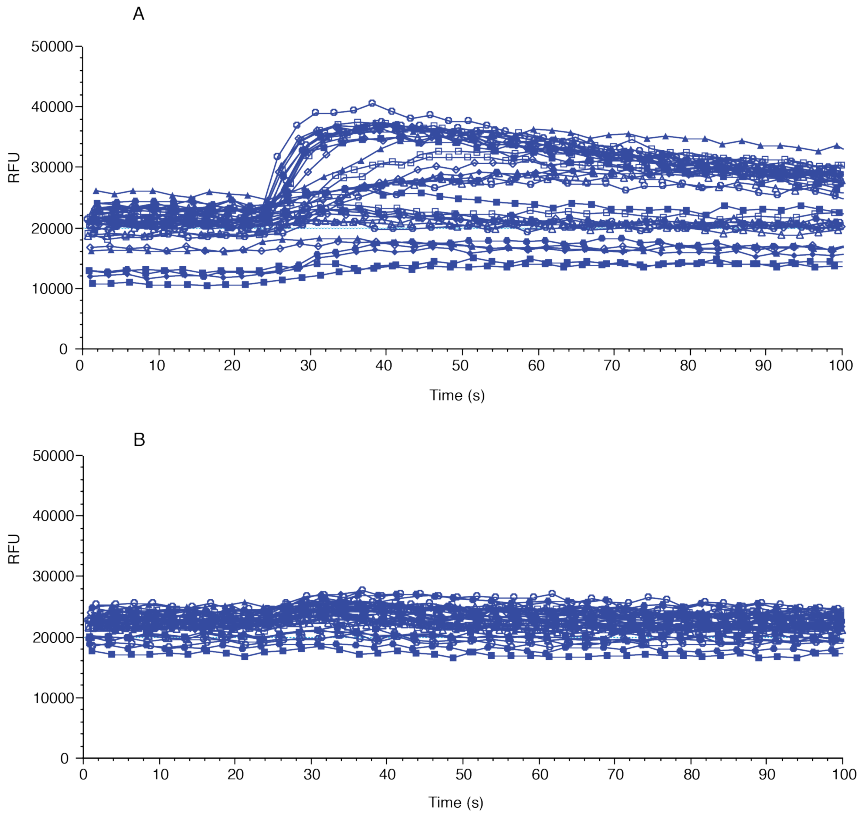

Figure 3-10 Calcium flux assay for wt hD4R-1D4 and serine and threonine to alanine mutants with the ligand quinpirole.

A) Representative calcium flux for wt hD4R-1D4 in the presence of $G_{qi}5$ when stimulated with 0-800 nM quinpirole at 20 sec. B) Representative calcium flux for hD4R-1D4 with 15 serine and threonine to alanine mutations, in the presence of $G_{qi}5$ when stimulated with 0-800 nM quinpirole at 20 sec.

Two threonine residues – T61 at the TM1/cytoplasm border and T401 at the TM7/cytoplasm border – were required to restore calcium flux capabilities to hD4.4R. It is possible that mutation of these residues disrupted receptor folding and membrane insertion. A receptor mutant where only 13 cytoplasmic serine and threonine residues were mutated to alanine were able to induce calcium flux, and this mutant is referred throughout this thesis as the serine and threonine null mutant (STØ hD4.4R-1D4) (Figure 3-11). It should be noted that it remains possible that the threonine residues at the TM/cytoplasm border could be ubiquitinated. Additionally, the exogenous 1D4 epitope tag on the hD4R C-term contains one serine and two threonine residues. A second mutant, KSTØ hD4.4R-1D4 was also generated; it combines the 13 cytoplasmic serine/threonine-to-alanine mutations with the four lysine-to-arginine mutations present in KØ hD4.4R-1D4 (Figure 3-11).

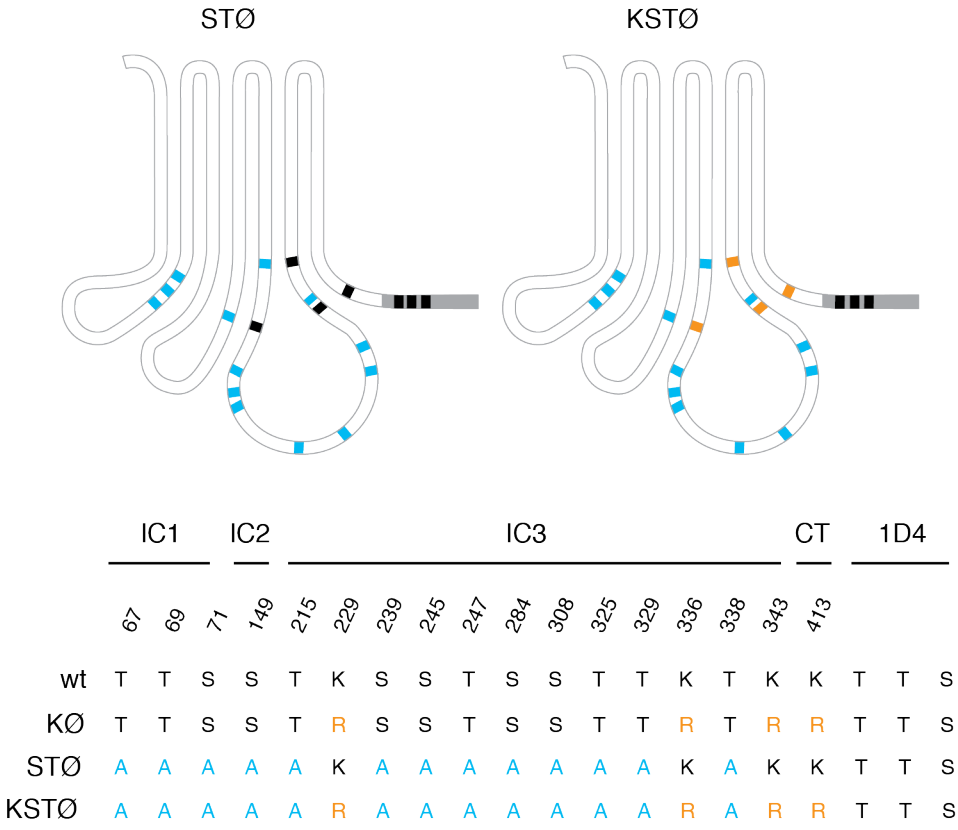

Figure 3-11 STØ and KSTØ mutants of hD4R-1D4.

hD4R mutants with potentially ubiquitinatable residues (black), lysine to arginine mutations (orange), and serine or threonine to alanine mutations (blue), and the 1D4 epitope (gray) denoted in graphical presentations (top) and residue number table (bottom).

3.1.6 STØ and KSTØ hD4R flux calcium

Calcium flux assays were performed for STØ and KSTØ hD4.4R-1D4. The EC_{50} for quinpirole with STØ hD4.4R-1D4 and KSTØ hD4.4R-1D4 were both approximately 10 nM (Figure 3-12). While these mutants are clearly capable of binding quinpirole and activating a G protein, their EC_{50} is shifted 10-fold compared with wt hD4.4R-1D4. This change may be due to a role for one or more of the mutated serine or threonine residues in mediating calcium flux independent of protein misfolding. It is possible that such substantial mutation of the cytoplasmic surface of the receptor disrupts G protein coupling, including pre-coupling of the G protein and GPCR, which has been proposed to modulate agonist affinity. Despite the difference in calcium flux performance and the presence of potentially ubiquitinatable residues, these mutants were deemed the best possible negative control for determining the role of serine and threonine residues in hD4R degradation.

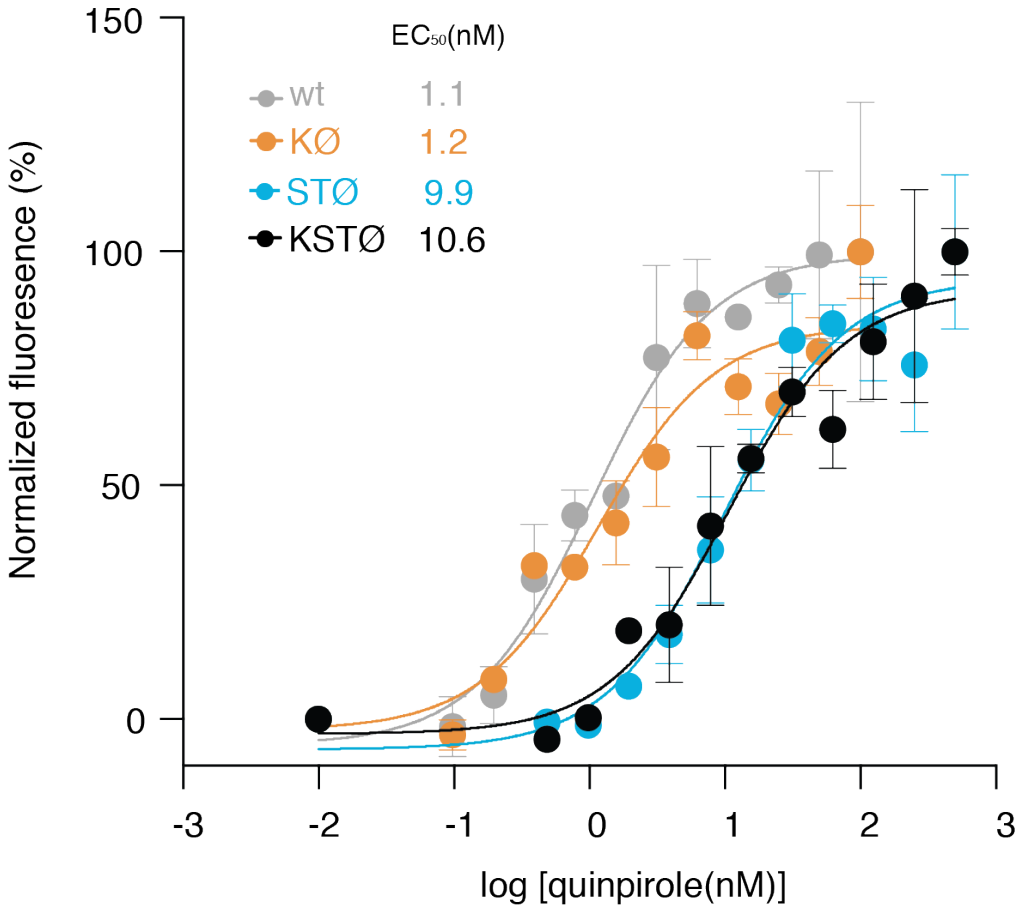

Figure 3-12 Calcium flux of hD4R-1D4 mutants.

Representative dose curve of wt hD4R-1D4 (gray), KØ hD4R-1D4 (orange), STØ hD4R-1D4 (blue), and KSTØ hD4R-1D4 (black) stimulated with quinpirole in the presence of $G_{qi}5$. EC_{50} of STØ hD4R-1D4 is 9.9 nM and EC_{50} of KSTØ hD4R-1D4 is 10.6 nM.

3.1.7 Mutation of hD4R serine and threonine residues increases hD4R protein levels

If ester ubiquitination regulates hD4R protein levels, then STØ and KSTØ mutants should have increased protein levels compared with wt hD4R. Therefore, the protein levels of STØ hD4.4R-1D4 and KSTØ hD4.4R-1D4 were compared with wt and KØ hD4.4R-1D4 (Figure 3-13). Strikingly, mutation of cytoplasmic serine and threonine residues in STØ hD4.4R-1D4 substantially increased protein levels, and an additive effect between lysine, serine, and threonine levels was observed in KSTØ hD4.4R-1D4. These data support the hypothesis that lysine, serine, and threonine residues in the wt receptor all regulate protein degradation.

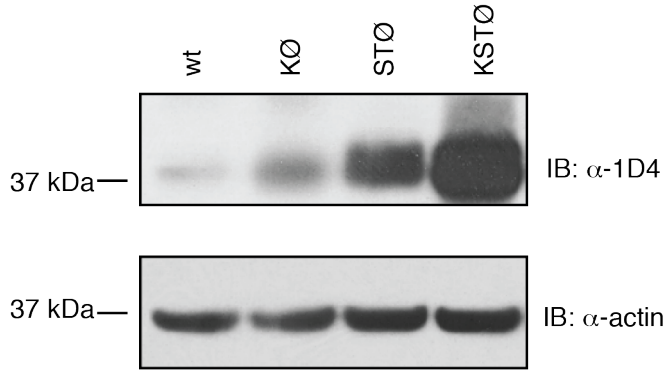

Figure 3-13 Protein levels of STØ and KSTØ hD4R-1D4.

HEK293T cells transiently transfected with hD4R-1D4 mutants were solubilized. Normalized cellular lysates were subjected to SDS-PAGE and immunoblot analysis with 1D4. Sample processing controls were subjected to immunoblot with anti-actin antibody.

3.1.8 Serine and threonine residues contribute to hD4R proteasomal degradation

The STØ hD4.4R-1D4 and KSTØ hD4.4R-1D4 mutants were also subjected to proteasome inhibition experiments. STØ hD4.4R-1D4 protein levels increased approximately 2-fold between 1 pM and 1 μM concentrations of bortezomib (Figure 3-14). The increase STØ hD4.4R-1D4 protein level upon bortezomib treatment was less than that of wt hD4R-1D4. The combined increase for STØ hD4.4R-1D4 (2-fold) and KØ hD4.4R-1D4 (3-fold) is approximately the total increase for wt (5-fold). Additionally, the KSTØ hD4.4R-1D4 mutant shows little to no increase in protein expression, as was originally anticipated for the KØ hD4.4R-1D4 mutant. The slight increase in protein levels at 1 μM could be due to ubiquitination of the serine and threonine residues present at TM/cytoplasm borders and/or the 1D4 epitope tag. Together, these bortezomib dose curves support the hypothesis that lysine, serine, and threonine residues all contribute to the proteasomal degradation of wt hD4R.

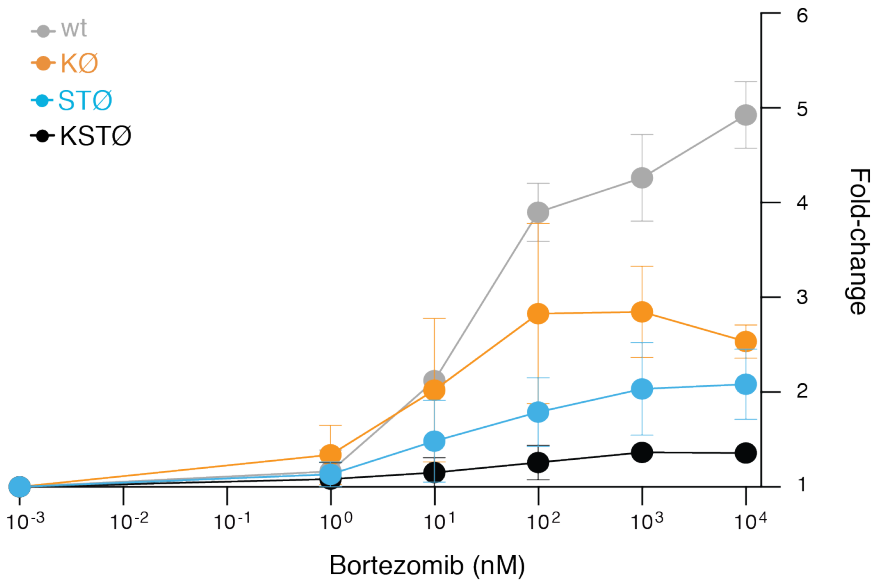

Figure 3-14 Proteasomal degradation of STØ and KSTØ hD4R-1D4.

HEK293T cells expressing hD4R-1D4 mutants were incubated with increasing concentrations of bortezomib for 12 hours. Normalized cellular lysates were subjected to SDS-PAGE and immunoblot analysis with 1D4. Immunoblot bands from 3 biological replicates were quantified via densitometry. The fold-change increase in intensity compared to the 1 pM bortezomib sample for STØ hD4R-1D4 and KSTØ hD4R-1D4 are plotted against bortezomib concentration. STØ hD4R-1D4 fold-change (blue) and KSTØ hD4R-1D4 fold-change (black) are compared to KØ hD4R-1D4 (orange) and wt hD4R-1D4 fold-change (gray).

3.1.9 Mutation of hD4R cysteine residues does not change hD4R protein levels

The fact that protein levels of KSTØ hD4.4R-1D4 are not substantially increased by bortezomib addition suggests that the majority of wt hD4R proteasomal degradation is due to ubiquitination on lysine, serine, and threonine residues and no others. However, the possibility that hD4R could be degraded after thioester ubiquitination of cysteine residues was still tested. There are two C-term cysteine residues on hD4R that are palmitoylated and required for proper receptor trafficking and function. The remaining cytoplasmic cysteine residues exist within the VNTR region. In order to simplify the mutagenesis approach the two repeat variant hD4.2R-1D4 was utilized for thioester ubiquitination studies. All 4 cytoplasmic, non-palmitoylated cysteine residues were mutated to alanine (CØ) (Figure 3-15). Protein levels of CØ hD4.2R-1D4 were not substantially increased compared with wt hD4.2R-1D4 (Figure 3-15). Therefore it is hypothesized that thioester ubiquitination of hD4R does not contribute to hD4R proteasomal degradation.

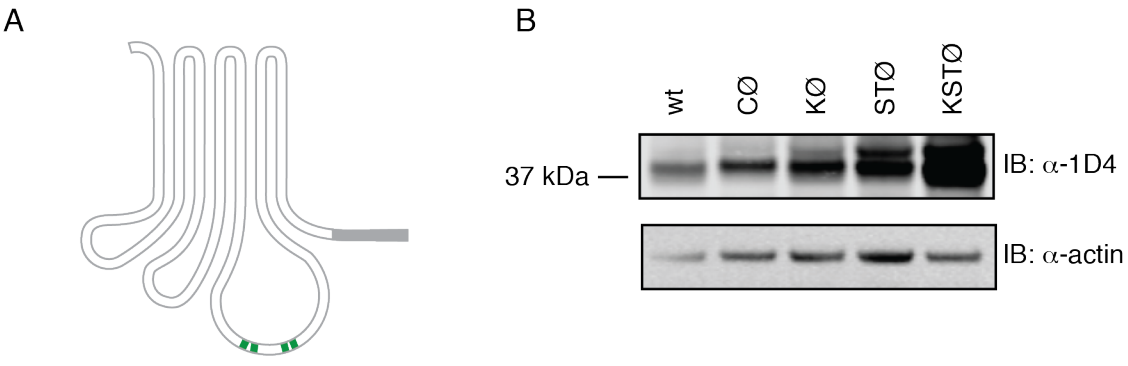

Figure 3-15 Protein levels of CØ hD4R-1D4.

A) Graphic representation of the cysteine to alanine mutations (green) in the CØ 2-repeat hD4R-1D4. The 1D4 epitope is shown in gray. B) HEK293T cells transiently transfected with 2-repeat hD4R-1D4 mutants were solubilized. Normalized cellular lysates were subjected to SDS-PAGE and immunoblot analysis with 1D4 and anti-actin antibody.

3.2 Ubiquitination of hD4R

3.2.1 IP demonstrates ubiquitination of hD4R

The data presented so far are consistent with ubiquitination mediating proteasomal degradation of hD4R; however, there is no evidence to show ubiquitin modification hD4R. IP experiments are standard in the field of ubiquitination biology, and were used to detect ubiquitination of hD4R. hD4.4R-1D4 was expressed in HEK293T cells and purified using the 1D4 antibody. The IP eluate was then tested for the presence of ubiquitin protein via SDS-PAGE and immunoblot. Initial experiments utilizing an antibody against endogenous ubiquitin for the immunoblot did not detect ubiquitin in 1D4 IP eluates. However, previous studies of GPCR ubiquitination were also unable to detect receptor modification using anti-ubiquitin antibodies. Instead, co-expressed a GPCR with a FLAG-tagged ubiquitin protein and detected ubiquitination using a anti-FLAG antibody (Marchese and Benovic, 2001). Therefore 3X-FLAG-ubiquitin was co-expressed with wt hD4.4R-1D4, and 1D4 IP eluates were analyzed by SDS-PAGE and immunoblot with anti-FLAG antibody (Fig 3-16). A high MW flag signal indicative of poly-ubiquitination was observed on the anti-FLAG immunoblot. These data support the hypothesis that wt hD4R is covalently modified by ubiquitination.

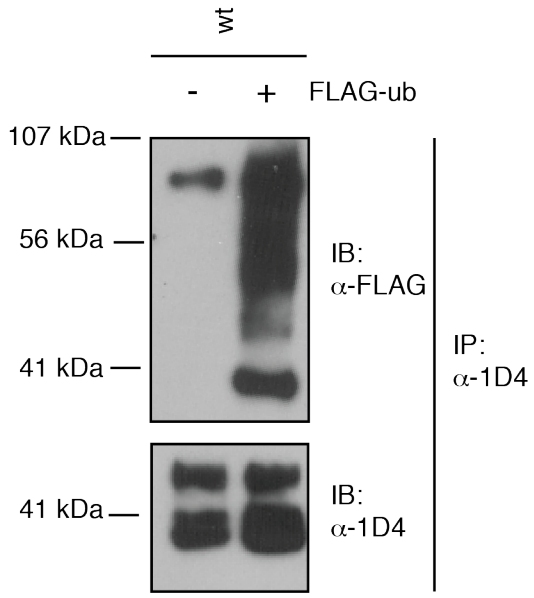

Figure 3-16 Detection of wt hD4R-1D4 ubiquitination via IP.

wt hD4R-1D4 was IP'd from HEK293T cell lysates and analyzed by SDS-PAGE and immunoblot with 1D4 and anti-FLAG antibody. Immunoblot with anti-FLAG antibody detects FLAG-ubiquitin.

3.2.2 IP demonstrates isopeptide and ester ubiquitination of hD4R

In order to determine the residues in wt hD4R to which ubiquitin is attached, the IP was repeated with KØ hD4.4R-1D4, STØ hD4.4R-1D4, and KSTØ hD4.4R-1D4, and eluates were treated with NaOH. Ester bonds that connect ubiquitin to serine or threonine residues are sensitive to base-catalyzed hydrolysis while the isopeptide bonds that attach ubiquitin to lysine residues are not. Therefore, if FLAG signal remains in the eluate after base treatment, it is

presumed to be the result of isopeptide-linked ubiquitin. Alternatively if FLAG signal disappears upon base treatment, it is presumed to be the result ester-linked ubiquitin. hD4.4R-1D4 were IP'd with limiting amounts of 1D4 antibody so that eluates for each IP contained approximately equal amounts of receptor, despite the substantially different levels of receptor in the cell lysate. Eluates were split and treated with NaOH (pH 12.3) or PBS (pH 7.6) and immunoblotted for both 1D4 and FLAG signal (Figure 3-17). In the case of wt hD4.4R-1D4, where lysine, serine, and threonine residues are present, FLAG signal was detected both in the presence and absence of NaOH. In the case of KØ hD4.4R-1D4, where serine and threonine are the only ubiquitinatable residues present, FLAG signal was diminished upon NaOH treatment, consistent with ester bond ubiquitination. The FLAG signal in STØ hD4.4R-1D4, where lysine residues are present, was maintained upon base treatment. Finally, the KSTØ hD4.4R-1D4 eluate showed little to no FLAG signal regardless of NaOH treatment, consistent with lack of ubiquitinatable residues. IP analysis suggests that ubiquitin molecules are attached to hD4R through isopeptide and ester bonds.

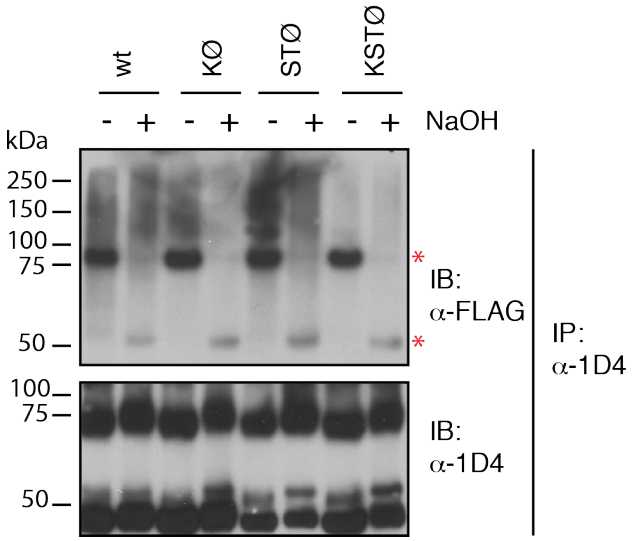

Figure 3-17 Detection of isopeptide bond and ester bond ubiquitination of hD4R via IP.

hD4R-1D4 mutants were IP'd from HEK293T cell lysates then treated -/+ NaOH before SDS-PAGE and immunoblot. Immunoblot with anti-FLAG antibody detects FLAG-ubiquitin. NaOH-sensitivity indicates the presence of ester-linked ubiquitination (at serine and threonine) and NaOH-insensitivity indicates isopeptide ubiquitination (at lysine). Red * show antibody bands from IP.

3.2.3 PLA demonstrates ubiquitination of hD4R

Detecting ubiquitination by IP has many drawbacks. PLA allows for detection of ubiquitination, but unlike IP, would also 1) provide information on the subcellular localization of ubiquitinated receptor 2) be adaptable to technically challenging systems like primary neurons and 3) allow for quantitative comparison between mutants. PLA has been utilized to detect PTMs, but has not previously been used to detect GPCR ubiquitination or ester ubiquitination of any

target proteins. To perform PTM detection via PLA, two primary antibodies raised in separate species are added to cells fixed on cover glass (in this case the 1D4 antibody and an antibody against endogenous ubiquitin). The cells are then incubated with orthogonal secondary antibodies to which DNA oligomers are attached. A solution containing DNA ligase enzyme and additional DNA oligomers is added to the cover glass. If the oligomers attached to the secondary antibodies against the two epitopes are within close proximity (theoretically 30 nm) the additional oligomers will bridge the antibody-attached oligomers forming a circular piece of DNA after ligation. Finally, a solution containing DNA polymerase, nucleotides, and fluorescent probes is added to the cover glass. If a circular piece of DNA has been formed, the polymerase will perform rolling circle amplification, and the fluorescent probes will adhere to the rolling circle amplification product (Figure 3-18). This will result in a dot detectable via fluorescence microscopy at the cellular location of the ligation product, inferred to be the location of ubiquitinated receptor (Söderberg et al., 2006).

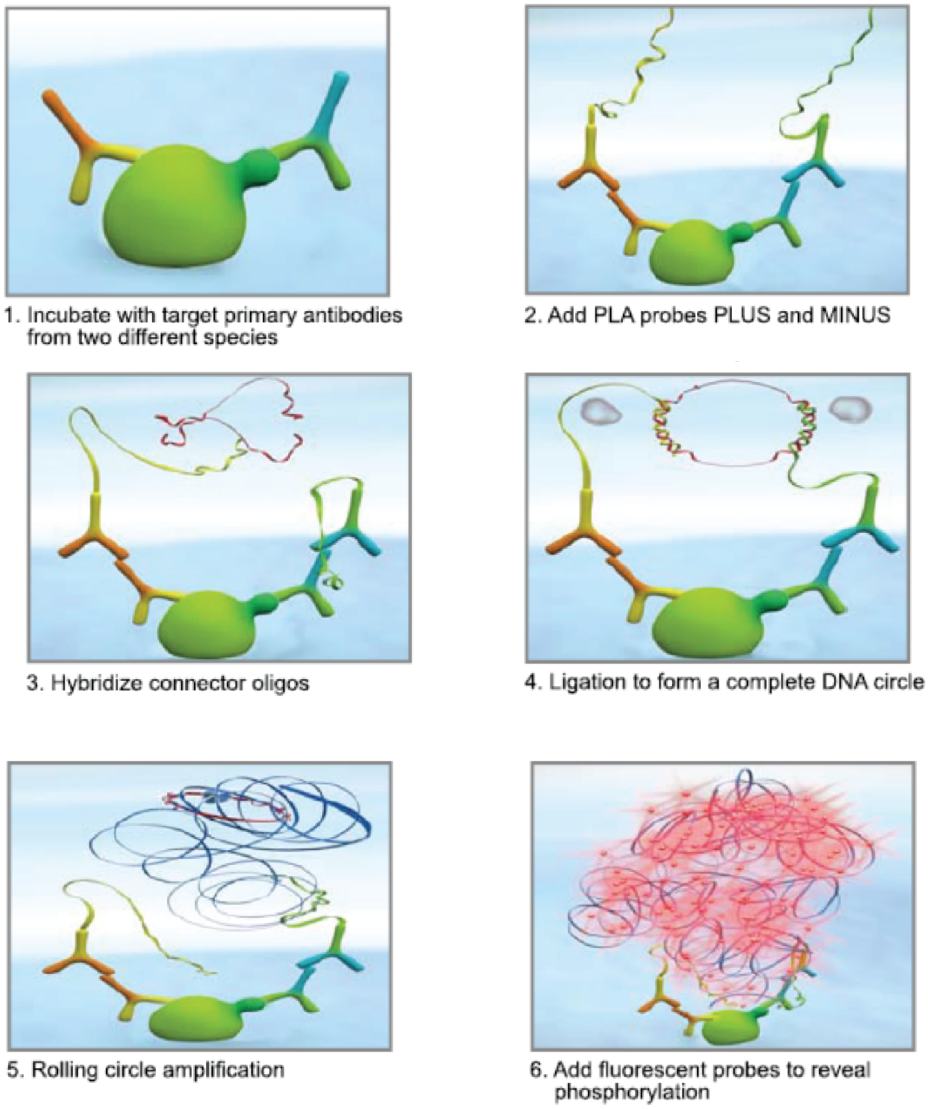

Figure 3-18 PLA protocol.

Adapted from OLINK Bioscience. The use of the 1D4 antibody and an antibody against endogenous ubiquitin in step 1 allows for detection of ubiquitinated hD4R in step 6.

Conditions of fixation, blocking, and antibody incubation for HEK293T cells expressing hD4.4R-1D4 were optimized using IF. IF with 1D4 and ubiquitin antibodies under optimized conditions are shown in Figure 3-19.

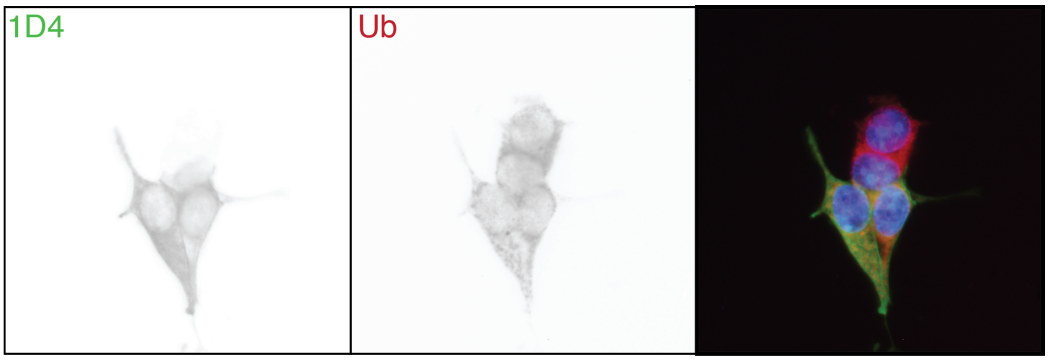

Figure 3-19 IF of wt hD4R-1D4 and endogenous ubiquitin.

HEK293T cells expressing wt hD4R-1D4 were fixed and incubated with 1D4 antibody (green), antibody against endogenous ubiquitin (red), and nuclear dye (blue).

3.2.3.1 Qualitative PLA in HEK293T cells

Qualitative PLA was performed on HEK293T cells transiently transfected with wt hD4.4R-1D4. Ubiquitinated wt hD4.4R-1D4 was detected, and the subcellular localization of the ubiquitinated receptors was determined. As shown in Figure 3-20, fluorescent dots representative of ubiquitinated receptor are present both 1) in an area close to the nucleus, potentially the ER, and 2) on or near the plasma membrane.

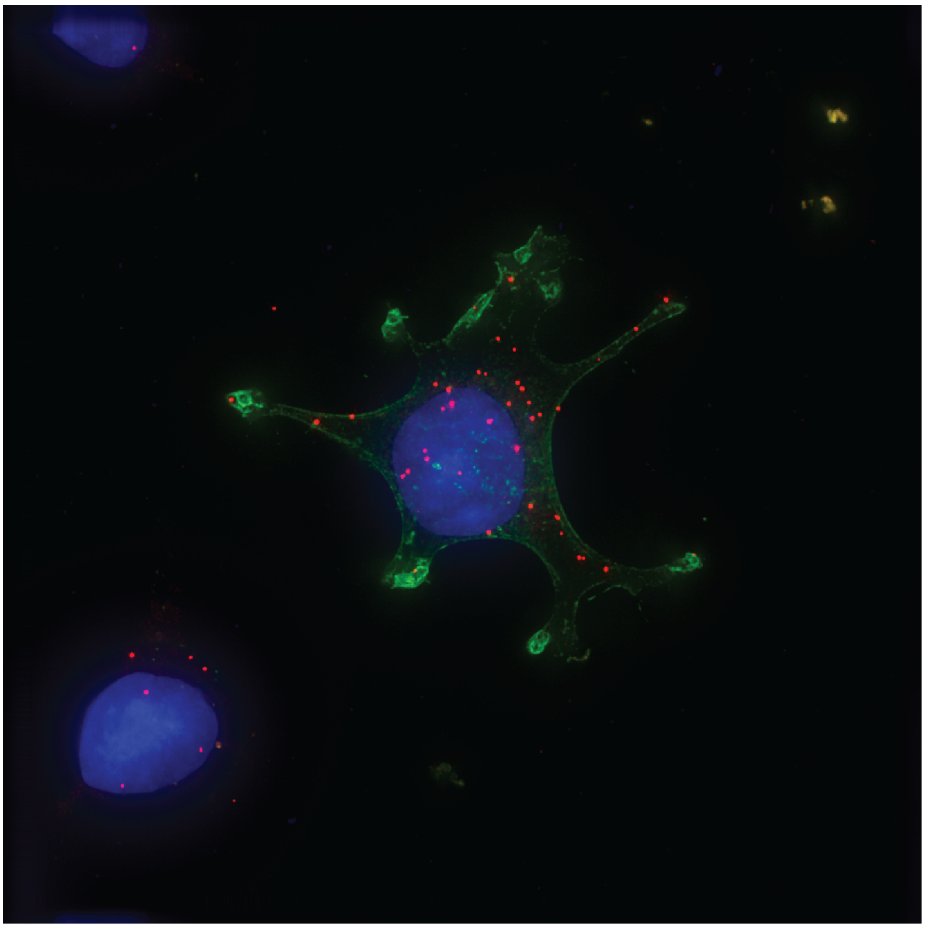

Figure 3-20 PLA of wt hD4R-1D4 in HEK293T cells.

HEK293T cells expressing wt hD4R-1D4 were fixed and incubated with 1D4 antibody and antibody against endogenous ubiquitin before performing PLA reaction. PLA dots (red) represent sites of close proximity between 1D4 and ubiquitin antibodies. A fluorescent secondary antibody recognizing 1D4 (green) was used to identify positively transfected cells. Cells were stained with a nuclear dye (blue). A maximum projection from the z-stack is shown.

3.2.3.2 Quantitative PLA in HEK293T cells

One potential criticism of the qualitative PLA shown in Figure 3-20 is that close proximity between 1D4 antibody and ubiquitin antibody could occur without covalent attachment between hD4R and ubiquitin. For example, an hD4R DRIP could be ubiquitinated, bringing the two antibodies within 30 nm, resulting in a fluorescent dot. In order to control for this possibility, quantitative PLA was performed on wt hD4.4R as well as hD4.4R mutants. PLA dots resulting from non-specific interactions would be present in cells expressing KSTØ hD4.4R-1D4, while dots resulting from covalent attachment of ubiquitin to hD4R should not. While it is possible that ubiquitination of the few remaining serine and threonine residues on the KSTØ hD4.4R-1D4 cytoplasmic surface (see section 3.1.5.), would result in PLA dots, IP experiments suggest that there is little to no covalent ubiquitination of this receptor mutant.

One of the greatest challenges for analyzing PLA on transfected cells is the low efficiency of lipid-based transfections. Transfected cells scarce in qualitative PLA samples, and for quantitative analysis high transfection efficiency was vital. Therefore a baculovirus infection system to efficiently deliver hD4R DNA into cells was developed. After cloning hD4.4R-1D4 open reading frames into the pFBDM plasmid viruses containing hD4.4R DNA were generated. A summer student from the Rockefeller University Summer Undergraduate

Research Fellowship program, Mariluz Soula, worked to optimize conditions for infecting HEK293T cells with baculovirus.

Using the baculovirus infection system instead of lipid-based transfection, Soula then performed quantitative PLA on HEK293T cells expressing wt hD4.4R-1D4, KØ hD4.4R-1D4, STØ hD4.4R-1D4, or KSTØ hD4.4R-1D4, or a negative control protein. Soula quantified the number of PLA dots per transfected cell for multiple fields of view for each condition. Some PLA dots were present, as before, in non-transfected cells. Single antibody experiments determined that this was due to lack of specificity of the endogenous ubiquitin antibody. The number of dots per transfected cell could not be calculated for the negative control since transfection efficiency could not be assessed. In order to account for non-specific PLA signal in the negative control, Soula subtracted the average number of dots per total number of cells in the negative control replicates from each hD4.4R-1D4 sample before calculating the final number of dots per transfected cell. Soula performed 4 biological replicates of this experiment, and the compiled data is shown in Figure 3-21. Despite the fact that there were still PLA dots in KSTØ hD4.4R-1D4 samples (even after controlling for the non-specific ubiquitin antibody), there was a statistically significant ($p<0.001$) difference in the number of dots for KSTØ versus wt hD4.4R-1D4. These data support the hypothesis that there is specific ubiquitin attachment to wt hD4R. Furthermore, the average numbers of PLA dots per cells transfected with STØ hD4.4R-1D4 and KØ hD4.4R-1D4 are intermediate – between KSTØ and wt - suggesting that both

isopeptide and ester bond ubiquitination are contributing to wt ubiquitination. The fact that KØ hD4.4R-1D4 PLA levels are most similar to wt and STØ levels are most similar to KSTØ may even suggest that the non-canonical ester bond modification is the predominant form of wt hD4R ubiquitination.

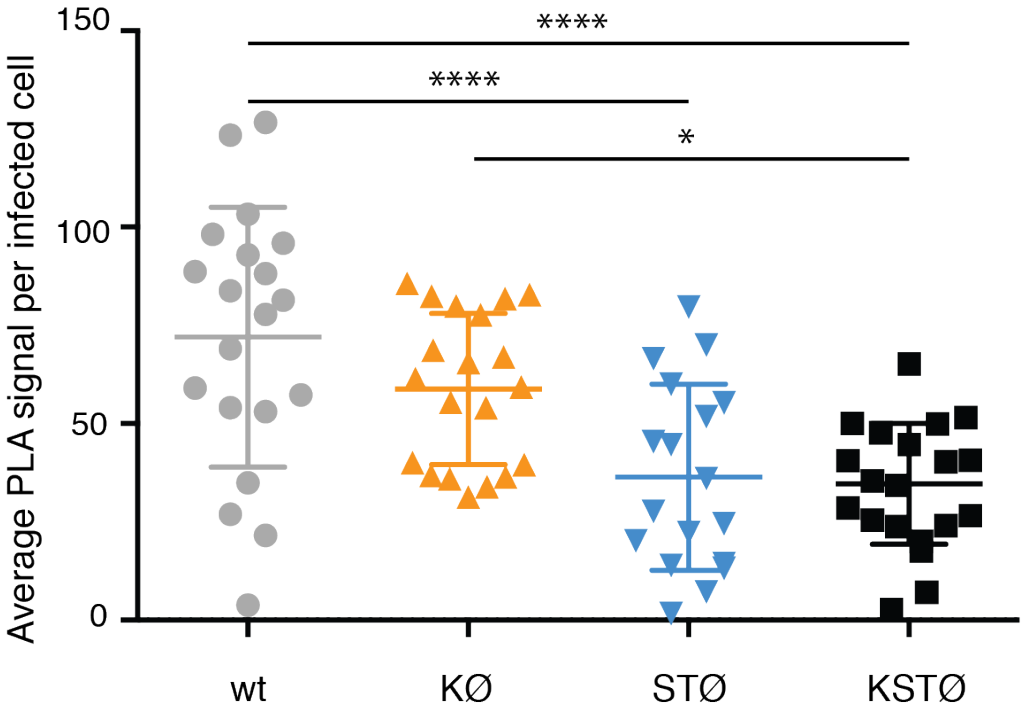

Figure 3-21 Quantitative PLA of hD4R-1D4 mutants.

HEK293T cells expressing wt hD4R-1D4 were fixed and incubated with 1D4 antibody and antibody against endogenous ubiquitin before performing the PLA reaction. The average number of PLA dots per infected cell are presented. Five biological replicates were performed per construct, totaling approximately 280 infected cells quantified for each. A one-way ANOVA followed by Tukey's multiple comparisons test was used to compare wt and mutant hD4R-1D4. **** represents $p \leq 0.001$ and * represents $p \leq 0.02$. All other comparisons (not indicated) had a $p \geq 0.05$.

3.2.3.3 Qualitative PLA in primary neurons

Data on hD4R ubiquitination has been generated in the HEK293T cell system. However, hD4R is predominantly expressed in the brain. Therefore a neuronal cell system would be more physiologically relevant for testing hD4R ubiquitination. Utilizing IP experiments would require dual transfection and substantial amounts of material, both of which would have been extremely difficult in primary neurons. PLA has been routinely used in neuronal systems (Schedin-Weiss et al., 2013). While visiting the center for Alzheimer's Research at the Karolinska Institutet, I worked with Sophia Schedin-Weiss to transfect cultured mouse cortical neurons with wt hD4.4R-1D4 and perform PLA to test for ubiquitinated receptor (Figure 3-22). These neurons expressed endogenous mD4R, and many ubiquitinatable residues are conserved between hD4R and mD4R, making this a suitably relevant cell system. As in the HEK293T system, PLA dots representative of ubiquitinated receptor appeared both in the soma of the neuron, likely in the ER, and also in the neurites, on or near the plasma membrane. These results demonstrates that while the consequences of hD4R ubiquitination so far have been shown in a model tissue culture system, the modification also occurs in primary mouse neurons.

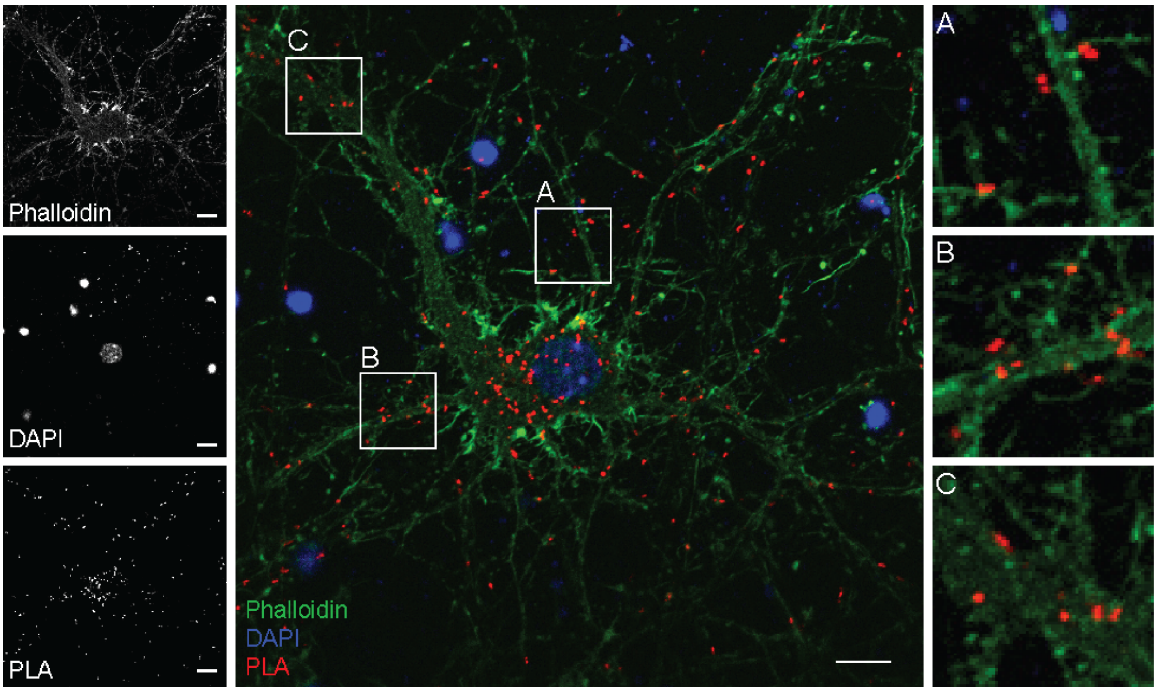

Figure 3-22 hD4R ubiquitination in neurons.

PLA analysis shows ubiquitinated wt hD4R-1D4 in transfected primary mouse cortical neurons. Phallodin (green) and DAPI (blue) show cellular architecture, while the PLA dots (red) represent ubiquitinated hD4R. Single channel isolations are shown on the left, a full-scale merge is shown in center, and on the right are zoomed-in views of areas highlighted in the center panel (A-C). Scale bars represent 10 µm.

3.3 Influence of VNTR on hD4R degradation

3.3.1 The 2-, 4-, and 7-repeat hD4R variants are degraded via isopeptide and ester bond ubiquitination

hD4R contains a VNTR in the human population. Ubiquitination and degradation have been shown in the most common variant, hD4.4R. To determine if protein degradation was consistent between hD4.4R and other common variants, multi-site mutagenesis was used to create a KØ, STØ, and KSTØ mutant of hD4.2R-1D4 and hD4.7R-1D4. Intriguingly, despite the fact that the 2, 4, and 7 repeat variants have drastically different numbers of total amino acids, the number of ubiquitinatable residues remains nearly constant. The most prevalent 4-repeat allele encodes for two serine residues within the 64 amino acid long repeat region. The most prevalent 2-repeat allele encodes for one serine residue within its 32 amino acid long repeat region, and the most prevalent 7-repeat allele encodes for one serine residue within its repeat region, despite containing 112 total amino acids total. Since the number of ubiquitinatable residues is similar between variants, it was hypothesized that 1) degradation via isopeptide and ester bond ubiquitination is consistent for all variants and 2) degradation of this receptor may be quite biologically important.

Protein levels for the wt and null mutants for each hD4R-1D4 variant were determined via SDS-PAGE and immunoblot. As shown in Figure 3-23, the

qualitative protein level patterns for receptor mutants are consistent between variants. For the 2-repeat, 4-repeat, and 7-repeat variants, wt protein levels were low and levels were increased in KØ and STØ. For the 2-repeat and 4-repeat variant there was an additive effect of lysine, serine, and threonine residues as seen in the very high protein levels for KSTØ. When normalizing for loading (as assayed by the actin immunoblot), it appears there is not an additive effect of lysine, serine, and threonine mutation for the 7-repeat variant. The reason for such a difference is not clear.

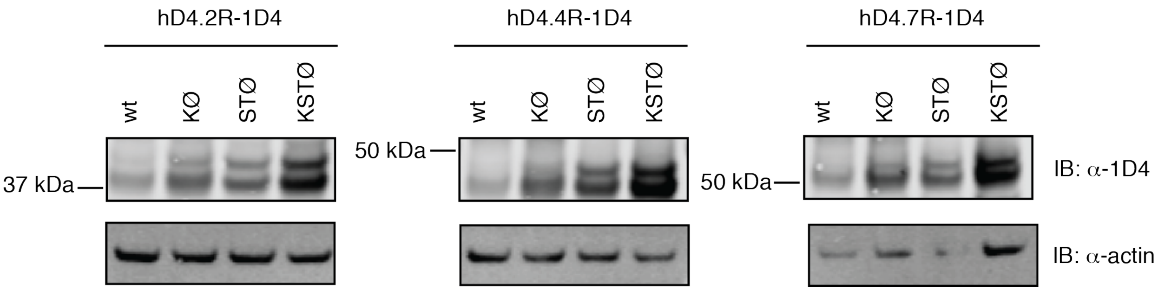

Figure 3-23 Protein levels of hD4R-1D4 VNTR variants.

HEK293T cells transiently transfected with wt, KØ, STØ, and KSTØ mutants of 2-repeat (hD4.2R-1D4), 4-repeat (hD4.4R-1D4), and 7-repeat (hD4.7R-1D4) variants were solubilized. Normalized cellular lysates were subjected to SDS-PAGE and immunoblot analysis with 1D4. The membrane was also probed with anti-actin antibody.

3.3.2 The VNTR repeat region is required for serine and threonine-mediated hD4R degradation

In order to understand the role that the repeat region might play in regulating receptor protein levels, KØ, STØ, and KSTØ mutants were created for a “no repeat” variant hD4.NRR-1D4. This variant does not exist in the human population, but was previously created to determine the role of the hD4R repeat region in G protein binding (Kazmi et al., 2000). This variant is missing not only the two serine residues within hD4.4R repeat region, but also four more serine/threonine residues flanking the repeat region. As shown in Figure 3-24, while KØ hD4.NRR-1D4 levels are greater than those of wt hD4.NRR-1D4, the STØ hD4.NRR-1D4 mutant has protein levels similar to wt hD4.NRR-1D4 levels. Additionally, KSTØ hD4.NRR-1D4 levels are equivalent to KØ hD4.NRR-1D4. This suggests that isopeptide but not ester bond ubiquitination is responsible for degradation of the no repeat variant.

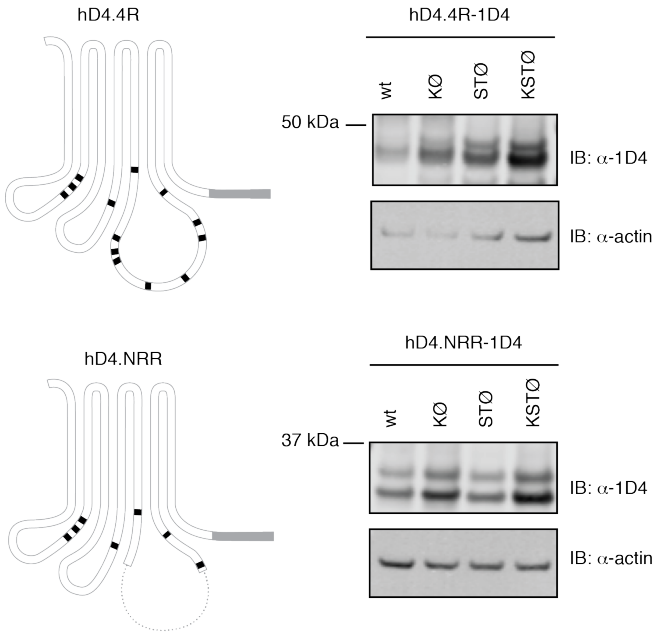

Figure 3-24 Protein levels of hD4R-1D4 no repeat variant.

Graphical representation of serine and threonine residues (black) in hD4R variants (left). HEK293T cells transiently transfected with wt, KØ, STØ, and KSTØ mutants of hD4.4R-1D4 (top) or hD4.NRR-1D4 (bottom) were solubilized. Normalized cellular lysates were subjected to SDS-PAGE and immunoblot analysis with 1D4 and anti-actin antibody (right).

The proteins levels of receptor mutants of the no repeat variant were quantified and graphed along with the protein levels of the 2-repeat, 4-repeat, and 7-repeat variant (Figure 3-25).

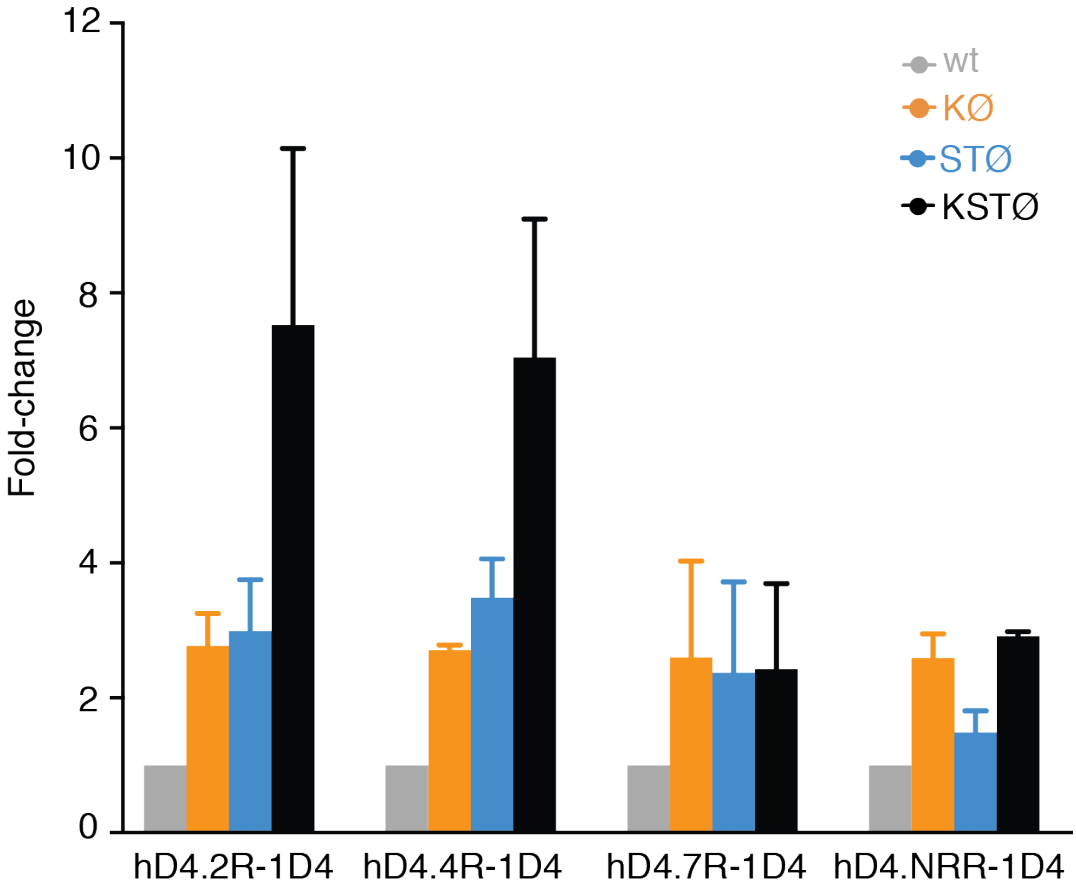

Figure 3-25 Quantification of hD4R-1D4 variant protein levels .

Immunoblots from Figure 3-23 and 3-24 were performed in triplicate. The protein levels were normalized for actin. The fold-change in mutant protein level compared to wt was calculated for each variant.

Again, it appears that the no-repeat variant is subject to degradation via isopeptide bonds but not ester bonds. There are multiple possible explanations for this observation. First, it could be that the only serine and threonine residues responsible for degradation of hD4.4R are the six (or a subset thereof) that are deleted in hD4.NRR. In order to test this possibility, a hD4.4R-1D4 mutant where only those six residues were mutated to alanine (Repeat:STØ hD4.4R-1D4) was created. If only those six residues were important for ester ubiquitin-based degradation, then the Repeat:STØ hD4.4R-1D4 mutant should have protein levels equal to STØ hD4.4R-1D4. However, as shown in Figure 3-25, Repeat:STØ hD4.4R-1D4 had levels closer to wt. In fact, the inverse of this mutant (where the six residues in and near the repeat region of hD4.4R are left intact and only the other cytoplasmic serine and threonine residues are mutated [NonRepeat:STØ hD4.4R-1D4]) has protein levels similar to STØ hD4.4R-1D4.

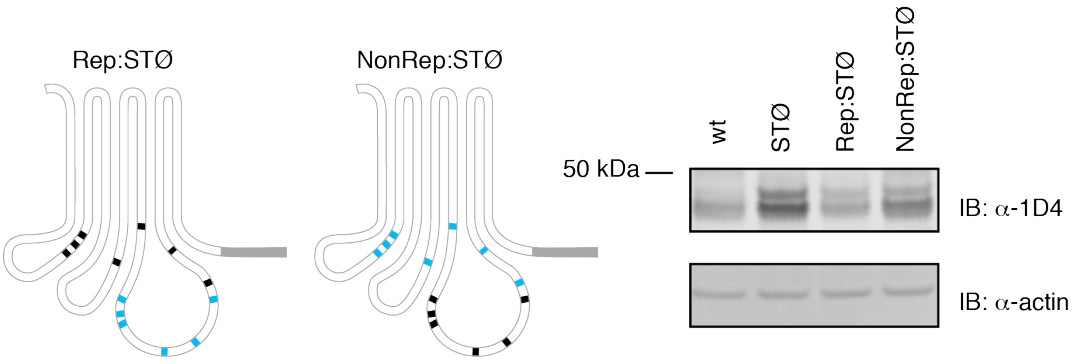

Figure 3-26 Role of hD4R repeat region in protein level regulation. .

Graphical representation of partial serine/ threonine to alanine mutants (blue, left). Residues were mutated exclusively in the repeat region (Rep) or exclusively outside the repeat region (NonRep). HEK293T cells transiently transfected with mutants of hD4.4R-1D4 were solubilized. Normalized cellular lysates were subjected to SDS-PAGE and immunoblot analysis with 1D4. The membrane was also probed with anti-actin antibody (right).

Based on these data, the most likely explanation for the difference between STØ mutants of hD4.4R and hD4.NRR is that the repeat regions – but not necessarily the ubiquitinatable residues within them -- are required for ester ubiquitin-based degradation of hD4.4R. For example it may be possible that the ubiquitination machinery required for ester ubiquitination (but not isopeptide ubiquitination) binds in the repeat region of hD4R.

CHAPTER 4: hD4R Dopamine Receptor Interacting Proteins (DRIPs)

4.1 DRIP GST pulldowns

The initial goal of my thesis research proposal was to gain a greater understanding of hD4R biology by identifying hD4R DRIPs. Specifically, I was interested in performing comparative, quantitative proteomics to identify hD4R DRIPs that interact non-uniformly with the hD4R variants. hD4R variants, – either 2 repeat, 4 repeat, 7 repeat, or the no repeat control – would be incubated with neuronal lysates, and interacting proteins would be co-purified with the receptors. Eluates of the purifications would be digested with trypsin, and labeled with isobaric tags before the samples were pooled. The isobaric tag would ensure that any given peptide present in each of the original eluates would have the same mass to charge ratio in the first round of mass spectrometry (MS). During the second round of MS a unique mass identifier would be released, providing a relative ratio of the given peptide in the original samples (Figure 4-1). Mass spectrometry analysis would provide 1) a list of hD4R DRIPs and 2) hD4R variant binding preferences for every DRIP.

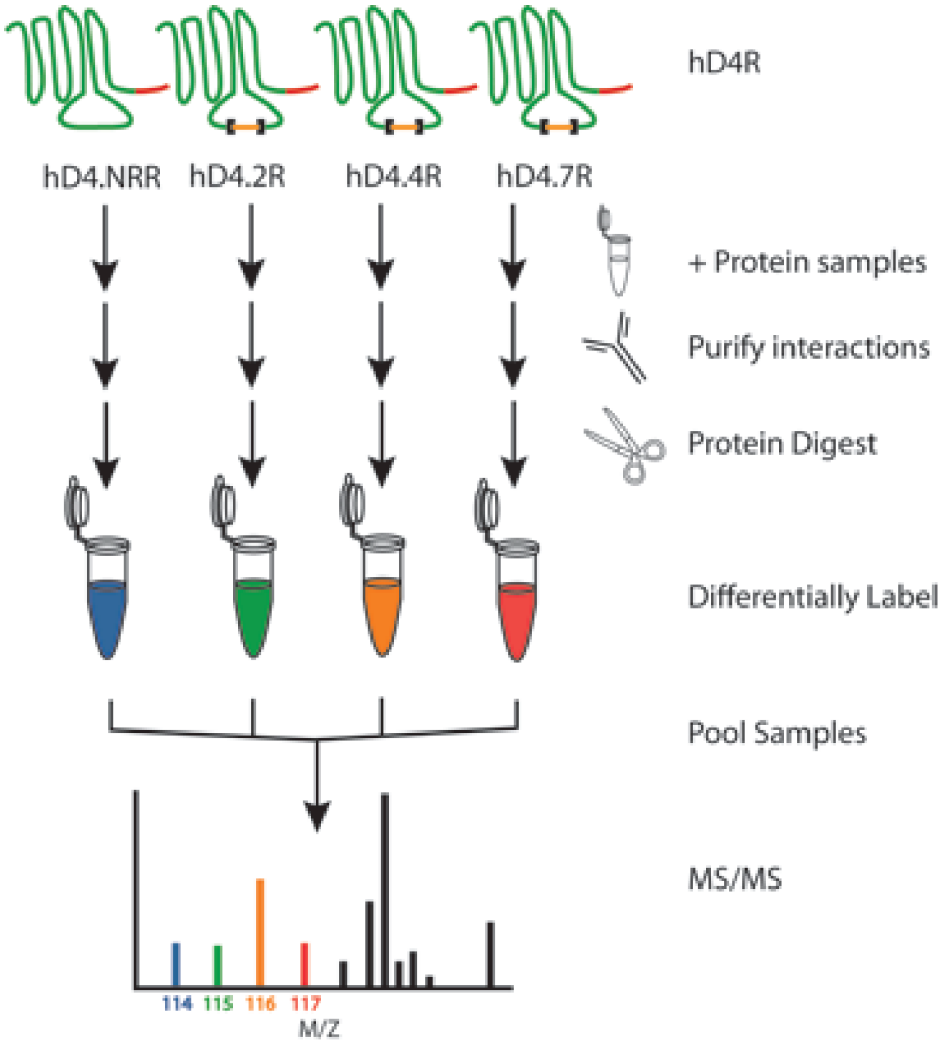

Figure 4-1 Identification of hD4R DRIPs using quantitative MS/MS.

hD4R variants would be isolated and incubated with neuronal lysates. Interacting proteins would then be purified by co-IP, and eluates would be digested and labeled with an isobaric tag (various colors). Samples would be pool and submitted to MS/MS analysis. Results would include a list of hD4R DRIPs and their relative ratios in the eluates.

4.1.1 Model DRIPs: Grb2 and Nck

As a first step to identify novel hD4R DRIPs, pulldowns were performed with hD4R and known DRIPs. The adaptor proteins growth factor receptor-bound protein 2 (Grb2) and non-catalytic region of tyrosine kinase adaptor protein (Nck) are both SH3 domain-containing proteins that have been previously shown to interact with the IC3 region of hD4R (John Oldenhof et al., 1998). Specifically, Grb2 and Nck interact with the SH3 binding domain that borders the VNTR region of hD4R. Oldenhof and colleagues found no difference in the affinity of Grb2 and Nck for VNTR variants. In order to facilitate identification and purification of DRIPs, GST-DRIP fusion proteins were created (Figure 4-2). A GST alone negative control, which should not interact with hD4R, was also generated. Protocols for GST-DRIPs expression in *E. coli* and GST-DRIP purification with glutathione sepharose were optimized.

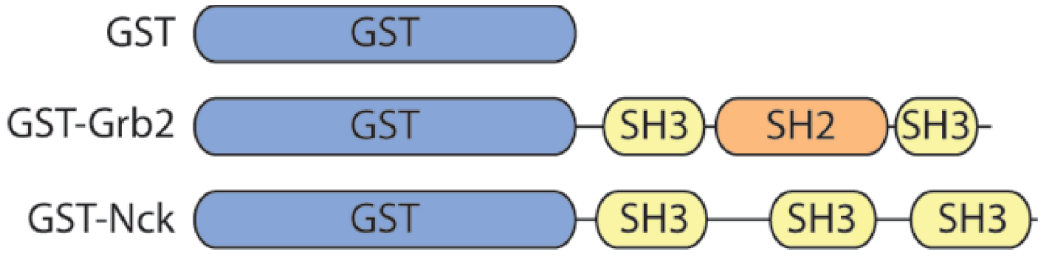

Figure 4-2 Model hD4R DRIPs.

GST-Grb2 and GST-Nck constructs were used to optimize hD4R DRIP co-IP conditions. GST alone served as negative control.

4.1.2 hD4R stabilized mutants

Purified hD4R protein was also required to perform hD4R/DRIP pulldowns. The 4-repeat variant hD4.4R-1D4 is the most common variant and was used for the first hD4R/DRIP pulldowns. Receptors needed to be isolated from intact cells so that the cytoplasmic domains of hD4R could be exposed to neuronal lysate proteins. However, simply solubilizing the cells could disrupt receptor folding. Therefore, membrane fractions of cells expressing hD4.4R-1D4 were isolated via ultracentrifugation in the presence of 35.5% sucrose solution (NEVILLE, 1960).

A substantial amount of purified receptor was required for hD4R/DRIP pulldowns. The wt hD4.4R-1D4 protein exists in low abundance in transfected HEK293T cells. However, a version of hD4R where all 4 lysine residues are mutated to arginine (KØ hD4.4R-1D4) exists at much higher levels in cell lysates (Fig. 3-2). Furthermore, functional studies show that KØ hD4R-1D4, which is stabilized against proteasomal degradation, is functional. In the calcium flux assay, KØ hD4.4R-1D4 and wt hD4.4R-1D4 have indistinguishable EC_{50} values for the ligand quinpirole (Fig. 3-7).

The lysine-to-arginine mutations in KØ hD4.4R-1D4 do not disrupt receptor function in calcium flux assays. Therefore it was hypothesized that these mutations would also not significantly disrupt most hD4R/DRIP interactions. In order to test the hypothesis, a preliminary pulldown between the purified GST-DRIPs and two variants of hD4.4R-1D4: wt and KØ was performed. Membrane

preparations from cells expressing either wt hD4.4R-1D4 or KØ hD4.4R-1D4 were added to sepharose beads with pre-bound GST-DRIPs. After the receptors and DRIPs were incubated for 2 hours, the beads were washed, and the bound proteins were eluted. The amount of GST-DRIP in each eluate was assayed via coomassie stained SDS-PAGE, and the presence of hD4.4R-1D4 was assayed via immunoblot with the 1D4 antibody. As shown in Figure 4-3, wt hD4.4R-1D4 and KØ hD4.4R-1D4 behaved similarly in the GST-DRIP expression assay. Neither receptor was detected in the eluates of glutathione beads coated in GST alone or GST-Nck. Both receptors were detected in the eluate of GST-Grb2-coated glutathione beads, at levels approximately proportional to the level of receptor input. It was concluded that wt and KØ hD4.4R-1D4 have a similar protein-protein interaction profile, including with the known DRIP Grb2. Since KØ hD4.4R-1D4 was equivalent in function and also had substantially increased protein levels, all further hD4R/DRIP experiments were performed with the KØ hD4.4R-1D4 protein.

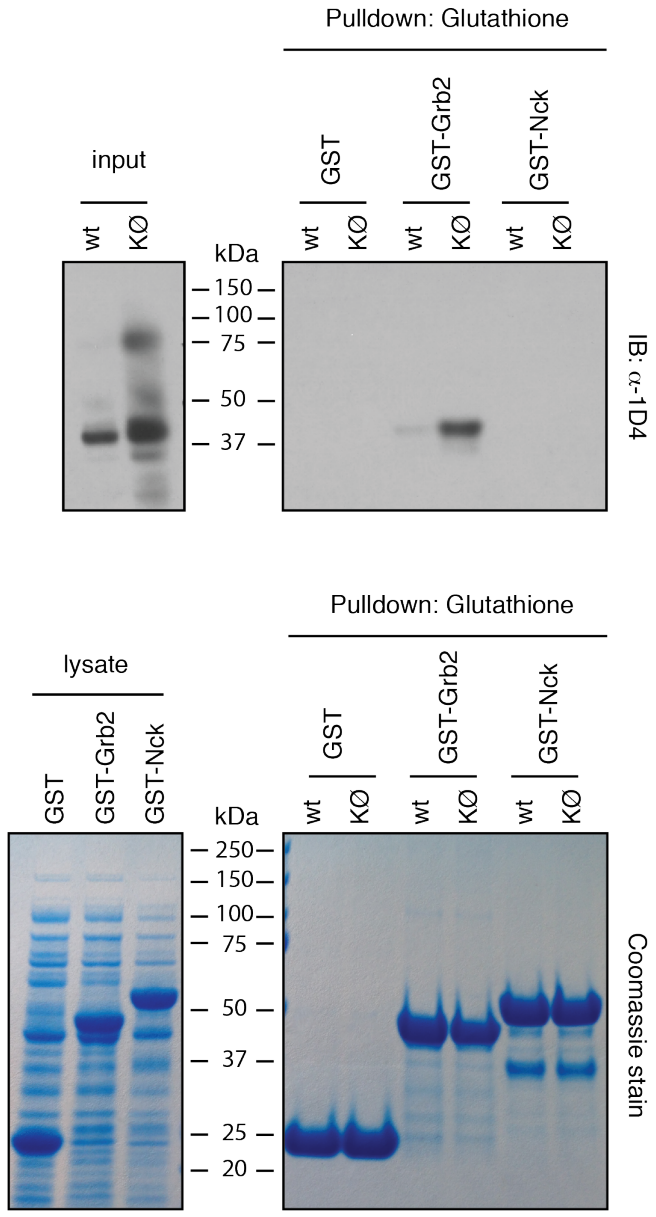

Figure 4-3 Using stabilized KØ hD4R-1D4 for DRIP identification.

Membrane preparations from cells expressing wt or KØ hD4R-1D4 were combined with glutathione beads coated in GST alone or GST-DRIPs. Eluates were tested for receptor presence via 1D4 immunoblot (top, IB) and GST or GST-DRIP levels via coomassie stain (bottom).

4.1.3 GST pulldowns

In order to further validate the hD4R/Grb2 interaction, glutathione beads coated in GST-DRIPs were used to pull down hD4R variants. As shown in Figure 4-3, hD4.4R-1D4 does not interact with the GST tag alone. Therefore, the successful pulldown of hD4.4R-1D4 with GST-Grb2-coated beads is likely due to direct interaction between Grb2 and hD4.4R-1D4. In order to confirm that the site of interaction between Grb2 and hD4R facilitating the pulldown is in fact the SH3 binding domains in hD4R IC3, pulldowns were conducted a “no repeat” (hD4.NRR-1D4) variant. The hD4.NRR-1D4 receptor has a deletion in IC3 that includes the repeat region and the flanking SH3 binding domain. The hD4.NRR receptor is not a naturally-occurring variant, but rather a laboratory-made control. GST-DRIP-coated gluthatione beads were incubated with membrane preparations from cells expressing either hD4.4R-1D4 or hD4.NRR-1D4. The GST-DRIP purification was evaluated by coomassie-stained SDS-PAGE while the hD4R/DRIP interaction was assayed by SDS-PAGE and immunoblot with the 1D4 antibody. Despite approximately equal receptor and DRIP input, hD4.4R-1D4 was eluted with GST-Grb2 while hD4.NRR-1D4 was not (Figure 4-4). Therefore, it was concluded that the point of interaction of Grb2 with hD4.4R-1D4 is in the region missing in hD4.NRR-1D4 – the SH3 binding domain and/or the repeat region.

GST-Nck did not appear to have a robust interaction with hD4R-1D4 (Figure 4-4). Oldenhof and colleagues did find that Nck had lower affinity than Grb2 for hD4R, and some long exposures suggested that there might be some hD4R-1D4 present in GST-Nck pulldowns (John Oldenhof et al., 1998). More importantly, Oldenhof and colleagues used different methods and buffers for their identification of hD4R DRIPs, which may explain the difference in results for GST-Nck and hD4R interactions. Based on the robust, SH3 domain-dependent interaction between hD4.4R-1D4 and GST-Grb2, GST-Grb2 was used as a model DRIP to optimize conditions for the identification of novel hD4R DRIPs.

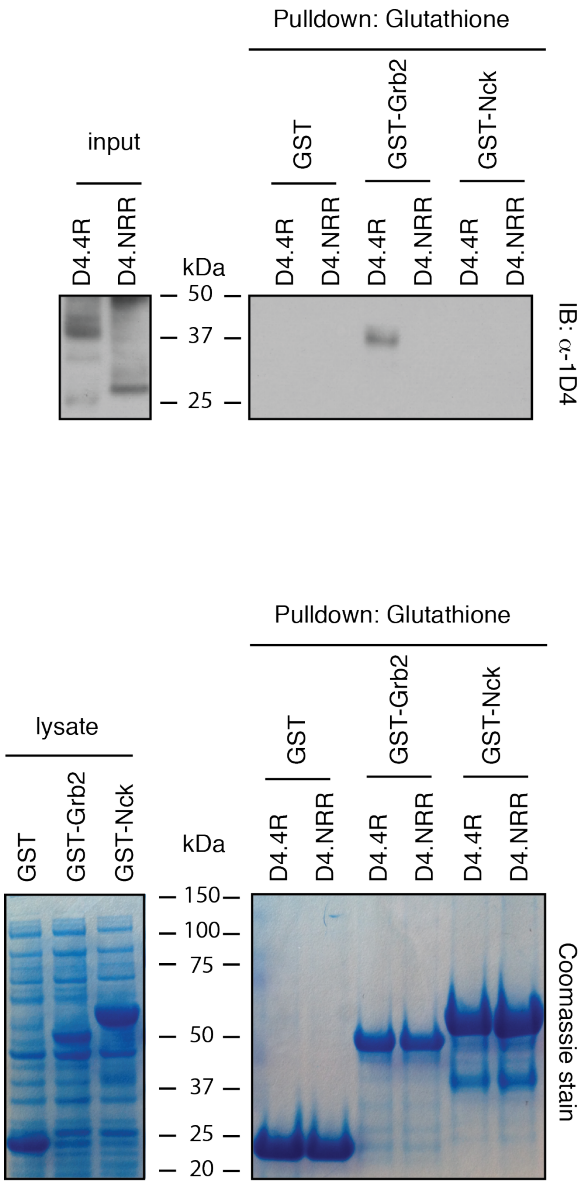

Figure 4-4 Specific interaction between Grb2 and the hD4R SH3 binding domain.

Membrane preparations from cells expressing 4-repeat (D4.4R) or no repeat (D4.NRR) KØ hD4R-1D4 were combined with glutathione beads coated in GST alone or GST-DRIPs. Eluates were tested for receptor presence via 1D4 immunoblot (top, IB) and GST or GST-DRIP levels via coomassie stain (bottom).

4.2 hD4R co-IPs

GST-DRIP-coated beads were successfully used to pull down hD4R and quickly and easily assay hD4R/Grb2 interactions. However, in order to efficiently identify new DRIPs, it would be necessary to isolate the receptor from the protein mixture and find DRIPs in the resulting eluate. Therefore, the interaction between hD4.4R-1D4 and GST-Grb2 was assayed using co-IP.

4.2.1 1D4 antibody co-IP

The 1D4 epitope is the 9 amino acids on the C-term of the prototypical GPCR rhodopsin (MacKenzie et al., 1984). The 1D4 epitope is widely used as a C-term epitope for GPCRs like hD4R, where specific antibodies against the endogenous protein sequence are not easily raised, and has been successfully used for enrichment of multiple GPCRs for proteomic studies (Wong, 2009). The monoclonal 1D4 antibody is commercially available from limited sources and at a very high cost. Therefore I worked with Manija A. Kazmi and Dr. W Vallen Graham to produce 1D4 antibody from the hybridoma cell line. We cultured the hybridoma cell line for 11 months in a hollow fiber cartridge, harvesting the growth medium every 48-72 hours. Protein G was then used to purify over 3 grams of 1D4 antibody. The resulting 1D4 antibody was utilized for IPs and immunoblots presented in this thesis.

In order to test the fidelity of the hD4R/Grb2 interaction, purified GST-DRIP proteins were combined with isolated membranes expressing hD4.4R-1D4 or hD4.NRR-1D4 and subsequently IP'd with 1D4 antibody. The eluates of the co-IP were then analyzed by SDS-PAGE and immunoblot. Immunoblot with the 1D4 antibody were used to assess hD4R protein levels, and an antibody against GST was used to assess the abundance of GST-DRIPs. In contrast to the highly specific interaction identified via GST pulldown, there was a substantial amount of GST-Grb detected in the eluate of the negative control, hD4.NRR-1D4 (Figure 4-5). Furthermore, GST alone could be detected in eluates of 1D4 co-IPs.

Given the low background in hD4R/DRIP interactions in GST pulldown experiments, it was hypothesized that non-specific interactions were an artifact of the 1D4 antibody co-IP procedure. Therefore, numerous alternative methods for preparation of hD4R-1D4 protein, preparation of DRIPs, and reaction conditions including buffer, time, and temperatures were tested. Co-IP between hD4R-1D4 and endogenous Grb2 in HEK293T cells via 1D4 antibody also resulted in detection of Grb2 in hD4.NRR-1D4 co-IP eluates. It was also determined that GST-Grb2 and GST alone could be detected in eluate of 1D4 antibody beads in the absence of hD4R-1D4. Therefore, it was hypothesized that the 1D4 antibody itself might be responsible for the non-specific detection.

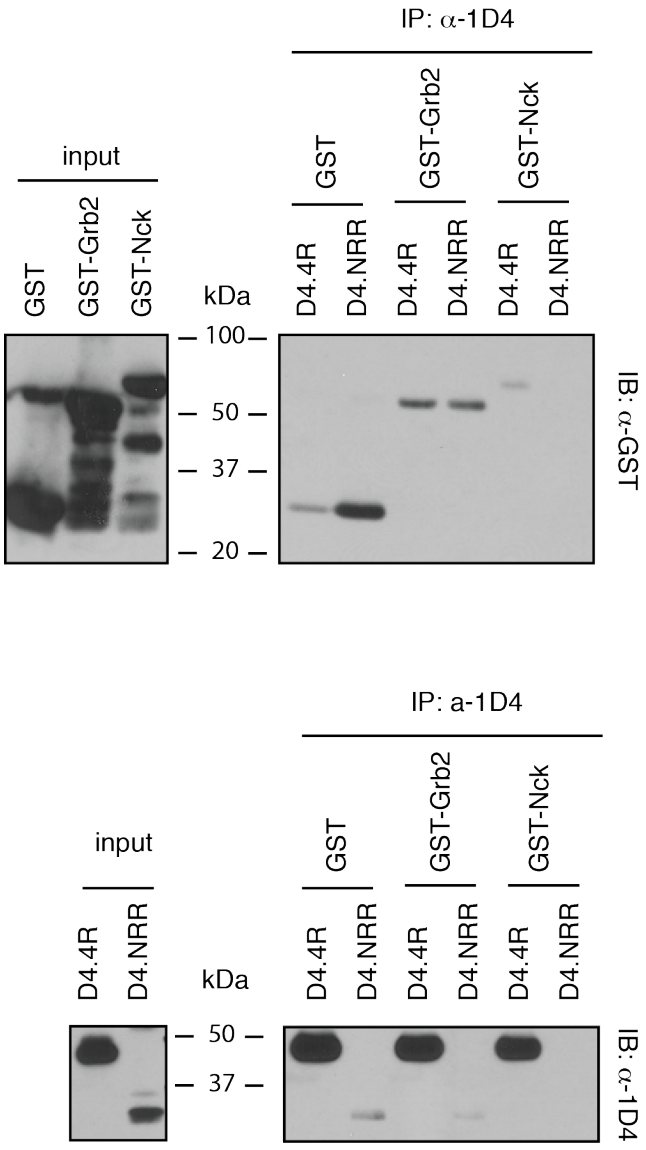

Figure 4-5 Non-specific interactions in 1D4 IPs.

Membrane preparations from cells expressing 4-repeat (D4.4R) or no repeat (D4.NRR) KØ hD4R-1D4 were combined with GST alone or GST-DRIPs. The 1D4 antibody was used to co-IP hD4R and DRIPs. Eluates were tested for GST or GST-DRIPs via immunoblot with anti-GST antibodies (top) and hD4R levels were tested via immunoblot with 1D4 antibody (bottom, IB).

4.2.2 Anti-myc antibody co-IP

Multiple epitope/antibody pairs were tested to find conditions that produced low background signal during co-IP. The Myc antibody showed low interaction with GST as compared to 1D4. Therefore, hD4.4R-1D4 and hD4.NRR-1D4 constructs with N-term myc epitopes were created. However, performing the pulldown assay with GST-DRIPs and isolated membranes from cells expressing myc-hD4R-1D4 also resulted in non-specific interactions between Grb2 and hD4.NRR (Figure 4-6).

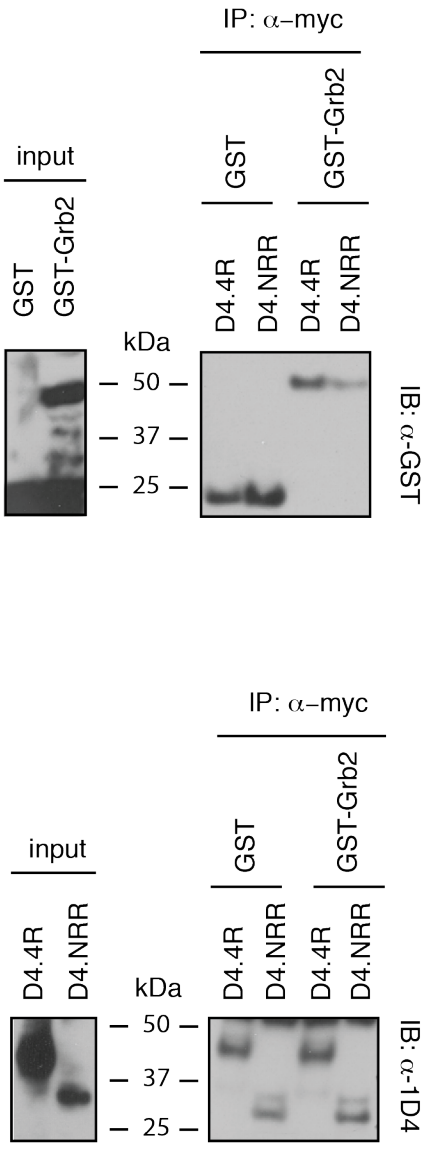

Figure 4-6 Non-specific interactions in myc IPs.

Membrane preparations from cells expressing 4-repeat (D4.4R) or no repeat (D4.NRR) KØ hD4R-1D4 were combined with GST alone or GST-DRIPs. The myc antibody was used to co-IP hD4R and DRIPs. Eluates were tested for GST or GST-DRIPs via immunoblot with anti-GST antibodies (top) and hD4R levels were tested via immunoblot with 1D4 antibody (bottom, IB).

4.2.3 Anti-OLLAS antibody co-IP

The rat antibody against the E. coli OmpF Linker and mouse Langerin fusion Sequence epitope (OLLAS) was developed at The Rockefeller University in 2007. The antibody has high specificity and affinity for the OLLAS epitope, and has been shown to be superior to many commercially available antibodies for use in IPs (Park et al., 2008). Like the 1D4 antibody, the antibody against OLLAS is not readily commercially available. Therefore, together with Manija A. Kazmi and Dr. W Vallen Graham, I cultured the anti-OLLAS antibody hybridoma cell line in a hollow fiber cartridge for 6 months. Over 300 mg of anti-OLLAS antibody was purified using protein G. The resulting antibody was used for IP and immunoblots within this thesis.

A hD4R construct with a C-term OLLAS epitope was created, as well as an OLLAS epitope-containing rhodopsin construct. These constructs were successfully expressed in HEK293T cells, as assayed via immunoblot with the anti-OLLAS antibody. The C-term OLLAS epitope did not disrupt hD4R functionality as assayed by calcium flux assay on the hD4.4R-OLLAS receptor.

Conditions for IP of hD4R-OLLAS and rhodopsin-OLLAS were optimized. However GST-Grb2 was detected in the eluate of the IP of hD4.NRRR, which does not contain the SH3 binding domain through which Grb2 interacts with hD4R.

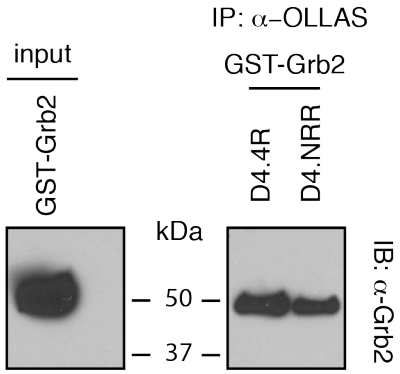

Figure 4-7 Non-specific interactions in OLLAS IPs.

Membrane preparations from cells expressing 4-repeat (D4.4R) or no repeat (D4.NRR) KØ hD4R-1D4 were combined with GST alone or GST-DRIPs. The OLLAS antibody was used to co-IP hD4R and GST-Grb2. Eluates were tested for Grb2 via immunoblot with anti-Grb2 antibody.

Due to the high background signal in co-IP-based hD4R/DRIP interaction studies and the interesting cell biological studies of hD4R protein regulation that were ongoing (see Chapter 3), attempts at identifying novel hD4R DRIPs were discontinued.

CHAPTER 5: Discussion and future perspectives

5.1 hD4R DRIPs

I proposed a method for the identification of novel hD4R DRIPs. A protocol to detect hD4R/DRIP interactions using GST-DRIPs and glutathione-based pulldowns was successfully developed. In order to identify unknown hD4R DRIPs, however, protein complexes would need to be purified using an epitope on the receptor, not the DRIP. Therefore several attempts were made to co-IP DRIPs with epitope-tagged hD4R. In all cases of co-IP, non-specific interactions were detected. Therefore identification of novel hD4R DRIPs was not pursued further.

5.1.1 Future perspectives on DRIP identification

The identification of hD4R DRIPs could still be conducted via co-IP with an antibody against a C-term or N-term epitope on hD4R. While qualitative immunoblots detected prohibitively high levels of non-specific binding, it is possible that a quantitative method such as comparative proteomics with tandem mass tags (TMT) or isobaric tags for relative and absolute quantitation (iTRAQ) could detect differences in the amount Grb2 in the co-IP eluates for hD4R with and without the SH3 binding domain. If significantly more Grb2 co-IP'd with the

SH3 domain-containing variant hD4.4R-1D4 compared with the hD4.NRR-1D4, then the quantitative comparative proteomics technique would corroborate Oldenhof's original result. Therefore the technique could be confidently used to identify novel DRIPs. If there was not a detectable more Grb2 in eluates of hD4.4R co-IP than in eluates of hD4.NRR co-IP, Grb2 would be classified as a non-DRIP in the proteomics assay. However, previous studies by Oldenhof and colleagues and my own glutathione-based pulldowns show that Grb2 is in fact a specific DRIP – meaning the proteomics result would be a false negative. It would be possible to conduct the proteomics screen for DRIPs with the understanding that the false-negative rate may be high. That would not, however, diminish the integrity of any positive hits in the screen. It may be that a number of DRIPs exist with specificity for hD4R that is greater than the specificity of the Grb2/hD4R interaction, and those potential DRIPs could be discovered using the approach outlined in Figure 4-1.

5.1.2 Degradation-resistant hD4R as a tool

The wt hD4R receptor is substantially degraded via the proteasome, leading to low receptor levels. Therefore biochemical and structural studies of the receptor that require large amounts of protein have been a struggle. The attempt at identifying hD4R DRIPs presented in this thesis was facilitated by the use of a degradation-resistant hD4R mutant. A mutant form of hD4R where the only four

lysine residues in the receptor are mutated to arginine (KØ) has much higher protein levels than wt (Fig 3-2) since proteasomal degradation of the mutant receptor is partially inhibited (Fig 3-8). The KØ mutant receptor has an EC_{50} for the agonist ligand quinpirole (as assayed via intracellular calcium release [Fig 3-7]) unchanged from that of wt receptor. Additionally, the KØ and wt receptors have a similar profile of hD4R DRIP interactions (Fig 4-3).

The KØ mutant receptor may be of value for a number of other experiments. Determining the physical structure of cytosolic proteins such as kinases through techniques such as x-ray crystallography and protein NMR has greatly advanced the ability to target these proteins with small molecule drugs. Many attempts have been made to generate GPCR structures and to discover potential drugs capable of targeting the receptors. GPCR structural studies are challenging because of the highly unstable nature of these receptors outside of the native membrane environment. Structural studies of hD4R specifically are furthermore complicated because of the low protein levels in cell expression systems. The use of KØ hD4R would facilitate structural studies would by allowing for the purification of a greater amount of receptor without compromising the functional integrity of the protein.

In the time since the hD4R/Grb2 interaction experiments were performed, it has been discovered that mutation of cytoplasmic serine and threonine residues to alanine leads to further stabilization of hD4R (Fig 3-13). The STØ and KSTØ mutants might also be useful in studies of hD4R that require large

amounts of purified protein; however, the STØ and KSTØ mutants did have a 10-fold shift in EC_{50} for quinpirole compared with wt receptor. The function of these mutants should be further characterized before use in structural studies of hD4R.

5.1.3 OLLAS epitope applications

The OLLAS epitope and antibody pair was used to co-IP hD4R/DRIP interactions (Fig 4-7). In order to use the OLLAS epitope and antibody for co-IP, I optimized OLLAS epitope detection via immunoblot and OLLAS epitope purification via IP. I also helped to produce and purify over 300 mg of the antibody. The OLLAS epitope and antibody have since been utilized in other GPCR studies. Specifically, the epitope/antibody pair have been utilized to immobilize the chemokine receptor CCR5 in order to conduct single molecule studies of receptor/ligand interactions. The low dissociation constant of the epitope/antibody pair means that OLLAS is well-suited for immobilization of a receptor over a long period of time. The OLLAS-based immobilization technology is now being developed as a general enabling technology for pharmacological studies of GPCRs.

5.2 hD4R ubiquitination and degradation

The activation of D4R in the brain has numerous pre-synaptic and post-synaptic consequences (Vullhorst, 2013). A role is emerging for D4R in regulation of gamma-oscillation power, highlighting the specific importance of D4R in cognition compared with other dopamine receptors (Andersson et al., 2012a; Kocsis et al., 2013) . We have uncovered a molecular mechanism controlling cellular levels of the hD4R protein through ubiquitination, raising the possibility that hD4R function may be regulated by its protein abundance.

Canonically ubiquitination of GPCRs at the plasma membrane is ligand-dependent and promotes lysosomal degradation of internalized receptors over recycling back to the plasma membrane (Marchese and Benovic, 2001). Our data suggest a deviation from the canonical model of GPCR ubiquitination in two ways. First, we detected ubiquitination of hD4R through PLA and IP in the absence of exogenous ligand (Fig 3-17, Fig 3-20, Fig 3-21, Fig 3-22). Secondly, treatments with lysosomal and proteasomal inhibitors (Fig 3-5) demonstrate that ubiquitin-dependent degradation of hD4R is proteasomal. Taken together, our data support a model of extensive proteasomal degradation of hD4R following ligand-independent isopeptide ubiquitin.

Our results are potentially consistent with a role for ubiquitination and proteasomal degradation of misfolded GPCRs in the ER, as is the case for the δ opioid receptor (Petaja-Repo et al., 2001). PLA can be used to visual the

subcellular localization of ubiquitinated receptor, and demonstrated that a perinuclear population of ubiquitinated hD4R exists. It is possible that the perinuclear population of hD4R is ubiquitinated in the ER due to misfolding and subsequently degraded by the proteasome. However, in both primary mouse cortical neurons and HEK293T cells, ubiquitinated receptors were also detected at the plasma membrane. Previous reports show that ubiquitinated receptors at the plasma membrane are often degraded via lysosomes, but the chloroquine dose curve experiments show that hD4R is not lysosomally degraded (Fig 3-5). The consequences of ubiquitination of hD4R in the plasma membrane are not clear, but may be an example of proteasomal degradation of a plasma membrane protein or a currently unappreciated role in controlling hD4R signaling beyond degradation.

We detect a role for ester bond ubiquitination in hD4R degradation. We have demonstrated that the lysine-less KØ hD4R-1D4 mutant is ubiquitinated and proteasomally degraded (Fig 3-17, Fig 3-21, Fig 3-8). Additionally, we have made a cytoplasmically serine-less and threonine-less mutant STØ hD4R-1D4 (Fig 3-11) that still retains protein function (Fig 3-12). We have confirmed the that the non-lysine ubiquitination is specifically ester bond ubiquitination through quantifying the ubiquitination and proteasomal degradation of STØ hD4R-1D4 (Fig 3-17, Fig 3-21, Fig 3-14). Finally, we made a functional lysine-less, and cytoplasmically serine-less and threonine-less mutant KSTØ hD4R-1D4 (Fig 3-12) where ubiquitination and proteasomal degradation are substantially

diminished (Fig 3-17, Fig 3-21, Fig 3-14). Combined with the fact that cytoplasmic cysteines did not influence hD4R protein levels (Fig 3-15), the lack of increase in KSTØ protein levels upon bortezomib treatment suggest that isopeptide and ester bond ubiquitination – but not thioester ubiquitination – regulate hD4R protein levels via proteasomal degradation.

The hD4R contains a VNTR in IC3. It is important to note that the 16-amino acid repeat sequence is not perfectly replicated in each repeat region. While all repeat segments are prline-rich, the amino acid identity between proline residues is variable both within a given allele and amongst the alleles present in the human population. Intriguingly, despite the substantial differences in total amino acid number among hD4R variants, the ubiquitinatable residues (lysine, serine, threonine) are nearly constant for the most common 2-repeat, 4-repeat, and 7-repeat alleles (Chang, 1996). For the 2-repeat, 4-repeat, 7-repeat, and a non-physiological no-repeat variant, the hD4R-1D4 protein is not degraded efficiently when lysine to arginine mutations are introduced. For all physiological variants tested (2-repeat, 4-repeat, and 7-repeat) efficient degradation is also inhibited by serine to alanine and threonine to alanine mutation. For the 2-repeat and 4-repeat variants, protein levels are substantially higher when lysine, serine, and threonine mutations are combined, indicating that both ester and isopeptide ubiquitination are likely to contribute to degradation of these receptor variants. The biological significance of the lack of additive effect for the 7-repeat variant and lack of ester ubiquitination for the no-repeat variant is not clear at this time.

5.2.1 Identifying E3 ligases responsible for hD4R ubiquitination

Attempts have been made to determine the ubiquitination machinery responsible for hD4R degradation. Two likely candidates are the E3 ubiquitin ligases KLHL12 and Hrd1, both of which are endogenous in HEK293T cells. KLHL12 was previously found to interact with the IC3 of hD4R via a yeast two-hybrid screen and to promote receptor ubiquitination, on lysine and non-lysine residues (Rondou et al., 2008) (Skieterska et al., 2015). However, over-expression of KLHL12 did not decrease hD4R protein levels, as would be predicted if it initiated hD4R degradation (Rondou et al., 2010). Hrd1 is an ER-associated E3 ubiquitin ligase that promotes ubiquitination of ERAD substrates including GPCRs (though it has not previously been linked to hD4R) and has been shown to promote ester ubiquitination (Shimizu et al., 2010).

If KLHL12 or Hrd1 promoted hD4R ubiquitination and subsequent degradation, hD4.4R-1D4 protein levels would increase upon siRNA knockdown of the responsible E3 ligase. HEK293T cells were transfected with wt hD4.4R-1D4 and siRNA against either KLHL12 or Hrd1 and then monitored hD4.4R-1D4 protein levels. Treatment with siRNA did not change hD4.4R-1D4 levels, though in the case of Hrd1, knock-down of the protein was not apparently successful, and in the case of KLHL12 the level of knockdown could not be determined due to the lack of suitable antibody (previous reports all monitored epitope-tagged protein, not endogenous).

Future attempts to identify the E3 ligase(s) responsible for hD4R degradation should consider a CRISPR based deletion of the ligases if they are not essential genes. Furthermore, future knockdown or knockout attempts should be assay by monitoring RNA levels of KLHL12 – eliminating the need for an antibody against the endogenous protein. Additionally, a dominant-negative Hrd1 construct has been reported 4 (Kikkert et al., 2004). If Hrd1 is responsible for hD4R ubiquitination and subsequent degradation, co-transfection of hD4R and the dominant negative Hrd1 gene should increase hD4R protein levels.

Intriguingly, the hD4.NRR-1D4 receptor mutant seems to be degraded via isopeptide but not ester bond ubiquitination (Fig 4-24). Mutating the serine and threonine residues in hD4.4R-1D4 that are deleted in hD4.NRR does not phenocopy STØ hD4.4R-1D4, suggesting that the presence of the repeat region itself is required for hD4R ester ubiquitination. A likely explanation is that the E3 ligase required for ester ubiquitination binds in the hD4R repeat region. Intriguingly, such a hypothesis would suggest that separate enzymes are required for isopeptide versus ester ubiquitination.

5.2.2 Ubiquitination and phosphorylation

A ubiquitinated GPCR at the plasma membrane must be internalized before it can be lysosomally degraded. GPCR desensitization via internalization is canonically dependent upon agonist-induced phosphorylation of cytoplasmic

serine and threonine residues via G protein-coupled receptor kinases. A single serine or threonine residue cannot be simultaneously phosphorylated and ubiquitinated. Suggestively, hD4R has been previously shown to be resistant to agonist-induced desensitization via the canonical pathway (Spooren et al., 2010). The same study qualitatively detected basal phosphorylation of one of the six cytoplasmic serine residues, but none of the cytoplasmic threonine residues in the hD4R IC3 loop. It is intriguing to hypothesize that phosphorylation may regulate which hD4R residues are available for ester ubiquitination – and vice versa.

5.2.3 Biological consequences of hD4R degradation

Non-isopeptide ubiquitination was first discovered in 2005 when Cadwell and Coscoy reported ubiquitination of a “Lysine-less” MHC-I cytoplasmic domain through a viral E3 ligase (Cadwell and Coscoy, 2005). More recent examples show that lysine-less proteins can be ubiquitinated in mammalian, insect, plant, and yeast cells regardless of viral infection (Shimizu et al., 2010) (Boban et al., 2015) (Gilkerson et al., 2015) (Domingues and Ryoo, 2012) . Ester and thioester ubiquitination have been detected in cases where massive, rapid degradation of the target protein has been advantageous. For example, a number of studies have shown that viral ubiquitination of host defense proteins (including MHC proteins and BST-2/thetherin) leads to substantial degradation – presumably

promoting viral success (Cadwell and Coscoy, 2005) (Tokarev et al., 2011) (Magadán et al., 2010) (Ishikura et al., 2010) (Herr et al., 2009). Additionally, the neural transcription factor Ngn2 needs to be active only during a precise window in development, suggesting that rapid degradation of the protein may be required for preventing aberrant activity after this window has passed (Vosper et al., 2009).

Several substrates of ester ubiquitination are targets of the ERAD pathway. ERAD promotes swift and substantial degradation of misfolded proteins in the ER in order to support cell survival (Christianson and Ye, 2014). It is possible that ester ubiquitination of misfolded hD4R protein in the ER promotes rapid degradation via the ERAD pathway (see section 5.2). However, we also observe hD4R ubiquitination outside of the ER, suggesting the modification is acting outside of the ERAD system.

One alternative reason – beyond ERAD degradation of misfolded proteins - that massive degradation of hD4R could be biologically advantageous is that hD4R has a role in the circadian cycle. Soon after the discovery of the *DRD4* gene, *DRD4* mRNA was detected at high levels in the retina, (Matsumoto et al., 1995) and many years later was also observed at high levels in the pineal gland (Kim et al., 2010). D4R protein function in the retina is important for circadian, light-adapted vision (Jackson et al., 2012). In the pineal gland, the presence of D4R at sunrise inhibits melatonin synthesis and release, while its absence at sunset allows for melatonin production (González et al., 2012b). While

transcription and translation of D4R are known to follow a circadian rhythm in the retina and pineal gland, massive proteasomal degradation of hD4R via isopeptide and ester ubiquitination may enable a rapid decrease in protein levels at sunrise. Previous evidence exists for degradation-regulated circadian protein rhythms; studies have shown that the ubiquitin-proteasome system and specifically KLHL proteins are important for maintaining retinal health (Campello et al., 2013).

5.3 Ester and thioester ubiquitination

5.3.1 Known cases of ester and thioester ubiquitination

Non-isopeptide ubiquitination has been reported for a total of 22 proteins spread over 5 species. The current list of proteins known to be ubiquitinated by ester and/or thioester bonds is presented in Table 5.1.

5.3.2 Under-recognition of ester and thioester ubiquitination

Isopeptide ubiquitination has been recognized for much longer than ester or thioester ubiquitination, and a great many examples of isopeptide ubiquitination have been discovered. Isopeptide ubiquitination has been detected on at least 5000 proteins in the human proteome alone (Kim et al., 2011). Ubiquitination originally was defined by the isopeptide bond linkage. In their 1980 publication, Ciechanover and Hershko characterized the linkage between proteins destined for degradation and the ubiquitin polypeptide as being resistant to treatment with basic or reducing agents (Ciechanover et al., 1980). Now, loss of ubiquitination upon NaOH treatment is used as the standard assay for detection of ester bond ubiquitination, and DTT sensitivity is used to detect thioester bond ubiquitination (Wang et al., 2007) (Tait et al., 2007).

Table 5- 1 Cases of ester and thioester ubiquitination

Target proteins and gene names are listed along with non-lysine residues that are known to be ubiquitinated by ester bonds (serine [S] and threonine [T]) or thioester bonds (cysteine [C]). Any enzymes known to be required for addition or removal of ubiquitin are listed, along with literature references.

Protein	Gene	Residue	Enzymes	References
Major histocompatibility complex I	*HLA.A2, HLA.B7*	CST	Mir1, mK3	Cadwell (2005), Cadwell (2008), Wang (2007), Herr (2009)
Peroxin 20	*PEX20*	C		Leon (2007)
Peroxisomal targeting signal 1 receptor	*PEX5*	C	Pex12p, Pex4p, USP9X	Carvalho (2007), Williams (2007), Grou (2012), Schwartzkopff (2015)
BH3-interacting domain death agonist	*BID*	C		Tait (2007)
Neurogenin-2	*NEUROG2*	CST		Vosper (2009), McDowell (2010)
CD4	*CD4*	ST	Vpu	Magadan (2010)
T cell antigen receptor α	*PTCRA*	S	Hrd1	Ishikura (2010)
Nonsecreted immunoglobulin light chain	*IGK*	ST	Hrd1	Shimizu (2010)
Immunoblobulin G1 Fab heavy chain	*VHCH1*	ST	Hrd1	Shimizu (2010)
α1-antitrypsin variant null (Hong Kong)	*SERPINA1*	ST	Hrd1	Shimizu (2010)
Homocysteine-responsive endoplasmic reticulum-resident ubiquitin-like domain member 1 protein	*HERPUD1*	ST	Hrd1	Shimizu (2010)
Transitional endoplasmic reticulum ATPase (p97)	*VCP*	ST	Hrd1	Shimizu (2010)
Bone marrow stromal antigen 2 (tetherin)	*BST2*	ST	Vpu	Tokarev (2011)
Neurogenin-3	*NEUROG3*	CST		Roark (2012)
Asi2	*ASI2*	ST	Doa10, Ubc6	Boban (2015)
Indole-3-acetic acid1 Auxin-responsive protein	*IAA1*	ST		Gilkerson (2015)
Vma12-*DegAB*		ST	Doa10, Ubc6	Weber (2016)
Protein transport protein SBH2	*SBH2*	ST	Doa10, Ubc6	Weber (2016)
Dopamine receptor 4	*DRD4*	ST	KLHL12	Peeler (in review), Skieterska (2015)

Ubiquitination was studied for 25 years before ester and thioester ubiquitin linkages were discovered. During those 25 years, many assumptions were made that must now be re-evaluated. For example, it is widely assumed that a lysine-free mutant protein is in fact a ubiquitin-free protein. Lysine-free mutants have served as the standard negative control to study the consequences of ubiquitination. The degradation of lysine-free mutants via the ubiquitin-proteasome system, however, has been well characterized multiple times since 2005, including in this thesis. In the case of hD4R and many other proteins, ester ubiquitination appears on the wt protein and lysine-null mutants. However, some researchers have found that proteins, which in wt form are only ubiquitinated via isopeptide bonds, can be ubiquitinated via ester and thioester bonds when lysine residues are mutated. Regardless of whether ester ubiquitination of a given protein is a normally occurring modification or an artifact of lysine mutation, the assumption that lysine-free mutants are also ubiquitin-free mutants should be revised. For example, Michael Tanowitz and Mark von Zastrow determined that the δ opioid receptor was degraded lysosomally, but that mutation of all cytoplasmic lysine residues did not significantly inhibit lysosomal degradation. They concluded, therefore, that ubiquitination was not required for lysosomal degradation of the receptor (Tanowitz and Zastrow, 2002). While isopeptide ubiquitination may not be necessary, it could be that ubiquitin attached through ester or thioester bonds are sufficient for degradation of this receptor.

Lysine-free ubiquitin is used to characterize whether a given protein is mono- versus poly-ubiquitinated, based on the assumption that poly-ubiquitin chains can only form through isopeptide bonds between ubiquitin molecules. While examples of ester or thioester-based polyubiquitination have not been described, there is no reason to think that ubiquitin itself could not be ubiquitinated on serine and/or threonine residues. Therefore, the use of a lysine-null ubiquitin construct for determination of mono- versus poly-ubiquitination should be reconsidered.

5.3.2.1 Mass spectrometry as a tool for studying ubiquitination

One reason that ester and thioester ubiquitination is under-recognized is the struggle to identify these bonds through MS/MS. MS/MS is a widely used tool in the study of PTMs, including isopeptide ubiquitination. MS/MS analysis is a standard assay for identifying ubiquitinated lysine residues for a given protein. Furthermore, quantitative proteomics has allowed for careful characterization of isopeptide ubiquitination, including the prevalence of specific linkages and ligase activity, on a global scale (Ordureau et al., 2015). In general, such MS/MS analysis has not detected ubiquitin linkages on serine, threonine, or cysteine residues. After the discovery of non-isopeptide ubiquitination, specific efforts were made to develop MS/MS techniques for the detection of ester and thioester ubiquitination. Using stable isotope labeling with amino acids in cell culture

(SILAC), one group was able to identify peptides that were likely to contain a ubiquitin modification, including peptides devoid of lysine residues. However, despite multiple efforts, they were unable to directly detect an ester or thioester linkage on any specific residues, though isopeptide linkages on lysine residues were readily detected (Anania et al., 2013). In the last year, however, the first report of MS/MS identification of an ester linkage between a serine residue and ubiquitin has been published. The base-sensitive ester bond was preserved only when peptide purification and subsequent resuspension was performed in the presence of 20 mM acetic acid (Weber et al., 2016). The identification of conditions for MS/MS that preserve the ester bond between serine and ubiquitin should lead to the increase in detection of non-isopeptide ubiquitination.

5.3.2.2 Mutational analysis for identification of ester and thioester ubiquitination

In addition to the challenge in detecting ester and thioester ubiquitination via MS/MS, the field of non-isopeptide ubiquitination is stunted by the difficulty in performing mutational analysis for ester and thioester ubiquitination. Lysine residue mutation has been vital to the field of isopeptide ubiquitination (though at times the results with these mutants have been misinterpreted). Removal of all serine and threonine residues in a given protein often requires a substantial number of mutations. Lysine residues comprise 5.6% of the total residues in the

human proteome. In contrast, serine and threonine residues together comprise over 13% of the amino acids in the human proteome. Substantial mutations can lead to serious protein misfolding, and therefore differences between wild type proteins and serine- and threonine-null mutants may result from factors other than the ubiquitination state of the protein. Researchers in the field of non-isopeptide ubiquitination have therefore struggled to find physiologically relevant negative controls (Tait et al., 2007). In this thesis I have demonstrated that mutation of all serine and threonine residues on the cytoplasmic surface and TM/cytoplasm border leads to a non-functional hD4R mutant. However, I was able to identify mutants where the majority of cytoplasmic serine and threonine residues are mutated, but the receptor is still functional – creating a physiologically relevant negative control for hD4R ester ubiquitination.

5.3.4 Serine and threonine residues in degradation motifs

As described more fully in section 1.5, non-isopeptide ubiquitination often leads to rapid, proteasomal degradation of the modified protein. In 1986 Scott Rogers and colleagues discovered that the presence of a motif rich in proline, glutamic acid, serine, and threonine residues (PEST motif) was correlated with short protein half-life specifically due to proteasomal degradation (Rogers et al., 1986). The PEST motif is found in 25% of eukaryotic proteins (Singh et al., 2006) and specifically prevalent in neurotransmitter receptor GPCRs (Tovo-Rodrigues

et al., 2014). Some evidence exists that suggests phosphorylation of serine residues in a PEST motif contribute to proteasomal degradation (García-Alai et al., 2006). However, it is also tempting to speculate that ester ubiquitination of the PEST motif may be signaling for the degradation of PEST domain-containing proteins.

5.3.5 Enzymes regulating ester and thioester ubiquitination

Understanding a given PTM requires an understanding of the proteins responsible for “writing” and “erasing” the modification. The field of isopeptide ubiquitination has carefully described the E1/E2/E3 enzyme cascade responsible for depositing the modification on target proteins, and more recently the role of DUBs in removing the modification has become more clear (Swatek and Komander, 2016).

A number of E2 and E3 ligases have been identified in the “writing” of ester and thioester ubiquitination as well, as shown in Table 5.1. The enzymes for ester and thioester ubiquitination seem to be a subset of the ligases responsible for isopeptide ubiquitination (as opposed to a distinct set). It is currently unclear what defines an E3 ligase capable of promoting ester and thioester ubiquitination. For example, the closely related MIR1 and MIR2 enzymes encoded by KSHV are both capable of inducing isopeptide ubiquitination of host MHC I molecules, while only MIR1 promotes thioester

ubiquitination (Cadwell and Coscoy, 2005). In yeast, the Ubc6 E2 enzyme seems to favor ubiquitination on serine and threonine residues while Ubc7 favors ubiquitination on lysine residues (Weber et al., 2016). As more examples of ester and thioester ubiquitination emerge, along with the responsible enzymes, characteristics common to enzymes responsible for non-isopeptide ubiquitination may emerge as well.

The removal of isopeptide ubiquitination by DUBs is now well characterized. DUBs, as currently defined, are a family of isopeptidases that function through an active site cysteine. One example of a DUB removing a non-isopeptide ubiquitin modification has been described thus far. The thioester ubiquitination of Pex5p seems to be removed by the protein USP9X. USP9X was shown to have thioesterase as well as isopeptidase activity (Grou et al., 2012). Further investigation of enzymes capable of removing ester and thioester ubiquitination should be performed. Additionally, the sensitivity of ester and thioester bonds to alkaline and reducing conditions, respectively, mean that these modifications may be removed through non-enzymatic methods within the cell. Careful analysis of subcellular localization and microenvironment would be required to determine the non-enzymatic loss of ester and thioester ubiquitination.

5.4 Conclusions

hD4R is ubiquitinated via isopeptide and ester bonds and subsequently degraded by the proteasome. Ubiquitination and degradation serve as a method for cellular control of hD4R protein levels. Protein levels of hD4R may contribute to the physiological consequences of hD4R signaling – including roles in cognition and human mental health. The generation of mutants which are resistant to ubiquitination and degradation provide tools to enhance the study of hD4R, especially structural studies. hD4R also serves as a model for the rarely described ester bond ubiquitin modification. hD4R may be the first example of a protein where ester and isopeptide ubiquitination are mediated by separate enzymes. PLA is a tool capable of assaying ester versus isopeptide ubiquitination quantitatively and in physiologically relevant model systems.

REFERENCES

Alonso, V., and Friedman, P.A. (2013). Minireview: Ubiquitination-regulated G Protein-Coupled Receptor Signaling and Trafficking. Molecular Endocrinology *27*, 558–572.

Anania, V.G., Bustos, D.J., Lill, J.R., Kirkpatrick, D.S., and Coscoy, L. (2013). A Novel Peptide-Based SILAC Method to Identify the Posttranslational Modifications Provides Evidence for Unconventional Ubiquitination in the ER-Associated Degradation Pathway. International Journal of Proteomics *2013*, 1–12.

Andersson, R.H., Johnston, A., Herman, P.A., Winzer-Serhan, U.H., Karavanova, I., Vullhorst, D., Fisahn, A., and Buonanno, A. (2012a). Neuregulin and dopamine modulation of hippocampal gamma oscillations is dependent on dopamine D4 receptors. Pnas *109*, 13118–13123.

Andersson, R., Johnston, A., and Fisahn, A. (2012b). Dopamine D4 Receptor Activation Increases Hippocampal Gamma Oscillations by Enhancing Synchronization of Fast-Spiking Interneurons. PLoS ONE *7*, e40906.

Asghari, V., Schoots, O., van Kats, S., Ohara, K., Jovanovic, V., Guan, H.C., Bunzow, J.R., Petronis, A., and Van Tol, H.H. (1994). Dopamine D4 receptor repeat: analysis of different native and mutant forms of the human and rat genes. Mol. Pharmacol. *46*, 364–373.

Asghari, V., Sanyal, S., Buchwaldt, S., Paterson, A., Jovanovic, V., and Van Tol, H.H.M. (1995). Modulation of Intracellular Cyclic AMP Levels by Different Human Dopamine D4 Receptor Variants. Journal of Neurochemistry *65*, 1157–1165.

Bai, L., Zimmer, S., Rickes, O., Rohleder, N., Holthues, H., Engel, L., Leube, R., and Spessert, R. (2008). Daily oscillation of gene expression in the retina is phase-advanced with respect to the pineal gland. Brain Research *1203*, 89–96.

Beaulieu, J.M., and Gainetdinov, R.R. (2011). The physiology, signaling, and pharmacology of dopamine receptors. Pharmacol Rev *63*, 182–217.

Benchenane, K., Tiesinga, P.H., and Battaglia, F.P. (2011). Oscillations in the prefrontal cortex: a gateway to memory and attention. Curr. Opin. Neurobiol. *21*, 475–485.

Benjamin, J., Li, L., Patterson, C., Greenberg, B.D., Murphy, D.L., and Hamer, D.H. (1996). Population and familial association between the D4 dopamine receptor gene and measures of Novelty Seeking. Nature Genetics *12*, 81–84.

Boban, M., Ljungdahl, P.O., and Foisner, R. (2015). Atypical Ubiquitylation in Yeast Targets Lysine-less Asi2 for Proteasomal Degradation. J. Biol. Chem. *290*, 2489–2495.

Breitschopf, K., Bengal, E., Ziv, T., Admon, A., and Ciechanover, A. (1998). A novel site for ubiquitination: the N-terminal residue, and not internal lysines of MyoD, is essential for conjugation and degradation of the protein. Embo J. *17*, 5964–5973.

Buck, L., and Axel, R. (1991). A novel multigene family may encode odorant receptors: a molecular basis for odor recognition. Cell *65*, 175–187.

Cadwell, K., and Coscoy, L. (2005). Ubiquitination on nonlysine residues by a viral E3 ubiquitin ligase. Science.

Campello, L., Esteve-Rudd, J., Cuenca, N., and Martín-Nieto, J. (2013). The ubiquitin-proteasome system in retinal health and disease. Mol. Neurobiol. *47*, 790–810.

Cardin, J.A., Carlén, M., Meletis, K., Knoblich, U., Zhang, F., Deisseroth, K., Tsai, L.-H., and Moore, C.I. (2009). Driving fast-spiking cells induces gamma rhythm and controls sensory responses. Nature *459*, 663–667.

Carvalho, A.F., Pinto, M.P., Grou, C.P., Alencastre, I.S., Fransen, M., Sá-Miranda, C., and Azevedo, J.E. (2007). Ubiquitination of mammalian Pex5p, the peroxisomal import receptor. J. Biol. Chem. *282*, 31267–31272.

Chen, Z.J., Parent, L., and Maniatis, T. (1996). Site-specific phosphorylation of IkappaBalpha by a novel ubiquitination-dependent protein kinase activity. Cell *84*, 853–862.

Chen, Z.J., and Sun, L.J. (2009). Nonproteolytic functions of ubiquitin in cell signaling. Molecular Cell *33*, 275–286.

Chini, B., and Parenti, M. (2009). G-protein-coupled receptors, cholesterol and palmitoylation: facts about fats. J. Mol. Endocrinol. *42*, 371–379.

Christianson, J.C., and Ye, Y. (2014). Cleaning up in the endoplasmic reticulum: ubiquitin in charge. Nat. Struct. Mol. Biol. *21*, 325–335.

Ciechanover, A., Elias, S., Heller, H., and Hershko, A. (1982). “Covalent affinity” purification of ubiquitin-activating enzyme. J. Biol. Chem. *257*, 2537–2542.

Ciechanover, A., Heller, H., Elias, S., Haas, A.L., and Hershko, A. (1980). ATP-dependent conjugation of reticulocyte proteins with the polypeptide required for protein degradation. Pnas *77*, 1365–1368.

Civelli, O. (2012). Orphan GPCRs and neuromodulation. Neuron *76*, 12–21.

Coward, P., Chan, S., Wada, H.G., and Humphries, G.M. (1999). Chimeric G proteins allow a high-throughput signaling assay of G i-coupled receptors. Analytical … *270*, 242–248.

de Mendoza, A., Sebé-Pedrós, A., and Ruiz-Trillo, I. (2014). The evolution of the GPCR signaling system in eukaryotes: modularity, conservation, and the transition to metazoan multicellularity. Genome Biol Evol *6*, 606–619.

Deshaies, R.J., and Joazeiro, C.A.P. (2009). RING domain E3 ubiquitin ligases. Annu. Rev. Biochem. *78*, 399–434.

DeWire, S.M., Ahn, S., Lefkowitz, R.J., and Shenoy, S.K. (2007). β-Arrestins and Cell Signaling. Http://Dx.Doi.org/10.1146/Annurev.Physiol.69.022405.154749 *69*, 483–510.

Domingues, C., and Ryoo, H.D. (2012). Drosophila BRUCE inhibits apoptosis through non-lysine ubiquitination of the IAP-antagonist REAPER. Cell Death Differ. *19*, 470–477.

Dong, C., Filipeanu, C.M., Duvernay, M.T., and Wu, G. (2007). Regulation of G protein-coupled receptor export trafficking. Biochim. Biophys. Acta *1768*, 853–870.

Dores, M.R., and Trejo, J. (2012). Ubiquitination of G Protein-Coupled Receptors: Functional Implications and Drug Discovery. Mol. Pharmacol. *82*, 563–570.

Dorsam, R.T., and Gutkind, J.S. (2007). G-protein-coupled receptors and cancer. Nat. Rev. Cancer *7*, 79–94.

Ebstein, R.P., Novick, O., Umansky, R., Priel, B., Osher, Y., Blaine, D., Bennett, E.R., Nemanov, L., Katz, M., and Belmaker, R.H. (1996). Dopamine D4 receptor (D4DR) exon III polymorphism associated with the human personality trait of Novelty Seeking. Nature Genetics *12*, 78–80.

Emmerich, C.H., Ordureau, A., Strickson, S., Arthur, J.S.C., Pedrioli, P.G.A., Komander, D., and Cohen, P. (2013). Activation of the canonical IKK complex by K63/M1-linked hybrid ubiquitin chains. Proc. Natl. Acad. Sci. U.S.a. *110*, 15247–15252.

Fredriksson, R., Lagerström, M.C., Lundin, L.-G., and Schiöth, H.B. (2003). The G-protein-coupled receptors in the human genome form five main families. Phylogenetic analysis, paralogon groups, and fingerprints. Mol. Pharmacol. *63*, 1256–1272.

Gainetdinov, R.R., Premont, R.T., Bohn, L.M., Lefkowitz, R.J., and Caron, M.G. (2004). DESENSITIZATION OF G PROTEIN–COUPLED RECEPTORS AND NEURONAL FUNCTIONS. Http://Dx.Doi.org/10.1146/Annurev.Neuro.27.070203.144206 *27*, 107–144.

García-Alai, M.M., Gallo, M., Salame, M., Wetzler, D.E., McBride, A.A., Paci, M., Cicero, D.O., and de Prat-Gay, G. (2006). Molecular basis for phosphorylation-dependent, PEST-mediated protein turnover. Structure *14*, 309–319.

Gilkerson, J., Kelley, D.R., Tam, R., Estelle, M., and Callis, J. (2015). Lysine Residues Are Not Required for Proteasome-Mediated Proteolysis of the Auxin/Indole Acidic Acid Protein IAA1. Plant Physiol. *168*, 708–720.

Gill, R.S., Hsiung, M.S., Sum, C.S., Lavine, N., Clark, S.D., and Van Tol, H.H.M. (2010). The dopamine D4 receptor activates intracellular platelet-derived growth factor receptor β to stimulate ERK1/2. Cellular Signalling *22*, 285–290.

Goldknopf, I.L., French, M.F., Musso, R., and Busch, H. (1977). Presence of protein A24 in rat liver nucleosomes. Pnas *74*, 5492–5495.

Goldstein, G., Scheid, M., Hammerling, U., Schlesinger, D.H., Niall, H.D., and Boyse, E.A. (1975). Isolation of a polypeptide that has lymphocyte-differentiating properties and is probably represented universally in living cells. Pnas *72*, 11–15.

González, S., Rangel-Barajas, C., Peper, M., Lorenzo, R., Moreno, E., Ciruela, F., Borycz, J., Ortiz, J., Lluís, C., Franco, R., et al. (2012a). Dopamine D4 receptor, but not the ADHD-associated D4.7 variant, forms functional heteromers with the dopamine D2S receptor in the brain. Molecular Psychiatry *17*, 650–662.

González, S., Moreno-Delgado, D., Moreno, E., Pérez-Capote, K., Franco, R., Mallol, J., Cortés, A., Casadó, V., Lluís, C., Ortiz, J., et al. (2012b). Circadian-related heteromerization of adrenergic and dopamine D_4 receptors modulates melatonin synthesis and release in the pineal gland. PLoS Biol. *10*, e1001347.

Grou, C.P., Francisco, T., Rodrigues, T.A., Freitas, M.O., Pinto, M.P., Carvalho, A.F., Domingues, P., Wood, S.A., Rodríguez-Borges, J.E., Sá-Miranda, C., et al. (2012). Identification of ubiquitin-specific protease 9X (USP9X) as a deubiquitinase acting on ubiquitin-peroxin 5 (PEX5) thioester conjugate. J. Biol. Chem. *287*, 12815–12827.

Herr, R.A., Harris, J., Fang, S., Wang, X., and Hansen, T.H. (2009). Role of the RING-CH domain of viral ligase mK3 in ubiquitination of non-lysine and lysine MHC I residues. Traffic *10*, 1301–1317.

Hershko, A., Ciechanover, A., Heller, H., Haas, A.L., and Rose, I.A. (1980). Proposed role of ATP in protein breakdown: conjugation of protein with multiple chains of the polypeptide of ATP-dependent proteolysis. Pnas *77*, 1783–1786.

Hershko, A., Heller, H., Elias, S., and Ciechanover, A. (1983). Components of ubiquitin-protein ligase system. Resolution, affinity purification, and role in protein breakdown. J. Biol. Chem. *258*, 8206–8214.

Hollingsworth, T.J., and Gross, A.K. (2012). Defective trafficking of rhodopsin and its role in retinal degenerations. Int Rev Cell Mol Biol *293*, 1–44.

Hu, H., Gan, J., and Jonas, P. (2014). Interneurons. Fast-spiking, parvalbumin^{+} GABAergic interneurons: from cellular design to microcircuit function. Science *345*, 1255263–1255263.

Hunt, L.T., and Dayhoff, M.O. (1977). Amino-terminal sequence identity of ubiquitin and the nonhistone component of nuclear protein A24. Biochemical and Biophysical Research ….

Ishikura, S., Weissman, A.M., and Bonifacino, J.S. (2010). Serine residues in the cytosolic tail of the T-cell antigen receptor alpha-chain mediate ubiquitination and endoplasmic reticulum-associated degradation of the unassembled protein. J. Biol. Chem. *285*, 23916–23924.

Jackson, C.R., Ruan, G.-X., Aseem, F., Abey, J., Gamble, K., Stanwood, G., Palmiter, R.D., Iuvone, P.M., and McMahon, D.G. (2012). Retinal Dopamine Mediates Multiple Dimensions of Light-Adapted Vision. J. Neurosci. *32*, 9359–9368.

Jean-Charles, P.Y., Snyder, J.C., and Shenoy, S.K. (2016). Ubiquitination and Deubiquitination of G Protein- Coupled Receptors (Elsevier Inc.).

John Oldenhof, Ross Vickery, Mordechai Anafi, James Oak, Andrew Ray, Oscar Schoots, Tony Pawson, Mark von Zastrow, A., Hubert H M Van Tol (1998). SH3 Binding Domains in the Dopamine D4 Receptor† (American Chemical Society).

Kazmi, M.A., Snyder, L.A., Cypess, A.M., Graber, S.G., and Sakmar, T.P. (2000). Selective Reconstitution of Human D4 Dopamine Receptor Variants with G iα Subtypes †. Biochemistry *39*, 3734–3744.

Kikkert, M., Doolman, R., Dai, M., Avner, R., Hassink, G., van Voorden, S., Thanedar, S., Roitelman, J., Chau, V., and Wiertz, E. (2004). Human HRD1 is an E3 ubiquitin ligase involved in degradation of proteins from the endoplasmic reticulum. J. Biol. Chem. *279*, 3525–3534.

Kim, J.-S., Bailey, M.J., Weller, J.L., Sugden, D., Rath, M.F., Møller, M., and Klein, D.C. (2010). Thyroid hormone and adrenergic signaling interact to control pineal expression of the dopamine receptor D4 gene (Drd4). Molecular and Cellular Endocrinology *314*, 128–135.

Kim, W., Bennett, E.J., Huttlin, E.L., Guo, A., Li, J., Possemato, A., Sowa, M.E., Rad, R., Rush, J., Comb, M.J., et al. (2011). Systematic and Quantitative Assessment of the Ubiquitin-Modified Proteome. Molecular Cell *44*, 325–340.

Kluger, A.N., Siegfried, Z., and Ebstein, R.P. (2002). A meta-analysis of the association between DRD4 polymorphism and novelty seeking. Molecular Psychiatry *7*, 712–717.

Kocsis, B., Lee, P., and Deth, R. (2013). Enhancement of gamma activity after selective activation of dopamine D4 receptors in freely moving rats and in a neurodevelopmental model of schizophrenia. Brain Struct Funct *219*, 2173–2180.

Komander, D., Clague, M.J., and Urbé, S. (2009). Breaking the chains: structure and function of the deubiquitinases. Nat. Rev. Mol. Cell Biol. *10*, 550–563.

Lavine, N., Ethier, N., Oak, J.N., Pei, L., Liu, F., Trieu, P., Rebois, R.V., Bouvier, M., Hébert, T.E., and Van Tol, H.H.M. (2002). G protein-coupled receptors form stable complexes with inwardly rectifying potassium channels and adenylyl cyclase. J. Biol. Chem. *277*, 46010–46019.

Léon, S., and Subramani, S. (2007). A conserved cysteine residue of Pichia pastoris Pex20p is essential for its recycling from the peroxisome to the cytosol. J. Biol. Chem. *282*, 7424–7430.

Li, D., Sham, P.C., Owen, M.J., and He, L. (2006). Meta-analysis shows significant association between dopamine system genes and attention deficit hyperactivity disorder (ADHD). Hum. Mol. Genet. *15*, 2276–2284.

Li, W., Bengtson, M.H., Ulbrich, A., Matsuda, A., Reddy, V.A., Orth, A., Chanda, S.K., Batalov, S., and Joazeiro, C.A.P. (2008). Genome-wide and functional annotation of human E3 ubiquitin ligases identifies MULAN, a mitochondrial E3 that regulates the organelle's dynamics and signaling. PLoS ONE *3*, e1487.

Li, Y.M., Pan, Y., Wei, Y., Cheng, X., Zhou, B.P., Tan, M., Zhou, X., Xia, W., Hortobagyi, G.N., Yu, D., et al. (2004). Upregulation of CXCR4 is essential for HER2-mediated tumor metastasis. Cancer Cell *6*, 459–469.

Lichter, J.B., Barr, C.L., Kennedy, J.L., Van Tol, H.H.M., Kidd, K.K., and Livak, K.J. (1993). A hypervariable segment in the human dopamine receptor D4 (DRD4) gene. Hum. Mol. Genet. *2*, 767–773.

Lu, Y., Lee, B.-H., King, R.W., Finley, D., and Kirschner, M.W. (2015). Substrate degradation by the proteasome: a single-molecule kinetic analysis. Science *348*, 1250834.

MacKenzie, D., Arendt, A., Hargrave, P., McDowell, J.H., and Molday, R.S. (1984). Localization of binding sites for carboxyl terminal specific anti-rhodopsin monoclonal antibodies using synthetic peptides. Biochemistry *23*, 6544–6549.

Magadán, J.G., Pérez-Victoria, F.J., Sougrat, R., Ye, Y., Strebel, K., and Bonifacino, J.S. (2010). Multilayered mechanism of CD4 downregulation by HIV-1 Vpu involving distinct ER retention and ERAD targeting steps. PLoS Pathog. *6*, e1000869.

Marchese, A., and Benovic, J.L. (2001). Agonist-promoted ubiquitination of the G protein-coupled receptor CXCR4 mediates lysosomal sorting. J. Biol. Chem. *276*, 45509–45512.

Matsumoto, M., Hidaka, K., Tada, S., Tasaki, Y., and Yamaguchi, T. (1995). Full-length cDNA cloning and distribution of human dopamine D4 receptor. Brain Res. Mol. Brain Res. *29*, 157–162.

Mazzuco, T.L., Chabre, O., Feige, J.J., and Thomas, M. (2007). Aberrant GPCR expression is a sufficient genetic event to trigger adrenocortical tumorigenesis. Molecular and Cellular Endocrinology *265-266*, 23–28.

McDowell, G.S., Kucerova, R., and Philpott, A. (2010). Non-canonical ubiquitylation of the proneural protein Ngn2 occurs in both Xenopus embryos and mammalian cells. Biochem. Biophys. Res. Commun. *400*, 655–660.

Meltzer, H.Y. (1991). The mechanism of action of novel antipsychotic drugs. Schizophr Bull *17*, 263–287.

Moore, A.R., Ceraudo, E., Sher, J.J., Guan, Y., Shoushtari, A.N., Chang, M.T., Zhang, J.Q., Walczak, E.G., Kazmi, M.A., Taylor, B.S., et al. (2016). Recurrent activating mutations of G-protein-coupled receptor CYSLTR2 in uveal melanoma. Nature Genetics *48*, 675–680.

Mrzljak, L., Bergson, C., Pappy, M., Huff, R., Levenson, R., and Goldman-Rakic, P.S. (1996). Localization of dopamine D4 receptors in GABAergic neurons of the primate brain. Nature *381*, 245–248.

NEVILLE, D.M. (1960). The isolation of a cell membrane fraction from rat liver. J Biophys Biochem Cytol *8*, 413–422.

Olsen, S.K., and Lima, C.D. (2013). Structure of a ubiquitin E1-E2 complex: insights to E1-E2 thioester transfer. Molecular Cell *49*, 884–896.

Olson, M.O., Goldknopf, I.L., Guetzow, K.A., James, G.T., Hawkins, T.C., Mays-Rothberg, C.J., and Busch, H. (1976). The NH2- and COOH-terminal amino acid sequence of nuclear protein A24. J. Biol. Chem. *251*, 5901–5903.

Ordureau, A., Münch, C., and Harper, J.W. (2015). Quantifying ubiquitin signaling. Molecular Cell *58*, 660–676.

Overington, J.P., Al-Lazikani, B., and Hopkins, A.L. (2006). How many drug targets are there? Nat Rev Drug Discov *5*, 993–996.

Pappa, I., Mileva-Seitz, V.R., Bakermans-Kranenburg, M.J., Tiemeier, H., and van IJzendoorn, M.H. (2015). The magnificent seven: A quantitative review of dopamine receptor d4 and its association with child behavior. Neuroscience & Biobehavioral Reviews *57*, 175–186.

Park, S.H., Cheong, C., Idoyaga, J., Kim, J.Y., Choi, J.-H., Do, Y., Lee, H., Jo, J.H., Oh, Y.-S., Im, W., et al. (2008). Generation and application of new rat monoclonal antibodies against synthetic FLAG and OLLAS tags for improved immunodetection. J. Immunol. Methods *331*, 27–38.

Petaja-Repo, U.E., Hogue, M., Laperriere, A., Bhalla, S., Walker, P., and Bouvier, M. (2001). Newly synthesized human delta opioid receptors retained in the endoplasmic reticulum are retrotranslocated to the cytosol, deglycosylated, ubiquitinated, and degraded by the proteasome. J. Biol. Chem. *276*, 4416–4423.

Qin, L., Liu, W., Ma, K., Wei, J., Zhong, P., Cho, K., and Yan, Z. (2016). The ADHD-linked human dopamine D4 receptor variant D4.7 induces over-suppression of NMDA receptor function in prefrontal cortex. Neurobiol. Dis. *95*, 194–203.

Regard, J.B., Sato, I.T., and Coughlin, S.R. (2008). Anatomical profiling of G protein-coupled receptor expression. Cell *135*, 561–571.

Rogers, S., Wells, R., and Rechsteiner, M. (1986). Amino acid sequences common to rapidly degraded proteins: the PEST hypothesis. Science *234*, 364–368.

Rondou, P., Haegeman, G., Vanhoenacker, P., and Van Craenenbroeck, K. (2008). BTB Protein KLHL12 targets the dopamine D4 receptor for ubiquitination by a Cul3-based E3 ligase. J. Biol. Chem. *283*, 11083–11096.

Rondou, P., Skieterska, K., Packeu, A., Lintermans, B., Vanhoenacker, P., Vauquelin, G., Haegeman, G., and Van Craenenbroeck, K. (2010). KLHL12-mediated ubiquitination of the dopamine D4 receptor does not target the receptor for degradation. Cellular Signalling *22*, 900–913.

Rotin, D., and Kumar, S. (2009). Physiological functions of the HECT family of ubiquitin ligases. Nat. Rev. Mol. Cell Biol. *10*, 398–409.

Sakmar, T.P., Menon, S.T., Marin, E.P., and Awad, E.S. (2002). Rhodopsin: insights from recent structural studies. Annu Rev Biophys Biomol Struct *31*, 443–484.

Schedin-Weiss, S., Inoue, M., Teranishi, Y., Yamamoto, N.G., Karlström, H., Winblad, B., and Tjernberg, L.O. (2013). Visualizing active enzyme complexes using a photoreactive inhibitor for proximity ligation--application on γ-secretase. PLoS ONE *8*, e63962.

Schlesinger, D.H., and Goldstein, G. (1975). Molecular conservation of 74 amino acid sequence of ubiquitin between cattle and man. Nature *255*, 423–424.

Schulman, B.A., and Harper, J.W. (2009). Ubiquitin-like protein activation by E1 enzymes: the apex for downstream signalling pathways. Nat. Rev. Mol. Cell Biol. *10*, 319–331.

Shimizu, Y., Okuda-Shimizu, Y., and Hendershot, L.M. (2010). Ubiquitylation of an ERAD substrate occurs on multiple types of amino acids. Molecular Cell *40*, 917–926.

Singh, G.P., Ganapathi, M., Sandhu, K.S., and Dash, D. (2006). Intrinsic unstructuredness and abundance of PEST motifs in eukaryotic proteomes. Proteins *62*, 309–315.

Skieterska, K., Rondou, P., Lintermans, B., and Van Craenenbroeck, K. (2015). KLHL12 Promotes Non-Lysine Ubiquitination of the Dopamine Receptors D4.2 and D4.4, but Not of the ADHD-Associated D4.7 Variant. PLoS ONE *10*, e0145654.

Sohal, V.S., Zhang, F., Yizhar, O., and Deisseroth, K. (2009). Parvalbumin neurons and gamma rhythms enhance cortical circuit performance. Nature *459*, 698–702.

Söderberg, O., Gullberg, M., Jarvius, M., Ridderstråle, K., Leuchowius, K.-J., Jarvius, J., Wester, K., Hydbring, P., Bahram, F., Larsson, L.-G., et al. (2006). Direct observation of individual endogenous protein complexes in situ by proximity ligation. Nat Meth *3*, 995–1000.

Spooren, A., Rondou, P., Debowska, K., Lintermans, B., Vermeulen, L., Samyn, B., Skieterska, K., Debyser, G., Devreese, B., Vanhoenacker, P., et al. (2010). Resistance of the dopamine D4 receptor to agonist-induced internalization and degradation. Cellular Signalling *22*, 600–609.

Swatek, K.N., and Komander, D. (2016). Ubiquitin modifications. Nature Publishing Group *26*, 399–422.

Szkudlinski, M.W., Fremont, V., Ronin, C., and Weintraub, B.D. (2002). Thyroid-stimulating hormone and thyroid-stimulating hormone receptor structure-function relationships. Physiol. Rev. *82*, 473–502.

Tait, S.W.G., de Vries, E., Maas, C., Keller, A.M., D'Santos, C.S., and Borst, J. (2007). Apoptosis induction by Bid requires unconventional ubiquitination and degradation of its N-terminal fragment. J. Cell Biol. *179*, 1453–1466.

Tanowitz, M., and Zastrow, Von, M. (2002). Ubiquitination-independent trafficking of G protein-coupled receptors to lysosomes. J. Biol. Chem. *277*, 50219–50222.

Thrower, J.S., Hoffman, L., Rechsteiner, M., and Pickart, C.M. (2000). Recognition of the polyubiquitin proteolytic signal. Embo J. *19*, 94–102.

Tokarev, A.A., Munguia, J., and Guatelli, J.C. (2011). Serine-threonine ubiquitination mediates downregulation of BST-2/tetherin and relief of restricted virion release by HIV-1 Vpu. J. Virol. *85*, 51–63.

Tovo-Rodrigues, L., Roux, A., Hutz, M.H., Rohde, L.A., and Woods, A.S. (2014). Functional characterization of G-protein-coupled receptors: a bioinformatics approach. Neuroscience *277*, 764–779.

Uhlhaas, P.J., and Singer, W. (2012). Neuronal dynamics and neuropsychiatric disorders: toward a translational paradigm for dysfunctional large-scale networks. Neuron *75*, 963–980.

Van Craenenbroeck, K., Clark, S.D., Cox, M.J., Oak, J.N., Liu, F., and Van Tol, H.H.M. (2005). Folding efficiency is rate-limiting in dopamine D4 receptor biogenesis. J. Biol. Chem. *280*, 19350–19357.

Van Tol, H.H., Wu, C.M., Guan, H.C., Ohara, K., Bunzow, J.R., Civelli, O., Kennedy, J., Seeman, P., Niznik, H.B., and Jovanovic, V. (1992). Multiple dopamine D4 receptor variants in the human population. Nature *358*, 149–152.

Van Tol, H.H.M., Bunzow, J.R., Guan, H.-C., Sunahara, R.K., Seeman, P., Niznik, H.B., and Civelli, O. (1991). Cloning of the gene for a human dopamine D4 receptor with high affinity for the antipsychotic clozapine. , Published Online: 18 April 1991; | Doi:10.1038/350610a0 *350*, 610–614.

Vassilatis, D.K., Hohmann, J.G., Zeng, H., Li, F., Ranchalis, J.E., Mortrud, M.T., Brown, A., Rodriguez, S.S., Weller, J.R., Wright, A.C., et al. (2003). The G protein-coupled receptor repertoires of human and mouse. Pnas *100*, 4903–4908.

Veldkamp, C.T., Seibert, C., Peterson, F.C., la Cruz, De, N.B., Haugner, J.C., Basnet, H., Sakmar, T.P., and Volkman, B.F. (2008). Structural basis of CXCR4 sulfotyrosine recognition by the chemokine SDF-1/CXCL12. Sci Signal *1*, ra4–ra4.

Vosper, J.M.D., McDowell, G.S., Hindley, C.J., Fiore-Heriche, C.S., Kucerova, R., Horan, I., and Philpott, A. (2009). Ubiquitylation on canonical and non-canonical sites targets the transcription factor neurogenin for ubiquitin-mediated proteolysis. J. Biol. Chem. *284*, 15458–15468.

Vullhorst, D. (2013). Dopamine, cognitive function, and gamma oscillations: role of D4 receptors. 1–19.

Wang, X., Herr, R.A., Chua, W.-J., Lybarger, L., Wiertz, E.J.H.J., and Hansen, T.H. (2007). Ubiquitination of serine, threonine, or lysine residues on the cytoplasmic tail can induce ERAD of MHC-I by viral E3 ligase mK3. J. Cell Biol. *177*, 613–624.

Weber, A., Cohen, I., Popp, O., Dittmar, G., Reiss, Y., Sommer, T., Ravid, T., and Jarosch, E. (2016). Sequential Poly-ubiquitylation by Specialized Conjugating Enzymes Expands the Versatility of a Quality Control Ubiquitin Ligase. Molecular Cell *63*, 827–839.

Wettschureck, N., and Offermanns, S. (2005). Mammalian G proteins and their cell type specific functions. Physiol. Rev. *85*, 1159–1204.

Young, B., Wertman, J., and Dupré, D.J. (2015). Regulation of GPCR Anterograde Trafficking by Molecular Chaperones and Motifs. Prog Mol Biol Transl Sci *132*, 289–305.

Zhang, X., and Kim, K.-M. (2016). Palmitoylation of the carboxyl-terminal tail of dopamine D4 receptor is required for surface expression, endocytosis, and signaling. Biochem. Biophys. Res. Commun. *479*, 398–403.

Zhen, X., Zhang, J., Johnson, G.P., and Friedman, E. (2001). D(4) dopamine receptor differentially regulates Akt/nuclear factor-kappa b and extracellular signal-regulated kinase pathways in D(4)MN9D cells. Mol. Pharmacol. *60*, 857–864.

Zhong, P., Liu, W., and Yan, Z. (2016). Aberrant regulation of synchronous network activity by the attention-deficit/hyperactivity disorder-associated human dopamine D4 receptor variant D4.7 in the prefrontal cortex. The Journal of Physiology *594*, 135–147.